Modeling and Performance Analysis of In-Building Distributed WLAN using CSMA with Spread Spectrum Signaling

by

Lawrence Tang

B.Eng.Sc., University of Western Ontario, 1992

A THESIS SUBMITTED IN PARTIAL FULFILLMENT OF
THE REQUIREMENTS FOR THE DEGREE OF
MASTER OF APPLIED SCIENCE

in

THE FACULTY OF GRADUATE STUDIES
DEPARTMENT OF ELECTRICAL ENGINEERING

We accept this thesis as conforming
to the required standard

THE UNIVERSITY OF BRITISH COLUMBIA

December 1995

In presenting this thesis in partial fulfilment of the requirements for an advanced degree at the University of British Columbia, I agree that the Library shall make it freely available for reference and study. I further agree that permission for extensive copying of this thesis for scholarly purposes may be granted by the head of my department or by his or her representatives. It is understood that copying or publication of this thesis for financial gain shall not be allowed without my written permission.

Department of Electrical Engineering

The University of British Columbia
Vancouver, Canada

Date Dec 18, 1995

DE-6 (2/88)

Abstract

In recent years, application of wireless technology in local area networks has become prominent due to its flexibility and ability to support portable terminals. This thesis considers a wireless local area network in a room with multiple stations accessing multiple radio bridges which are interconnected by a backbone network. Direct sequence spread spectrum signaling with a common spreading code and carrier sensing multiple access are employed. This system is analyzed with respect to uplink performance only as well as uplink/downlink performance.

The 1–persistent carrier sensing multiple access protocol performs well in the uplink model. However, it does not yield satisfactory results in the uplink/downlink model. In particular, the 1–persistent protocol is unable to balance uplink/downlink channel access, giving the uplink traffic much higher throughput than downlink traffic. This unbalanced channel access problem is solved by using a dual persistency carrier sensing protocol, which is shown to balance uplink and downlink throughput.

The relationships between packet duplications, hidden terminals and multiple packet receptions in the distributed wireless local network architecture are illustrated via eight system parameters. In particular, the number of radio bridges, the carrier sensing threshold and the type of power control method have the greatest influence on the system performance. These three parameters directly affect packet duplications, multiple packet receptions, the number of hidden terminals in the system, and the received signal-to-noise ratio and interference-to-signal ratio at each receiver.

In both the uplink only and uplink/downlink models, a higher number of radio bridges is found to be desirable since it allows multiple packet receptions. A moderate carrier sensing threshold is preferred since a low value causes packet duplications whereas a high value causes the system to saturate. Power-controlled transmission is desirable in terms of fairness because it equalizes capturing probabilities with respect to stations' distances from the radio bridges. Hidden terminals, which are detrimental to conventional carrier sensing systems, have a less detrimental effect in distributed wireless local area networks with multiple radio bridges due to the possibility of multiple packet receptions.

Table of Contents

List of Figures

List of Tables

Acknowledgment

I would like to express sincere gratitude to my supervisor, Dr. Victor C. M. Leung for his constant guidance and advise in this thesis. I also would like to thank Dr. R. W. Donaldson for introducing me to this research topic. My acknowledgment to the Canadian Institute for Telecommunications Research (CITR) and B. C. Science Council for their financial support of this research.

Chapter 1
Introduction

This introductory chapter gives the motivations on the research of wireless local area network. The objectives of this thesis are stated. The topics that will be covered in subsequent chapters are outlined at the end of this chapter.

1.1 Motivations

Interconnection of data terminals/workstations to networks using wired local area networks (LANs) has been in existence for many years. However, the locations of terminals are inflexible in these networks. Extra rewiring costs are incurred when terminals are added or rearranged within the network. Sometimes, in the installation of a network in an older building, laying the cables can be more expensive than the costs of terminals.

Wireless local area networks (WLANs), which provide tetherless connections among the terminals, eliminate the above disadvantages of wired LANs. In addition, WLANs can enhance the capabilities of networking. For example, WLANs may be used to network mobile and portable computers to provide personal communication services (PCS).

In a WLAN, wireless terminals access base stations to communicate with shared resources on the network, resulting in multiple access interference in the shared radio channel when contention-type medium access control (MAC) protocols are employed. Since most WLANs operate in an indoor environment, multipath interference is one of the dominant factors that degrades the performance of the system. Spread spectrum (SS) signaling is used to suppress many types of interference. SS signaling enables a receiver to correctly receive a packet despite the presence of other overlapping transmissions. Most of the previous research has emphasized code division multiple access (CDMA) techniques, which employ different spreading sequences for different terminals in the system. In contrast, a system that uses a

common spreading sequence is considered in this thesis. Using a common spreading code has the advantage of reducing the receiver complexity.

To provide radio coverage over a large area, the centralized cellular architecture is commonly used. The entire service area of a cellular wireless network is divided into cells. Each wireless terminal is allowed to communicate only with the base station of the cell in which it is located. An alternative approach is the distributed architecture, which employs multiple base stations, called radio bridges (RBs) in this thesis, to cover the whole service area in an overlapping coverage pattern. Any wireless terminal may have connectivity with multiple RBs simultaneously. The distributed architecture has the advantage of transparent handoff when a terminal is moved from one location to another, and multiple packet receptions when multiple terminals can simultaneously communicate with several RBs. Whereas most WLAN research and commercial products employ the centralized cellular architecture, the modeling and performance analysis of a distributed wireless in-building network employing a carrier sensing type protocol has not been previously considered, and is the subject of this thesis.

Direct sequence spread spectrum (DS/SS) is a commonly used SS signaling method, which directly modulates the data with a pseudonoise (PN) sequence with a much higher clock rate (chip rate) than the data. One problem in multiple access with DS/SS signaling is the near-far effect. In a centralized CDMA network, this problem is solved by controlling the transmission power of each terminal. However, this method is not applicable in distributed architectures and therefore it is necessary to find some new strategies suitable for distributed WLAN to mitigate the near-far problem.

1.2 Objectives

The objectives of this thesis are the followings :

1. To create a model for a distributed WLAN with multiple RBs which employs the carrier sensed multiple access (CSMA) protocol for the MAC layer and DS/SS signaling with a common spreading sequence in the physical layer.

2. To evaluate the performance (throughput, delay and fairness) of the CSMA protocol in the distributed WLAN architecture.
3. To develop a MAC protocol suitable for distributed WLANs when both uplink and downlink traffic share a common channel, and to examine the resulting performance.
4. To develope strategies for suppressing the near-far effect in distributed WLANs.
5. To investigate the effects of various design parameters on the performance of distributed WLANs.

1.3 Thesis Outline

Chapter 2 presents the problems of wired LANs and the advantages of WLANs. It discusses the technologies and architectures employed by existing WLANs and describes the investigation methods.

Chapter 3 defines the performance measures, explaining simulation parameters, assumptions, constraints and other precautions taken in the modeling of the distributed WLAN.

Chapter 4 investigates the uplink performance of a distributed WLAN in which uplink and downlink traffic employs different channels.

Chapter 5 discusses the problem of adopting the uplink CSMA protocol to a system in which uplink and downlink traffic shares a common channel and presents the solution by introducing a dual persistency CSMA protocol. Using this protocol, a complete distributed WLAN incorporating both uplink and downlink traffic in the same channel is analyzed. The effects of a number of design parameters on the throughput, delay and capturing probability of the system are examined.

Chapter 6 summarizes of the results and contributions of this research and presents other possible areas for future research.

Chapter 2
Background

In this chapter, the problems of wired LANs and the advantages of WLANs are discussed. Despite the flexibility and other advantages of WLANs, they have some drawbacks such as limited range and vulnerability to interference. Bursty traffic from random access terminals may also cause inefficient use of channel bandwidth. Spread spectrum modulation and contention medium access protocol are employed to overcome these problems.

2.1 Problems of Wired LANs

LANs provide communications linkages among the computer terminals, servers, printing devices and other peripherals. This allows an efficient and low cost approach to share information and facilities between many users. However, most LANs are not installed in such a way that can be expanded or modified easily. Even though wired LANs using coaxial cables are available off the shelves, the expense and the inconvenience of their installations are sometimes not bearable. An estimation made by Motorola indicates a total of US$1.12 billion per year for relocating LAN devices in the USA [1].

2.2 Wireless LANs

Use of radio channels instead of cables provides an alternative transmission medium for indoor LAN applications. Radio transmissions provide flexibility in terminal rearrangements, LAN configuration modifications and system expansions. Furthermore, WLANs support mobility of portable terminals. Due to the complexity and hence high cost of radio transceivers required in WLANs, the first time installation cost of a WLAN may exceed that of a wired LAN. However, in the long run, the cost of the network will become lower than a wired LAN owing to the reduction in the expenses and the inconvenience incurred to reconfigure the network. This leads to enormous interests in WLANs as evidenced by the increasing level of research and product development activities in this area.

In recent years, some commercial WLANs have come into the market. They can be classified into two types. The first type uses infrared (IR) as the medium for wireless networking. The second type uses radio communications.

2.2.1 Infrared WLAN

Infrared and visible light, being near in wavelength, behaves similarly. For instance, infrared light is reflected by mirrors but absorbed by dark objects. Infrared light penetrates glass but not walls. Thus an infrared signal is usually confined to a single compartment.

Infrared transmissions have an abundance of bandwidth, are free from Federal Communication Commission's (FCC) regulation, and are immune to radio interference. On the other hand, infrared signals are susceptible to shadowing caused by objects or people between the transmitter and receiver. Another disadvantage is their limited range (~5 m radius) due to the power limit on infrared transmitters imposed by safety considerations. Nevertheless, infrared channels have higher bandwidth and can support higher data rate compared to other wireless media. In [2], it is argued that data rates up to 100 Mbits/s are possible.

Infrared WLANs have two basic transmission methods :

1. Directed transmission : the transmitter and receiver are precisely aligned.
2. Diffuse transmission : signals are scattered off the walls and ceilings within a room.

Diffuse transmission is potentially more convenient to use but at the expense of lower data rate and shorter range. Early infrared systems can support a data rate ranging from 19.2 kbits/s to 1 Mbits/s, [2]. A commercial InfraLAN Technology directed transmission system is compatible with the Token Ring, having a data rate of 16 Mbit/s. In contrast, the Photonics Collaborate IR LAN which uses diffuse transmission can only support 1 Mbits/s [3].

2.2.2 Radio WLAN

The second type of WLANs uses radio communications. The development of WLAN has been concentrated in the USA since 1985 due to a decision by the FCC to allow the use of spread spectrum modulation techniques in the unregulated Industrial, Scientific and Medical (ISM) frequency bands (at 902–928 MHz, 2400–2500 MHz, and 5725–5825 MHz).

Currently the IEEE 802.11 working group is developing a standard for WLAN and the second draft [4] has been completed by the end of 1994.

Radio WLANs may have three architectures, i.e., peer-to-peer, centralized and distributed.

Peer-to-Peer This is also known as the ad hoc network. Any terminal can transmit to other terminals that are in radio range of one another, i.e. the network is fully connected [5]. However, since the attenuation of wireless signals is much more severe than in wired media, this architecture has limited range compared to the next two. This architecture is illustrated in figure 2.1.

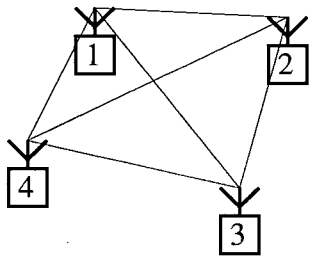

Figure 2.1 Peer-to-peer architecture

Centralized A significant amount of efforts have been spent on this architecture [6–14]. An example is the Wireless In-Building Network (WIN) proposed by Motorola [6, 7]. In this architecture, a group of wireless terminals communicate with one another only through a base station at the centre of its coverage area called a microcell. The overall coverage area can be expanded by using multiple base stations and each base station operates at a different frequency than adjacent base stations. Frequency can be reused at some microcells that are several cells apart, as in the cellular mobile radio network. Terminals that move into another microcell are required to exercise handoff procedures and frequency changes. Connections between base stations are provided by a wired LAN. Figure 2.2 shows an example of a centralized WLAN, where in each room there may be one or multiple microcells.

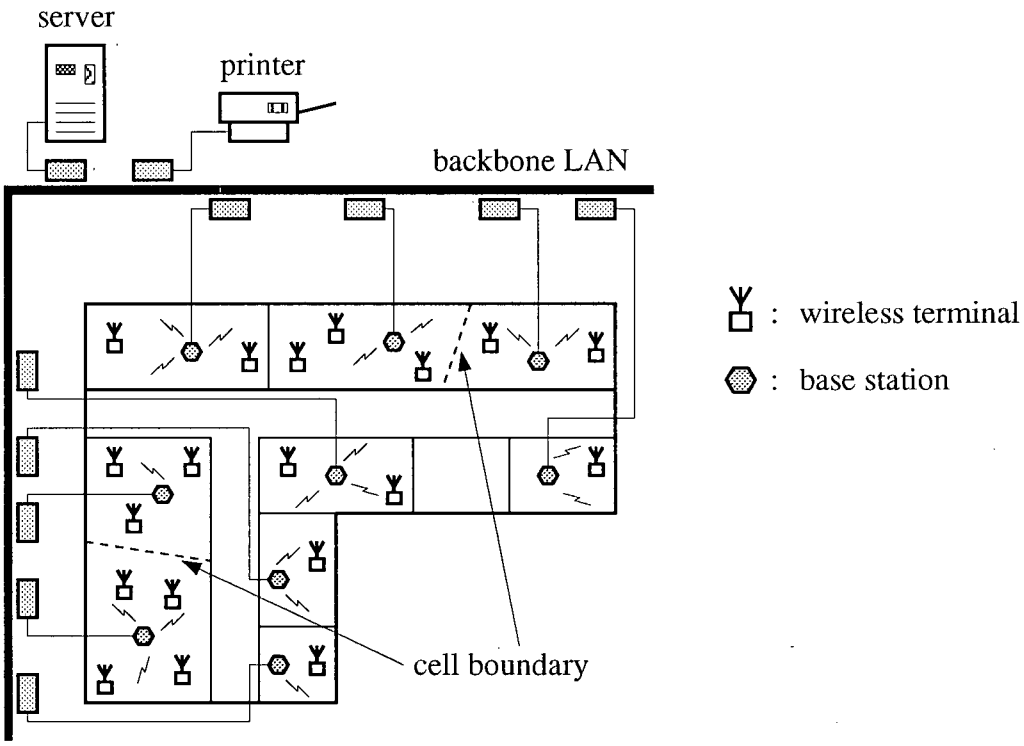

Figure 2.2 Centralized (cellular) architecture for
wireless in-building network with multiple base stations

Distributed Comparatively less attention is given to this architecture [15–19]. In [20], Serizawa has considered a model that allows wireless terminals to communicate with each other via the wired LAN equipped with multiple radio ports (or radio bridges, RBs, in the context of this thesis). However, [20] only analyzed the performance of a wired LAN but not the wireless channel. The major difference between the distributed architecture and the one base station per cell centralized architecture is that multiple RBs are allowed to communicate with each terminal and hence no microcell exists. The same frequency is used for the entire coverage area. All wireless terminals are interconnected by multiple RBs. The idea behind the distributed architecture is to gain the advantage of multiple packet receptions [21–24]. In a random access channel, two simultaneous transmissions to the same RB may result in destruction of both packets, depending on the capturing ability of the receivers. However, by putting in more RBs and each terminal having connectivity to more than one RBs, it is possible that both packets can be received and hence improve the throughput of the system.

Figure 2.3 depicts a possible configuration of a distributed WLAN. Note that there is no cell boundary in the entire coverage area.

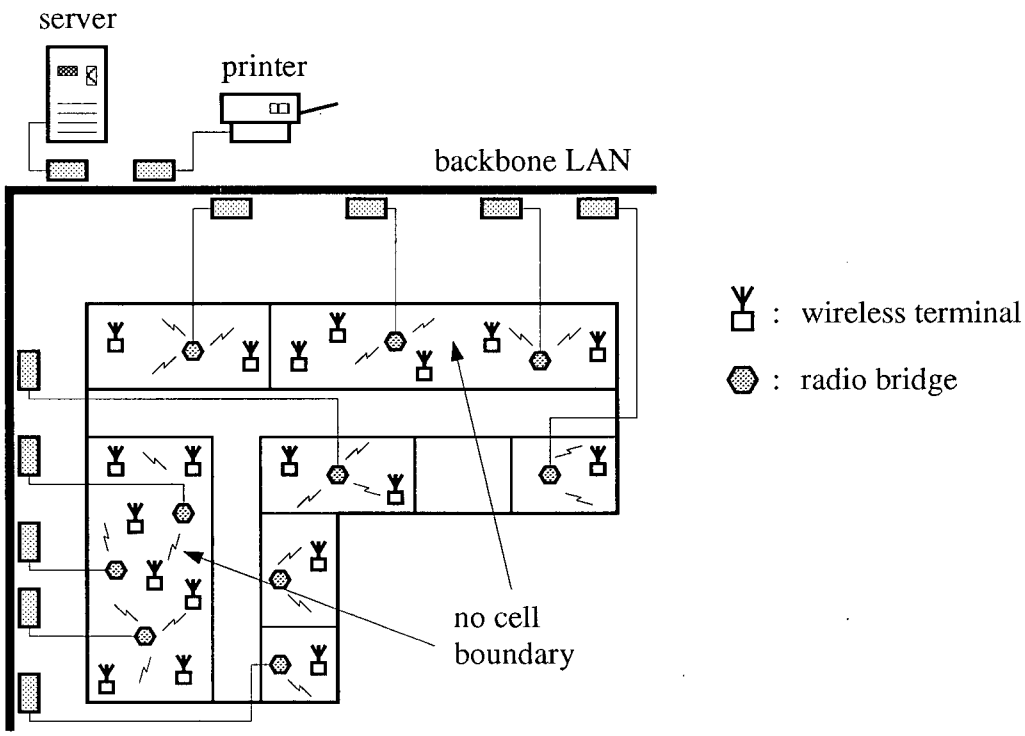

Figure 2.3 Distributed architecture for wireless in-building network with multiple radio bridges

Commercial WLANs employing radio transmissions include WaveLAN by NCR and Windata's Freeport wireless LAN. The WaveLAN employs the 902–928 MHz band. It is a peer-to-peer network architecture where terminals on the network communicate directly with any other terminals. All terminals compete for channel access using a CSMA/CA (collision avoidance) MAC protocol. WaveLAN employs DS/SS signaling with a chip rate of 22 Mchips/s and a data rate of 2 Mbit/s.

In Windata's WLAN, the two upper ISM bands are used. It is based on a hub configuration (centralized architecture), such that all interconnections between terminals — whether by radio or by a wired LAN — are routed via the hub. The 2400–2500 MHz band

is used as the uplink channel and the 5725–5825 MHz band is for the downlink. Windata again uses DS/SS modulation and is able to support data rates up to 5.7 Mbit/s.

2.3 Spread Spectrum Signaling

Literally, a spread spectrum system is one in which the transmitted signal is spreaded by means of a spreading code over a frequency band much wider than the minimum bandwidth required to transmit the information being sent.

Synchronized reception using the spreading code restores the information to its original bandwidth while spreading only interfering signals to the transmission bandwidth which are subsequently rejected by filtering at the information bandwidth. Since radio transmissions in WLANs are susceptible to interference from multipath reflections and other co-channel users, the use of SS signaling in WLANs could enhance system performance by suppressing interference.

One of the most popular SS methods to counteract interference is direct sequence (DS) or pseudonoise (PN) modulation. Direct sequence is the direct modulation of the data by a code sequence, usually a PN code, which has a much higher clock rate than the data rate. The product of the two signals then modulates a carrier by the most common biphase phase-shift keying (BPSK). The demodulation occurs at the receiver where the same sequence is used to correlate the received signal which is composed of the desired transmitted signal, reflected, delayed and possibly distorted replica of the transmitted signal, interference from other transmissions, and noise. The correlation of the desired signal and the spreading sequence produces a signal peak at the match filter output while attenuating any interfering signal by the processing gain, PG, if the signal is modulated by a different spreading sequence. A signal with the same spreading code as the desired signal with at least 1 chip offset in time is also suppressed. This phenomenon is know as the capture effect of spread spectrum signaling. The capture effect allows one of several colliding packets to be correctly received at the receiver, as opposed to the model used in [9, 10, 25], where all overlapped packets are assumed to be destroyed.

2.4 Medium Access Control Protocol

When a set of uncoordinated wireless terminals share a common channel, contentions will occur. In the absence of the capture effect, packet overlapping may lead to destruction of all colliding packets and hence the channel bandwidth is wasted. There are many MAC protocols for LANs, such as token passing, CDMA, Aloha and CSMA. The token passing type protocol includes the token ring and token bus. However, token passing type protocols may not be suitable for accessing the radio medium due to its broadcast nature [26].

CDMA is a MAC protocol and can be treated as an extension of DS/SS. It is widely used in centralized systems [5]. CDMA assigns a different spreading to each transmitter. Then at each receiver, as many match filters as the number of active users are used to demodulate the received signals. CDMA allows simultaneous transmissions and is a good example of using the SS capture effect. However, if the network population grows large, the receiver structure will become extremely complicated and there is a certain limit on the number of signals that can be simultaneously demodulated. Distributed WLANs require multiple simple receivers. Thus, in this thesis we investigate the performance of DS/SS signaling without CDMA.

Contention type protocols, where the entire bandwidth is provided to the terminals as a single channel, are well suited for bursty traffic. Aloha and CSMA are examples of such protocols. Aloha, while simple to analyze, is highly inefficient even in light traffic and is unstable under heavy traffic.

The first detailed analysis of the CSMA protocol can be found in [9] and later an immense number of variations and applications of CSMA have appeared in the literature [11, 20]. In this protocol, each terminal or node senses the presence of transmissions by its neighbors before it transmits. Thus CSMA permits terminals to dynamically acquire the state of the channel and prevent most of the collisions. CSMA may be advantageously employed for random access by uncoordinated users with bursty traffic. Its performance also does not degrade drastically when the normalized offered traffic is slightly greater than one, provided that the propagation delay is small and the sensing procedure has a good estimate of the state of the channel.

There are two possible ways that collisions may still occur despite the CSMA strategy. The first is due to nonzero propagation delay in sensing the state of the channel before a carrier arrives. This factor is not significant because the propagation delays over indoor wireless channels are very small compared to wired systems since signals are travelling at the speed of light. The second cause of collision is the hidden terminal problem [27] which results when a terminal's transmission can not be heard by other terminals in the network. When a transmitting terminal is hidden from a sensing terminal, the latter will treat the channel as idle and start a transmission, leading to a collision.

An unslotted version of the CSMA MAC protocol is considered in this thesis for two reasons. First, synchronization required in a slotted system is difficult to achieve in wireless communications. The transceivers in a synchronous system are far more complex than those found in an asynchronous system. Second, when a wireless terminal has linkages to more than one RBs and there are different propagation delays to the different RBs, it becomes difficult for the terminal to decide which RB it should synchronize to.

Chapter 3
Modeling of Distributed WLAN using CSMA with Capture

A model of a distributed WLAN using CSMA with capture is created and simulated using Simscript II.5. The system parameters as well as two power control methods and two capture schemes are introduced here. This chapter explains why and how the parameters are chosen. All the methods or parameters, except the CSMA protocol, are equally applicable to both the uplink model (chapter 4) or the uplink/downlink model (chapter 5).

3.1 Physical Environment

In this section, the physical environment and other properties in the model design are described.

3.1.1 Room Dimension

The room is modelled as a 40x40 m^2 square with four walls. Duchamp [28] used a range of distance from 10 to 56 m between the transmitter and the receiver. This room size will allow some hidden terminals to exist for different values of carrier sensing threshold. The square shape allows us to produce symmetric reflected signals. Room dimension of other sizes will be considered in subsequent simulations. If the room dimension is increased but the number of RBs remains unchanged, the positions of terminals and RBs are adjusted accordingly, reducing the terminal density. We expect to see a worse throughput than before because increasing the room dimension increases the number of hidden terminals that carrier sensing fails to detect.

3.1.2 Number of RBs

The number of RBs plays an important role in the system throughput. Multiple RBs allow reception of several simultaneous transmissions (see section 2.2.2, paragraph on distributed

architecture). Simulations are run for system with 1 to 5 RBs. All RBs are interconnected by a backbone LAN. An uplink packet directed to another terminal, which is out of the range of the receiving RB, will be forwarded to the nearest RB of the designated terminal.

3.1.3 Terminal Distribution

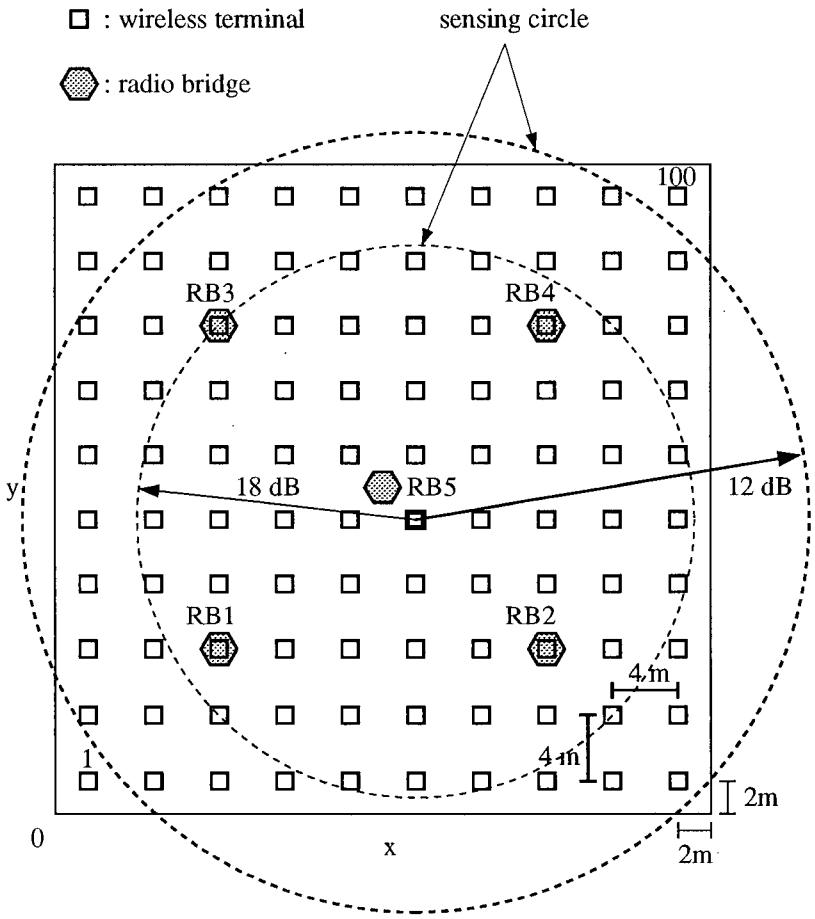

Figure 3.1 Physical model

There are N stations or terminals uniformly distributed across the room. The maximum number of stations is $N = 100$. The reason of having 100 fixed stations is that this number of station can form a grid pattern inside a room. This permits us to measure capturing probability at each geographical location during the course of simulation. This grid pattern also allows us to model the situation of having other terminals nearby. Smaller population

sizes with $N = \{49, 81\}$ are used to compare the effects of population size to the system performance. Figure 3.1 shows the case of $N = 100$ and RB = 5.

3.1.4 Signal Propagation Model

A common signal propagation model used to calculate the signal strength as a function of distance is the inverse distance power model [29],

$$\Gamma = \frac{1}{d^{\beta}} \tag{3.1}$$

where Γ is the normalized received signal power, d is the distance between the transmitter and the receiver, and β is a power attenuation factor. The value of β in an indoor environment is a function of building type and objects between the transmitter-receiver. Two measurement were made in two buildings and β was found to have a value of 3.54 and 4.33 [30]. An average $\beta = 4$ is used in this thesis.

3.1.5 Reflection of Signals

In this thesis we consider multipath signals that are due to signal reflected from lateral walls. Signals reflected from the ceiling, from the floor and multiple reflected signals are ignored. The ceiling and floor reflections are ignored because the path difference are too small to consider in our model. They are simply not resolvable due to the limits of time resolution of DS/SS. A possible combination of direct and multipath signals that may appear at a RB is shown in figure 3.2. The signals consist of one direct signal and four reflected signals. We assume that the reflected signals obey the law of reflection and that the incident angle is equal to the reflected angle. We further assume that there is no loss of power when a signal is reflected once and that the signal attenuation is solely due to path losses.

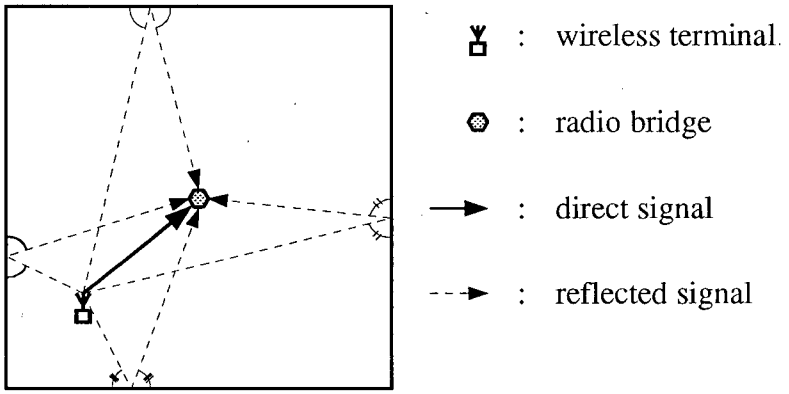

Figure 3.2 A possible signal combinations arrive at a RB in an indoor environment

3.1.6 Propagation Delay

To calculate the propagation delay between a transmitter and a receiver, it is first necessary to find the distance, d, between the two points and it is given by :

$$d = \sqrt{x^2 + y^2 + z^2} \tag{3.2}$$

where x, y, and z are the differences between the Cartesian coordinates of the two points. There are three possible combination transmitter-receiver pairs :

(i) station to station pair (z = 0 m)

(ii) station to RB pair (z = 2 m)

(iii) RB to station pair (z = 2 m)

Once the distances are calculated, the propagation delay is given by :

$$delay = \frac{d}{c} = \frac{d}{3.0 \times 10^8} \quad sec \tag{3.3}$$

This delay can then be normalized with respect to the packet length, i.e. the normalized propagation delay, a :

$$a = \frac{delay}{packet\ lenght} = \frac{d}{3.0 \times 10^8 \times packet\ length} \tag{3.4}$$

Because this is a wireless network, the value of a found from equation (3.4) is very small compared to the usual value in a wired network. In our model, the two diagonal stations

are the farthest apart. For this pair of station, the value of a is 3.25×10^{-5}, with respect to a packet length of 5.2224 ms. Therefore the propagation delay does not affect the system performance as far as the CSMA protocol is concerned.

3.2 Signaling Model

This section explains the relations of signal-to-noise ratio, interference-to-signal ratio and bit error rate. In addition, it explains the capturing methods, power control schemes and multipacket receptions in details.

3.2.1 Spread Spectrum Signaling

Spread spectrum signaling is employed in this wireless system. Spread spectrum allows capturing even if there are several packets in collision. Packets that are not locked on at the receiver are considered as interference and their correlation with the spreading code at the receiver are suppressed by the ratio of processing gain, *PG*, to the maximum odd autocorrelation, *oddM*, i.e. *PG/oddM*. *PG* is defined as :

$$PG = \frac{BW_{RF}}{BW_{info}} \tag{3.5}$$

where BW_{RF} is the RF bandwidth of the transmitted SS signal and the BW_{info} is the baseband bandwidth of the information.

Define $\hat{x}$ as a vector of length L whose element is $x_j \in \{+1, -1\}$, i.e.

$$\hat{x} = (x_0, x_1, ..., x_{L-1}, x_L) \tag{3.6}$$

and let x be the periodic sequence generated by $\hat{x}$, i.e.

$$x = \ ..., x_{-2}, x_{-1}, x_0, x_1, x_2, ..., x_{L-1}, x_L, ... \tag{3.7}$$

To define *oddM*, it is necessary first to define the aperiodic correlation function :

$$C_x(l) = \sum_{j=0}^{L-1-l} x_j x_{j+l} \qquad 0 \le l < L \tag{3.8}$$

Then the odd autocorrelation function $\hat{\theta}_x$ is defined as :

$$\hat{\theta}_x(l) = C_x(l) - C_x(L-l) \tag{3.9}$$

The function $\hat{\theta}_x$ has the property that

$$\hat{\theta}_x(l) = \begin{cases} L & l \bmod L = 0 \\ \hat{\theta}_x \leq oddM & l \bmod L \neq 0 \end{cases} \tag{3.10}$$

Therefore *oddM* is defined as $\max\{|\ \hat{\theta}_x(l)\ |: 1 \leq l < L\}$. This odd autocorrelation is applicable to interfering signals, which data transitions are not aligned with those of the desired signal at the receiver.

The values of the *PG* and the corresponding maximum *oddM* of the m-sequence can be found in [31, 32]. Table 3.1 tabulates the *PG* and maximum *oddM* for different n, where n is the degree of the PN sequence generator polynomial.

Table 3.1 Processing Gain and maximum odd autocorrelation values

Polynomial degree, n	$PG = 2^n - 1$	max *oddM*
5	31	7
6	63	11
7	127	17
8	255	25
9	511	41
10	1023	65
11	2047	87

3.2.2 Interfering Signals

When multipath interference and multiple access interference are taken into consideration, the probability of a bit error P_e is given by the following equation [31],

$$P_e = Q\left(\sqrt{2 \times SNR} \times \left(1 - \frac{oddM}{PG} \times max(ISR)\right)\right) \tag{3.11}$$

where SNR is the signal-to-noise ratio, and ISR is the interference-to-signal power ratio at the receiver. As the actual ISR changes over the packet duration, the maximum value used in (3.11) represents the worst case situation (see figure A.1 in Appendix A). The value of SNR is the ratio of the received power to the noise power. The received power is given by the transmitted power attenuated according to equation (3.1) and the noise power is assumed

to be constant for all receivers. The interference power is the sum of the received power of all other packets that are not locked on by the receiver, including all multipaths and direct path signals. ISR is defined as the ratio of interference power to received signal power.

From equation (3.11), the packet error rate *PER* is given by :

$$PER = \left(1 - (1 - P_e)^{bit}\right) \tag{3.12}$$

where *bit* is the number of bits per packet. This *PER* is used to determine the success or failure of packet reception at the receiver. Since P_e is calculated using the maximum ISR for the entire packet, this is equivalent to having the maximum interference power over the entire packet duration and hence (3.12) gives the worst case PER.

3.2.3 Power Control Methods

In the investigation of the performance of WLAN, two power control methods are introduced. These two methods have great influence on the carrier sensing as will be explained in section 3.2.5. The two methods are :

1. Fixed power method (FP). In this method, every station transmits with the same power, no matter how far the station is from the RB. The transmit power is fixed so that the corner stations produce a 10 dB SNR at the centre of the room.
2. Adjusted power method (AP). In this method, every station adjusts its transmitting power such that its signals have a SNR of *SNratio* dB at the second nearest RB. *SNratio* is a fixed parameter specified for the system and it has a major impact on the sensing range of the terminals. By using this method, some stations may have a sensing circle covering three RBs but some may not. However, the minimum number of RB that can capture a station's transmission is two.

3.2.4 Signal Capturing Mechanism

In [14, 19], a capturing scheme based on the signal with the higher power being captured at the receiver is used. In this thesis, another capturing scheme is introduced and compared. These two schemes are :

1. Power capture (PC). Capturing is based on the highest received signal power at the receiver.
2. Time capture (TC). Capturing is based on the earliest arrival once the receiver is available.

In conjunction with the PC scheme, a parameter called capture guard time, *mdatatime*, is introduced. The function of *mdatatime* is to define a time frame in which capturing may occur. A diagram is shown in figure 3.3 where *mdatatime* is specified in the units of data bits. In that figure, packet 0 is the earliest arrival at the receiver and packet 1 and 2 are within the capturing time frame *mdatatime* = 4 of packet 0. Within the time frame, capturing is based on the received signal level such that the strongest signal will prevail. Thus capturing of packet 1 or 2 instead of packet 0 is possible. Packets arriving after *mdatatime* relative to the first arrival are treated as interference and thus they will not be captured.

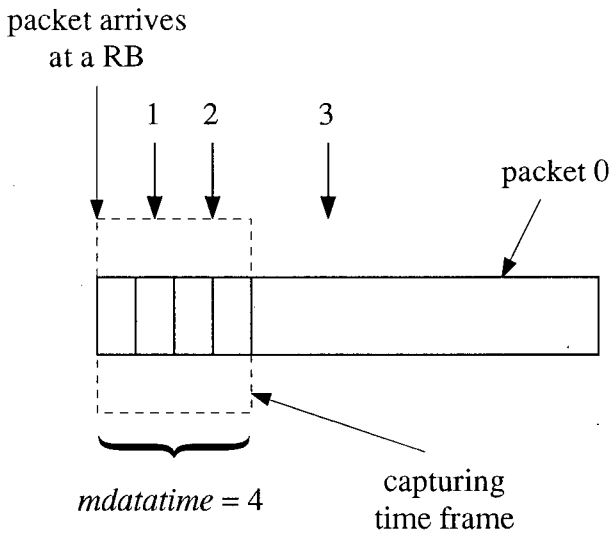

Figure 3.3 Functionality of *mdatatime*

In the TC scheme, the RB threshold, *RBTH*, is a parameter used by the receivers so that a receiver will not lock onto weak packets from terminals that are far away from the receiver. From figure 3.4, for example, if station1 transmits a packet and station100 transmits a packet after the propagation delay from station1 to RB4, then RB4, as well as other RBs, will lock onto the packet from station1 (the first arrival), even though packet100 has higher power

at RB4. However, in this situation, an increase in the number of RBs can not improve the system throughput since all RBs capture the same (the first) packet. It also prevents us to gain the advantage of using multiple RBs. Hence, the *RBTH* can prevent packet1 from being captured by RB4. It should be noted that *RBTH* is used only in the TC scheme.

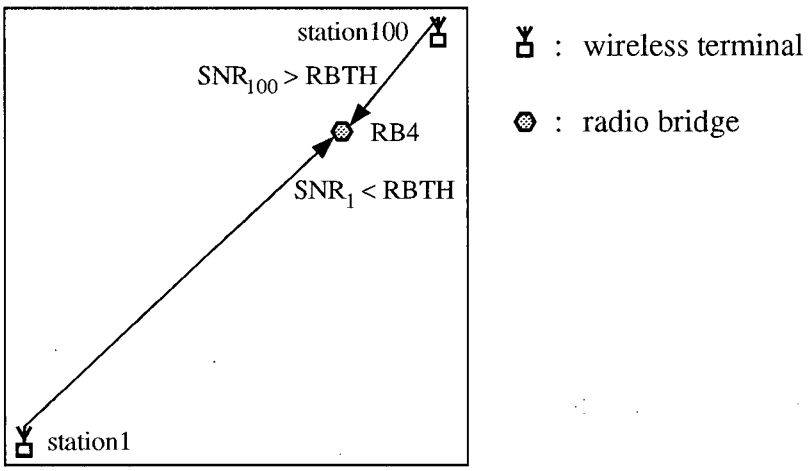

Figure 3.4 Functionality of *RBTH*

3.2.5 Carrier Sensing Threshold

When a terminal or a RB senses the channel, there exists some limitations on the range it can hear. Therefore, a parameter called carrier sensing threshold, *THSNR*, measured in dB, is introduced here. The value of *THSNR* represents the minimum SNR for a signal to be detected by a sensing terminal. It is used by each ready-to-send station to determine the state of the channel (idle or busy). If a station senses the channel and finds a SNR greater than the *THSNR*, the channel is considered as busy for that station. A larger value of *THSNR* indicates a smaller range and hence more hidden terminals, as indicated by the sensing circles in figure 3.1. Any station within the circle will produce a SNR greater than the value indicated and thus the station at the centre of the circle will sense a busy channel. Note that in figure 3.1, those circles are constructed based on the FP method. In the case of the AP method, the sensing threshold boundary may not form a circle since the stations have different transmitting powers.

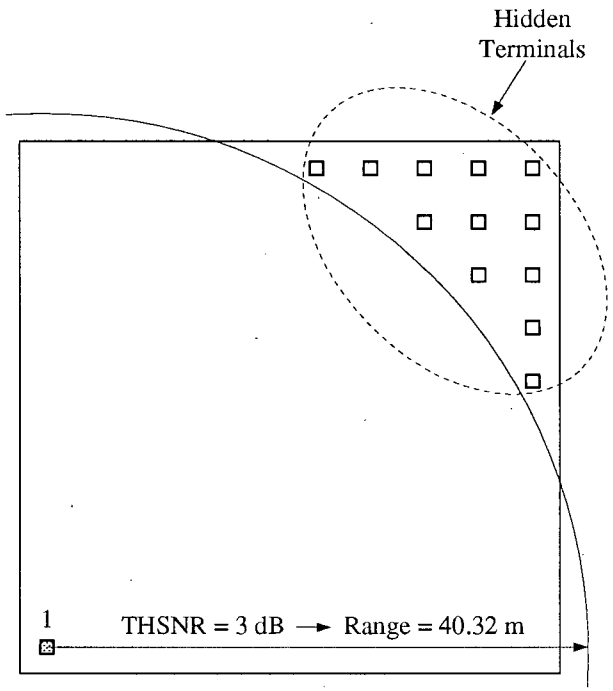

Figure 3.5 Range of hearing

THSNR is also used to control the number of hidden terminals in the system. Figure 3.5 depicts the range of hearing when *THSNR* = 3 dB. By using different *THSNR*, different ranges of hearing exists among the stations. This closely resembles a practical system where different terminals at different geographical locations have different number of hidden terminals. Hidden terminals are detrimental to the performance of CSMA since a channel sensed idle may in fact be busy, causing collisions between packets sent by terminals hidden from each others.

3.2.6 Multiple Packet Receptions and Duplication Problem

With the terminals having linkages to more than one RBs, more than one packets can be received by different RBs during the same time due to multiple packet receptions. Therefore multiple packet receptions can improve the system throughput. However, terminals with linkages to more than one RBs also cause the problem of duplicated packet receptions. Duplicated packets prevent possible receptions of other packets and this is the reason why using many more RBs may not give a proportional gain in throughput.

3.3 Multiple Access Model

This section describes the multiple access model used in the WLAN investigation. Assumptions made in the model are then discussed.

3.3.1 CSMA Protocol

The terminals are each equipped with a transmitter and a receiver and they share a single radio channel. Each terminal can be transmitting, receiving or idle but can not transmit and receive simultaneously.

The channel access employs the CSMA protocol [9, 33]. A terminal determines from the *THSNR* if the channel is idle before initiating a transmission. If the channel is sensed idle (*THSNR* > SNR), the terminal transmits the packet. Otherwise, the terminal backoffs for some multiples of packet length to avoid a collision which could occur if two stations try to transmit shortly after the channel becomes idle. Transmissions from the hidden terminals will cause collisions at the receiver. However, correct packet reception may still be possible due to the capture effect. Two types of CSMA protocol will be used for an uplink only channel and for an uplink/downlink shared channel. Specific details on the two protocols will be given in the later chapters.

3.3.2 Finite Population Singular Buffer Terminal

The system has a finite population of terminals and each terminal only has a single buffer [34]. The finite population model is necessary because terminals need to have fixed locations in the model. In this case, new packets will only be generated at the terminals which are idle. If a terminal is currently transmitting a packet, waiting for acknowledgment, or backlogged for retransmission, no new packet will be generated. The single buffer assumption allows us to calculate the lower bound of delay since no packet is being stored to wait for transmission.

3.3.3 Random Backoff Delay

The random backoff delay, *prno*, is for controlling the maximum multiple of packet length to backoff when a station has a collision or when the channel is sensed busy. The

equation used in the backoff is :

$$delay = (1 + prno \times random.no) \times packet.length \tag{3.13}$$

where *random.no* is a random number uniformly distributed between 0 and 1.

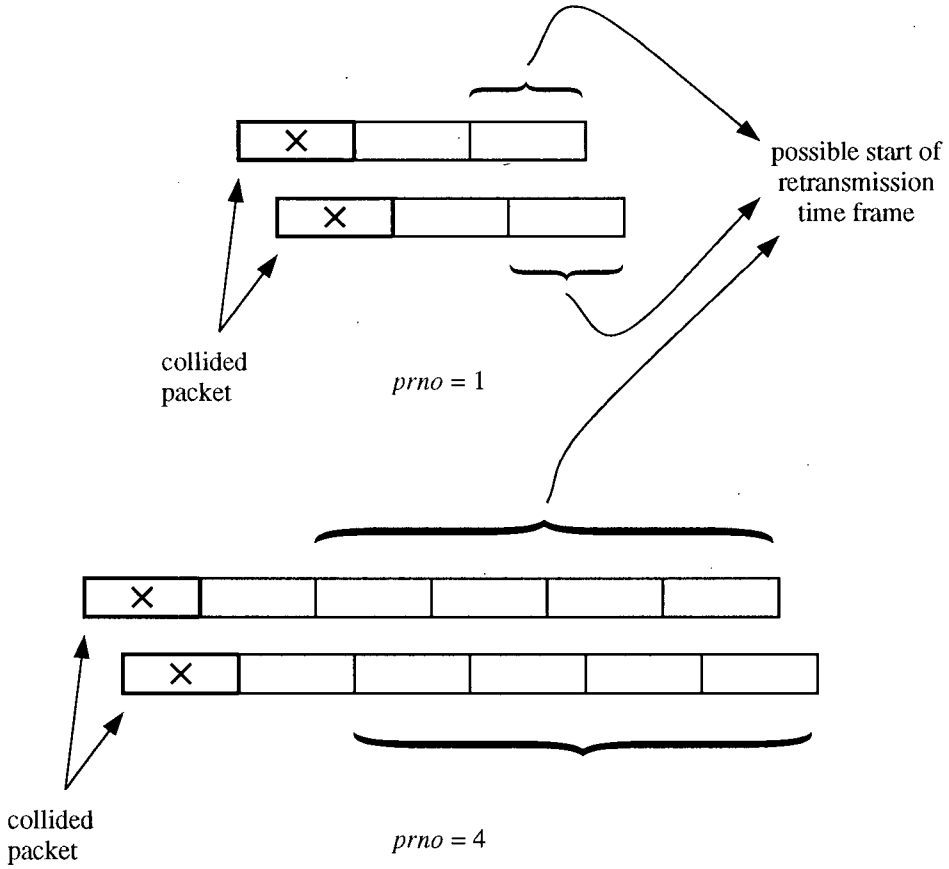

Figure 3.6 Random Backoff, *prno* = {1, 4}

To explain the usefulness of *prno* we first contrast two values of random backoff for *prno* = {1, 4}. By substituting *prno* = 1 into equation (3.13), we get a maximum *delay* = 2 packet lengths and likewise for *prno* = 4, the maximum *delay* = 5 packet lengths. With *prno* = 1, the *delay* or start of retransmission is bounded between 1 to 2 packet lengths after the collision and we have a situation in figure 3.6. After two packets have collided, the start of retransmission of the two packets may take place anywhere inside the bracket. The larger the value of *prno* is, the less likely the same two stations' retransmissions will overlap again.

Figure 3.6 shows that a subsequent collision between the same two stations is more likely when *prno* = 1 than when *prno* = 4. Thus, larger *prno* have the effect of smoothing out the retransmissions over the 1+*prno* packet length duration. Although a large *prno* value may avoid most of the repeated collisions, it will cause the system to experience longer delays.

3.4 Performance Evaluation Criteria and Modeling Parameters

The definitions of the performance measure parameters and other simulation parameters are presented in this section. The ranges of their values are tabulated for references.

3.4.1 Throughput, Channel Traffic and Delay

Throughput is defined as the ratio of the time spent in transmissions of successfully received packets to the maximum time available for transmissions. From figure 3.7, the duration in transmitting a packet is t_s and the maximum time for transmissions is T. Therefore, if one successful transmission occurs over this time interval, the normalized throughput S is given by :

$$S = \frac{t_s}{T} \tag{3.14}$$

and similarly, the normalized channel traffic G is given by :

$$G = \frac{4 \times t_s}{T} \tag{3.15}$$

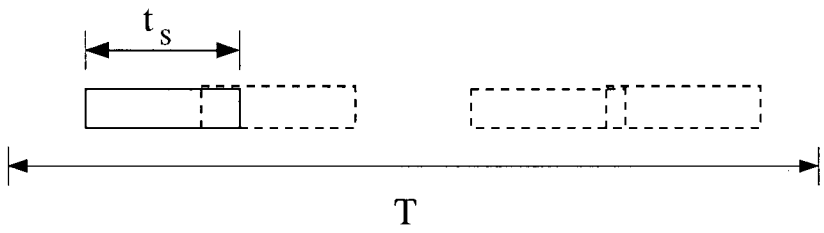

Figure 3.7 Definition of S and G

Normalized delay is another measure of the system's performance. The delay of interest here is the average time delay experienced by all stations for uplink transmissions. It is

defined as the time between the arrival of a new packet and the acknowledgment on successful reception at the RB. The delay consists of the following components.

1. Waiting delay. When a new packet arrives a terminal and needs to backoff due to the channel being sensed busy.
2. Propagation delay. The time elapsed between the beginning of transmission of the first data bit and the arrival of the first data bit at the receiver.
3. Retransmission delay. If a packet is collided or lost, the transmitter will backoff and reschedule another transmission later in time. This backoff period is considered as the retransmission delay.
4. Reception delay. The time to receive a data packet or an acknowledgment packet, from the arrival of the first bit at the receiver.

Upon completion of the simulation, each station has accumulated its own delay statistics for uplink transmissions. The time delay is calculated by averaging the delay experienced by the N stations and by normalizing it with respect to the packet length.

3.4.2 Normalized Arrival Rate

The normalized arrival rate, λ, is an input parameter that controls the generation of new packets at an idle terminal. With a given λ and the assumption of Poisson arrivals, the interarrival time of the packets can be expressed as :

$$average\ interarrival\ time = \frac{1}{\lambda} \tag{3.16}$$

This interarrival time determines how often an idle terminal generates a packet. Then the combination of λ, *THSNR* and retransmission determine the actual traffic on the channel.

RBs do not generate new packets themselves. Downlink packets transmitting from the RBs depend on the number of successful uplink packets. Thus the average arrival rate for the RBs λ_{RB} is :

$$\lambda_{RB} = \frac{S_{uplink}}{Number\ of\ RB} \tag{3.17}$$

3.4.3 Simulation Parameters

The following two tables summarize the fixed and variable parameters in the simulations. The parameters in table 3.2 are fixed to maintain a consistent system for comparison. The variable parameters in table 3.3 are the subject of investigation.

Table 3.2 Fixed parameters in simulation

Fixed Parameters	Explanations	Value used
SNratio	Signal to noise ratio for power control method	10 dB
RBTH	RB capture threshold	10 dB
chip rate	chip rate of spreading code	50 Mchips/s
PG	Processing gain	255
oddM	Odd autocorrelation	25
bit	Number of bits in a packet	1024
ackbit	Number of bits in an ack packet	128
t_s	packet duration	5.2224 ms
rfactor	Wall reflection factor	1.0
β	Power attenuation factor	4
END.TIME	Simulation time	100 s

Table 3.3 Variable parameters in simulation

Parameters	Explanations	Range
RB	Number of RBs	1 - 5
THSNR	Carrier sensing threshold	8, 10, 12, 14, 18 dB
Method	Power control method	Fixed or Adjusted
Scheme	Capture scheme	Power or Time
mdatatime	Capture guard time	2, 4, 6
prno	Random backoff time	5, 9, 13
N	Network size	49, 81, 100
room dimension	Room dimension	40, 60, 80 m^2

Chapter 4
Performance Analysis of Uplink Multiple Access

The reason for investigating only the uplink part of the system is that some WLANs utilize different channels for uplink/downlink traffic. For that situation, the analysis on uplink traffic will be applicable. The uplink transmissions employ multiple access and the downlink transmissions employ broadcasting.

4.1 CSMA Protocol for Uplink

The 1–persistent CSMA protocol is chosen for the uplink multiple access channel. As illustrated in figure 4.1, the protocol operates as follows :

1. When a terminal has a packet ready to transmit, it senses the state of the channel. If the channel is idle, the packet is transmitted.
2. Otherwise the terminal persists to sense the state of the channel and transmits the packet with probability 1 once the channel is sensed idle.

Ideally, 1–persistent CSMA does not let the channel become idle whenever there is a terminal with a packet to transmit. However, when two or more terminals become ready during a transmission period of some other terminals, they wait for the channel to become idle (at the end of the transmission period) and then they all transmit with probability one and cause a collision.

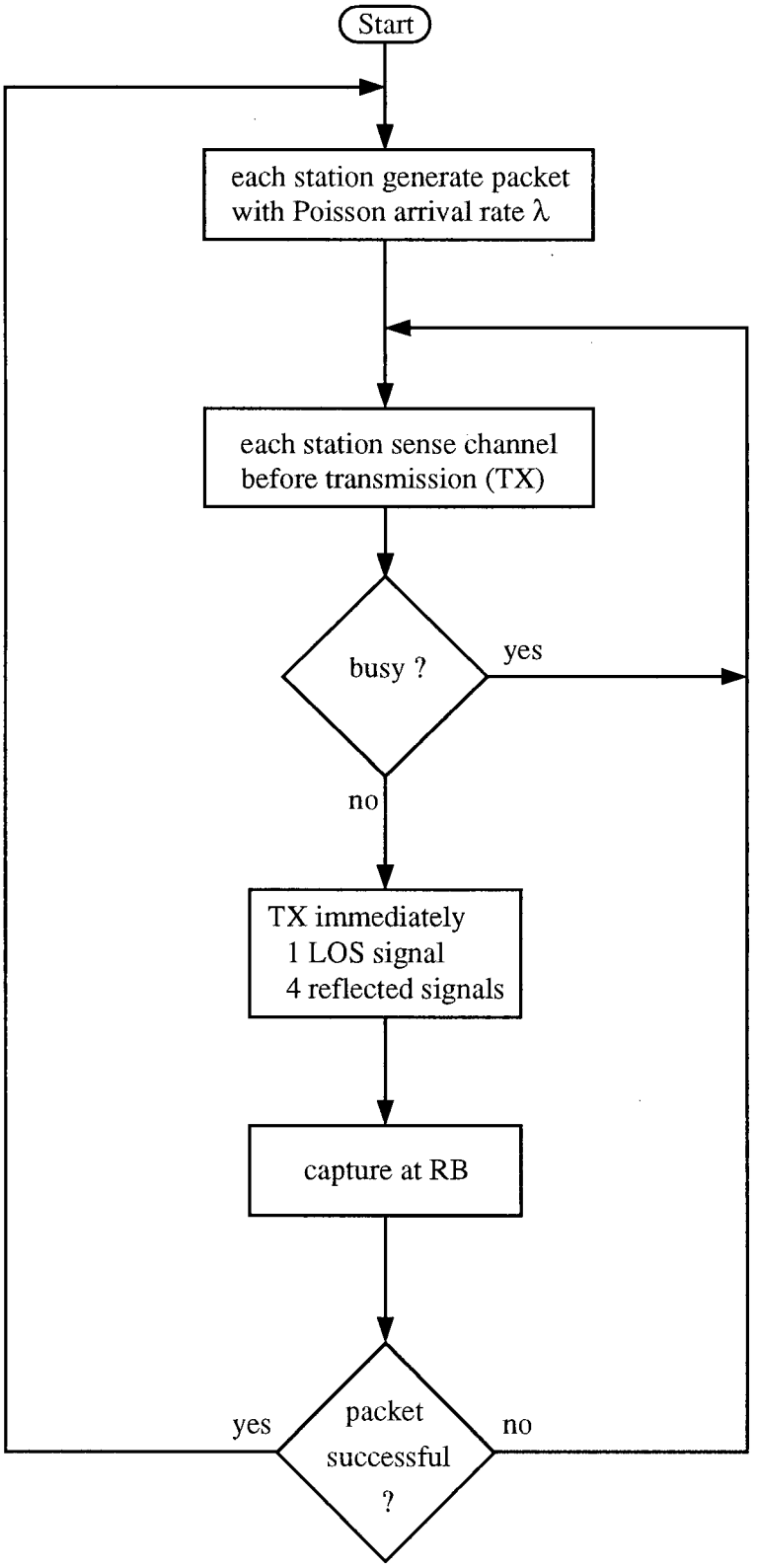

Figure 4.1 1–persistent CSMA protocol flowchart

4.2 Modeling Assumptions

The assumptions for the uplink only model are the same as those described in chapter 3.2.4 with the following exceptions :

1. The backoff delay is :

$$delay = (1 + prno \times random.no) \times max.propagation.length \tag{4.1}$$

   The backoff is a multiple of the maximum propagation delay rather than a multiple of the packet length in equation (3.13). This small delay allows us to model the continuous monitoring nature of the 1–persistent CSMA protocol.

2. It is assumed that on the reverse channel the acknowledgment received is immediate and without error.

3. *SNratio* in section 3.4.3 was defined as a fixed parameter. However, we consider a scenario using a higher *SNratio* to evaluate its effects in this chapter. We expect to see a higher S for the system employing the AP method.

4.3 Results and Discussion

4.3.1 Effects of Number of RBs

The result of S-vs.-λ with different number of RBs is depicted in figure 4.2. This result is generated with *THSNR* = 18 dB, FP method and PC scheme. The maximum achievable throughput aggregated over all terminals with different number of RBs in this figure are summarized in table 4.4.

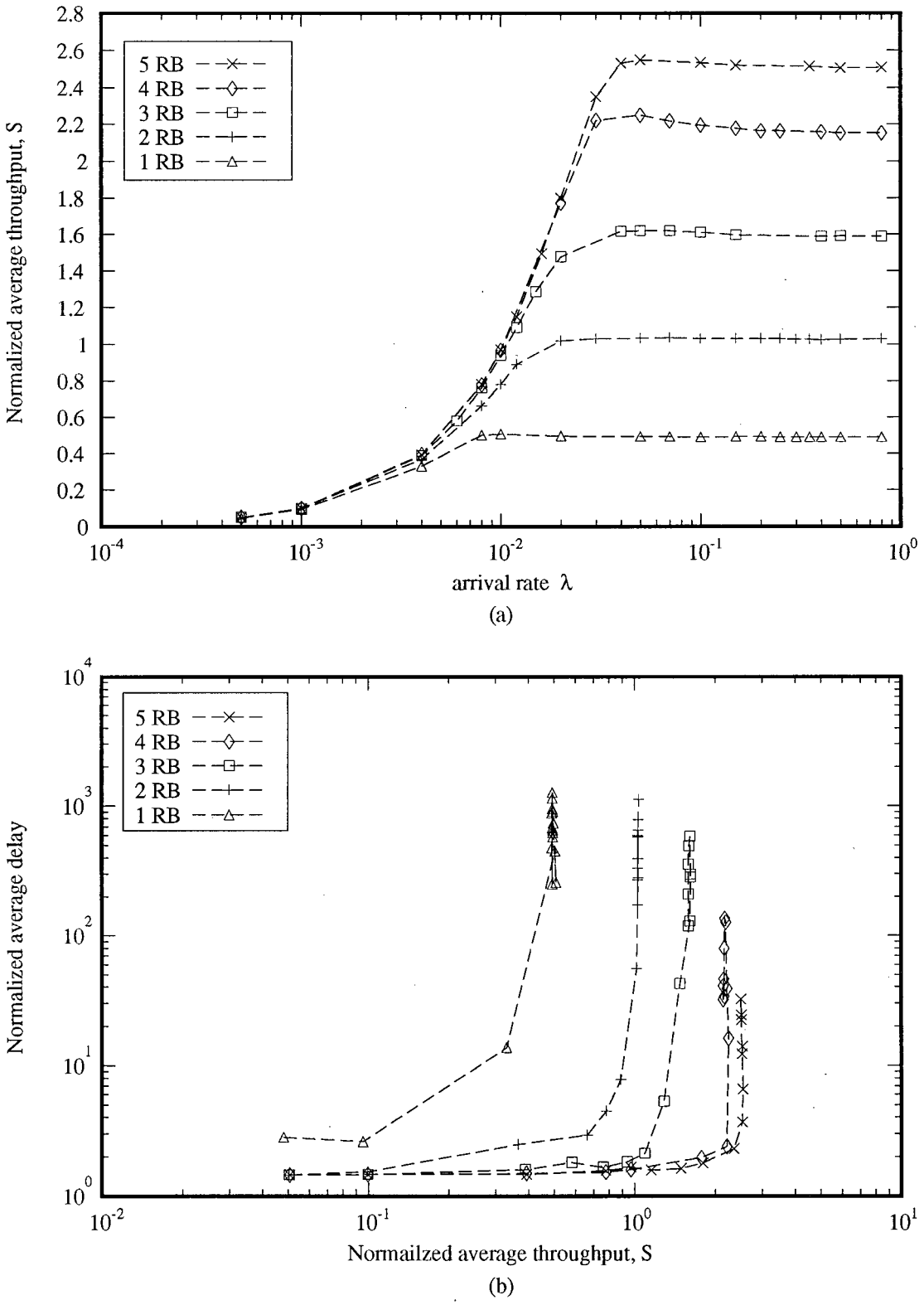

Figure 4.2 Uplink performance for different λ with FP, PC, *THSNR* = 18 dB and RB = {1–5}

Table 4.4 Maximum S for different number of RBs with $THSNR$ = 18 dB, FP, PC

Number of RBs	Max S	λ at max S
1	0.50908	0.008
2	1.03612	0.02
3	1.62169	0.04
4	2.25067	0.05
5	2.54887	0.05

With the maximum throughput obtained above, it is also desirable to examine the fairness of the system. In fact, a high throughput in figure 4.2a does not imply that every station can achieve the same throughput. Figure 4.3 shows the capturing probability, Pr_C, of each station inside the room. Pr_C is the ratio of the number of packets from a terminal successfully captured by the RBs to the total number of packets transmitted from the same terminal. It is obvious that those stations near the RBs have much better access to the RBs than those at the corners or near the walls when the number of RBs in the system is small, i.e. RB = {1, 2}. RB = {3} gives some improvements but the Pr_C is still not acceptable at some locations. It is apparent that RB = {4, 5} give fairer access to the stations. Once the arrival rate has exceeded the λ in table 4.4, the contribution to the throughput in figure 4.2a are mostly coming from the middle stations.

Figure 4.2b shows the delay-vs.-throughput performance of the system. As expected, five RBs give the highest throughput and the least average delay to the system since more packets can be received at one time. There is one phenomenon observed in these plots. At low λ, delay remains small but rising as throughput increases. Once the throughput has reached the maximum, further increase in λ will result in a slight drop in throughput in figure 4.2a but it will not drop down to zero. At this point, the delay-vs.-throughput curve starts to turn upward. From there on, the delays experienced by the stations fluctuate at some large values. This upward turning point is where the system comes into saturation.

This phenomenon is referred as saturation in capacity where the number of transmissions has reached a level that adversely affects the throughput of the channel, i.e. there are too

many interferers resulting in increased ISR at the RBs such that it becomes more difficult to receive a packet successfully.

Figure 4.2a gives the insights of the uplink system. At small value of λ, using multiple RBs does not result in very much difference in throughput because the RBs are capturing the same packet. At large values of λ, the gain in throughput as the number of RBs increases is due to multipacket receptions since more than one packets can be received successfully at different RBs per packet duration. Results shown in figure 4.2a are the combination of *THSNR*, hidden terminals, packet duplication and multiple packet receptions. *THSNR* = 18 dB allows some hidden terminals to exist for each terminal in the system. While the hidden terminals generate some traffic which interfere with the original terminal's transmission, they may contribute to the system throughput through multipacket receptions.

Although higher number of multipacket receptions can be achieved with more RBs, it does not necessary give an equal proportion of increase in S. When the number of RBs is increased from 4 to 5, less gain in S is obtained. This is due to the fact that when RBs become too close together, duplicated packets occur more easily.

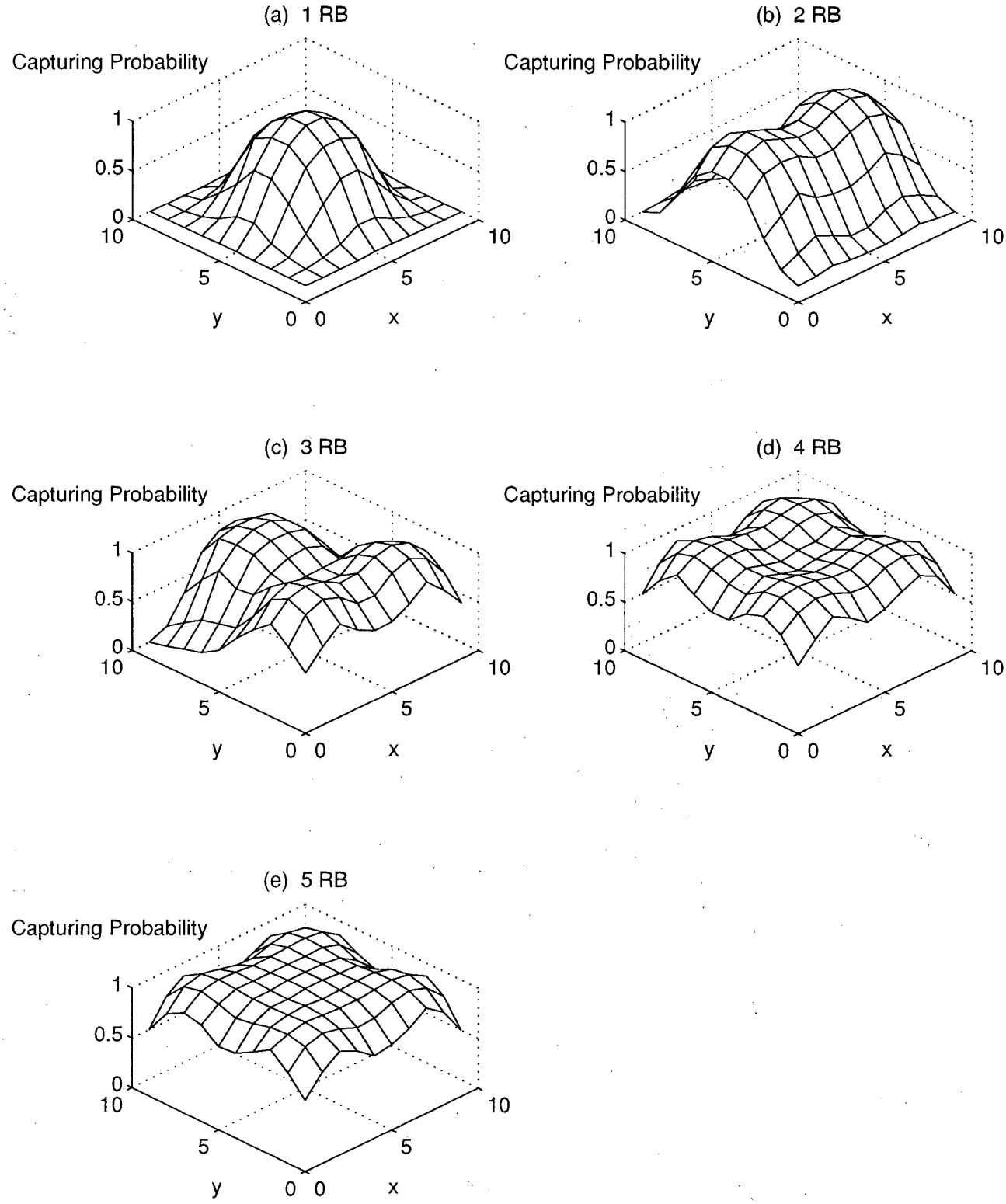

Figure 4.3 Capturing probability of stations with FP, PC, *THSNR* = 18 dB, λ = 0.02

4.3.2 Effects of Other Parameter Variations

Throughout tables 4.5 to 4.8, a name is given to each set of simulation parameters to facilitate the discussion when a particular set of parameters is referred to. From table 4.5 and 4.6, the PC scheme has a better throughput than the TC scheme in the FP method. From table 4.7 and 4.8, the PC scheme again has higher throughput than the TC scheme in the AP method. The AP method has higher maximum S than the FP method, except in FP6 and AP6.

Table 4.5 Maximum throughput with 5 RBs, FP method

	PC Scheme	TC Scheme
12 dB	FP1 : 2.410	FP2 : 1.601
14 dB	FP3 : 2.477	FP4 : 1.560
18 dB	FP5 : 2.540	FP6 : 1.391

Table 4.6 Maximum throughput with 5 RBs, FP, variation in some other parameters

	PC scheme	TC scheme
prno = 50	FP7 : 2.519	FP8 : 1.670
RBTH = 8 dB	FP9 : 2.410	FP10 : 1.312
SNratio = 12 dB	FP11 : 2.410	FP12 : 1.601

Table 4.7 Maximum throughput with 5 RBs, AP method

	PC scheme	TC scheme
12 dB	AP1 : 2.580	AP2 : 1.694
14 dB	AP3 : 2.620	AP4 : 1.517
18 dB	AP5 : 2.618	AP6 : 1.205

Table 4.8 Maximum throughput with 5 RBs, AP, variation in some other parameters

	PC scheme	TC scheme
prno = 50	AP7 : 2.703	AP8 : 1.816
RBTH = 8 dB	AP9 : 2.605	AP10 : 1.455
SNratio = 12 dB	AP11 : 2.608	AP12 : 1.980

Figures 4.4 and 4.5 depict the capturing probability of each station, using the parameters in tables 4.5 and 4.7, respectively. Going down from the top to bottom in each column of figure 4.4, it is apparent that the capturing probability for the corner stations drop as *THSNR* increases, yet the throughput increases. As more packets are allowed to be transmitted, the RBs have a better chance to capture different packets. When a higher *THSNR* is used in the PC scheme, centre stations have a power advantage over the corner stations. As the PC scheme selects the strongest signal out of all colliding packets, this signal gives a higher SNR and hence has a better chance to be received correctly. Therefore S increases as a result of more successful packets from centre stations and consequently the Pr_C of corner stations drops. See figure 4.4 (a, c, e).

On the other hand, a receiver employing the TC scheme locks onto the first arrival at the RB. Figure 3.1 indicates that a higher *THSNR* means a smaller sensing circle and hence less stations can be detected by the ready-to-send stations. Therefore, the sensing actions of each station do not give accurate information on the state of the channel and hence more hidden terminals exist. If the first arrival is from a corner station, any station that can not detect this corner station's transmission will transmit and interfere with the reception at the RB. Much lower Pr_C at the corners in the second column of figure 4.4 indicates that these stations' performance are adversely affected by the hidden terminals.

All results in table 4.6 use a *THSNR* = 12 dB. Thus the comparisons made in this paragraph are between table 4.5, *THSNR* = 12 dB and table 4.6. A longer random backoff *prno* improves the maximum S. The *RBTH* is used only in the TC scheme and thus there is no difference in S. A lower *RBTH* does not improve the Pr_C at all since a lower *RBTH* actually allows a RB to lock onto a weaker packet with a lower chance of correct reception. If *RBTH* is higher than *SNratio*, then some stations may not have linkage to more than one RBs, which is not desirable in the distributed system. The use of higher power for FP method does not seem to affect the maximum S.

The capturing probabilities using the AP method are shown in figure 4.5. As *THSNR* increases, an overall reduction in Pr_C is seen. However, the Pr_C of the corner station and its neighbours are similar. This shows the AP method can give far away stations fair access to

the channel. The improvement on fair channel access is particular pronounced when figures 4.4 (b, d, f) are compared with figures 4.5 (b, d, f).

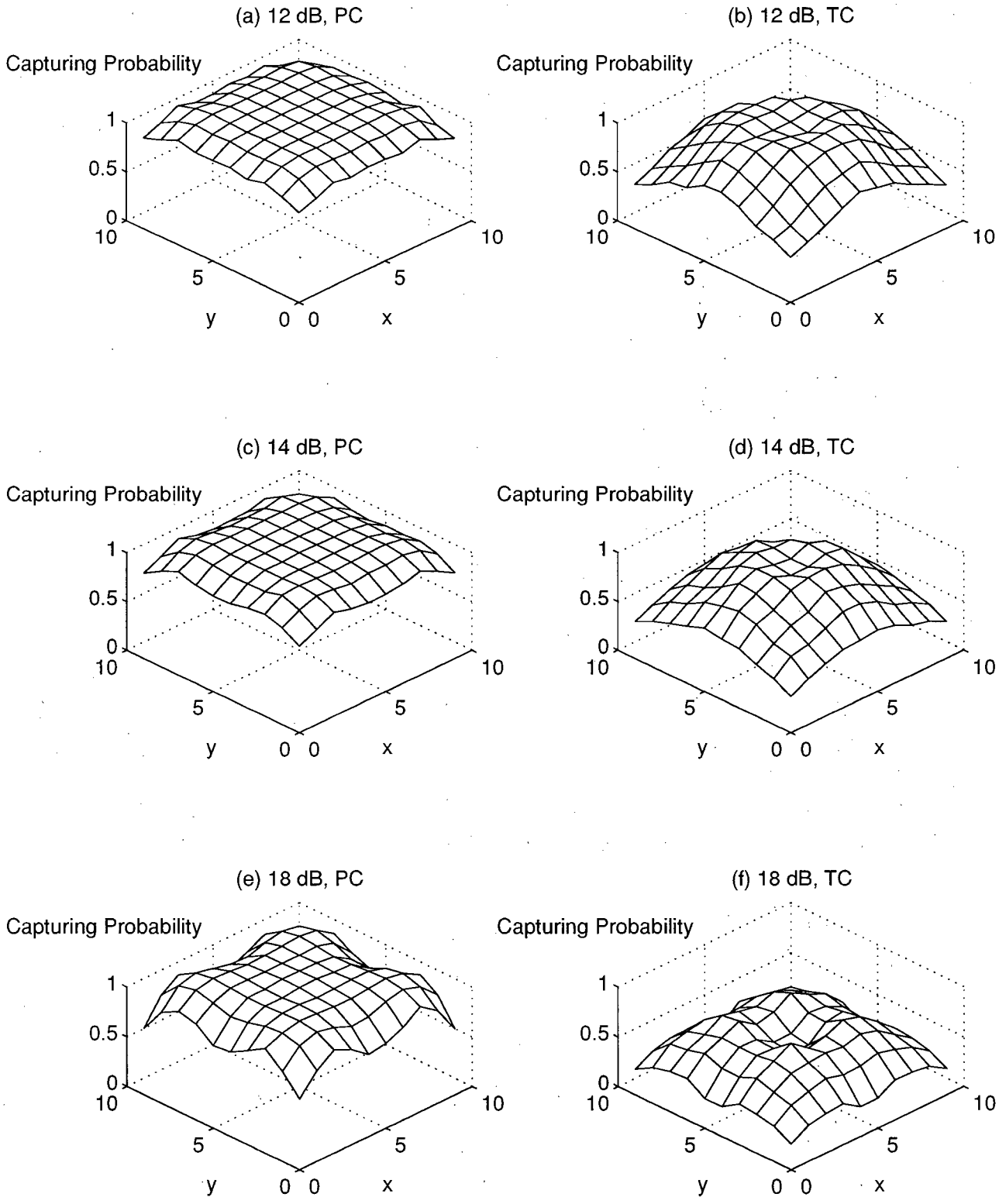

Figure 4.4 Capturing probability of each station for system parameters in table 4.5, 5 RBs, $\lambda = 0.02$

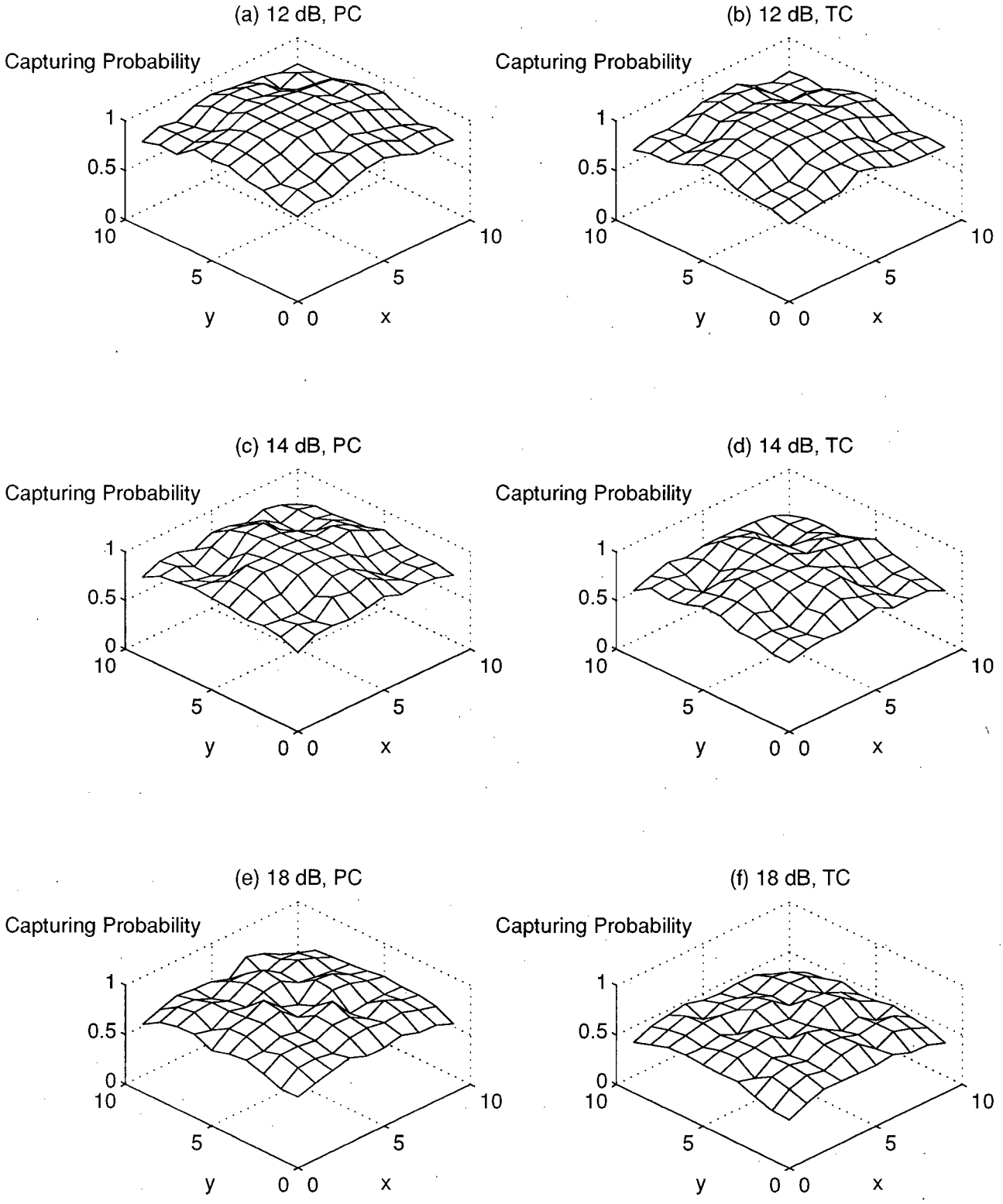

Figure 4.5 Capturing probability of each station for system parameters in table 4.7, 5 RBs, $\lambda = 0.02$

Based on the S-vs.-λ and delay-vs.-λ results in figures 4.6 to 4.9, table 4.9 summarizes the effects of varying the parameters on the system's throughput. It tabulates qualitatively the changes in throughput when a parameter is changed.

Table 4.9 Uplink throughput comparison

Variation of parameter	Power control method	PC scheme	TC scheme
Increase *THSNR*	FP	Improved	Worsen
	AP	Improved	Worsen
Increase *prno*	FP	Improved	Improved
	AP	Improved	Improved
Decrease *RBTH*	FP	N/A	Worsen
	AP	N/A	Worsen
Increase *SNratio*	FP	No effect	No effect
	AP	Improved/Worsen	Improved/Worsen

In figure 4.6, varying *THSNR* has different effects on the throughput using the two capture schemes. In the PC scheme, higher *THSNR* gives higher S while higher *THSNR* gives lower S in the TC scheme. Since the PC scheme selects the higher SNR packet to capture, a higher *THSNR* allows more packets into the channel and the RBs select the best signals. On the other hand, the TC scheme in figure 4.6c selects the first arrival, which may not be the strongest signal. Note that the almost identical S at low values of λ are due to packet duplications.

In figure 4.7a, a high *prno* improves S since collisions are reduced. A higher *SNratio* in FP method has no effect on the system throughput. Lowering *RBTH* decreases S significantly since the chance of success is lower.

An increase in *THSNR* from 12 dB to 14 dB in figure 4.8 actually causes the average S to rise. However, further increase to *THSNR* = 18 dB results in a drop in S because there are too many packets in the channel causing collisions. The gain in S from *THSNR* = 12 dB to 14 dB is due to multipacket receptions as the AP method allows more packets into the channel.

The *prno* value in figure 4.9 improves S compared to figure 4.8 for the respective capture scheme. *SNratio* = 12 dB improves the maximum throughput performance at some moderate

values of λ but degrades the S at high values of λ. This is due to higher interference from the other packets. Lowering *RBTH* in figure 4.9c results in lower S.

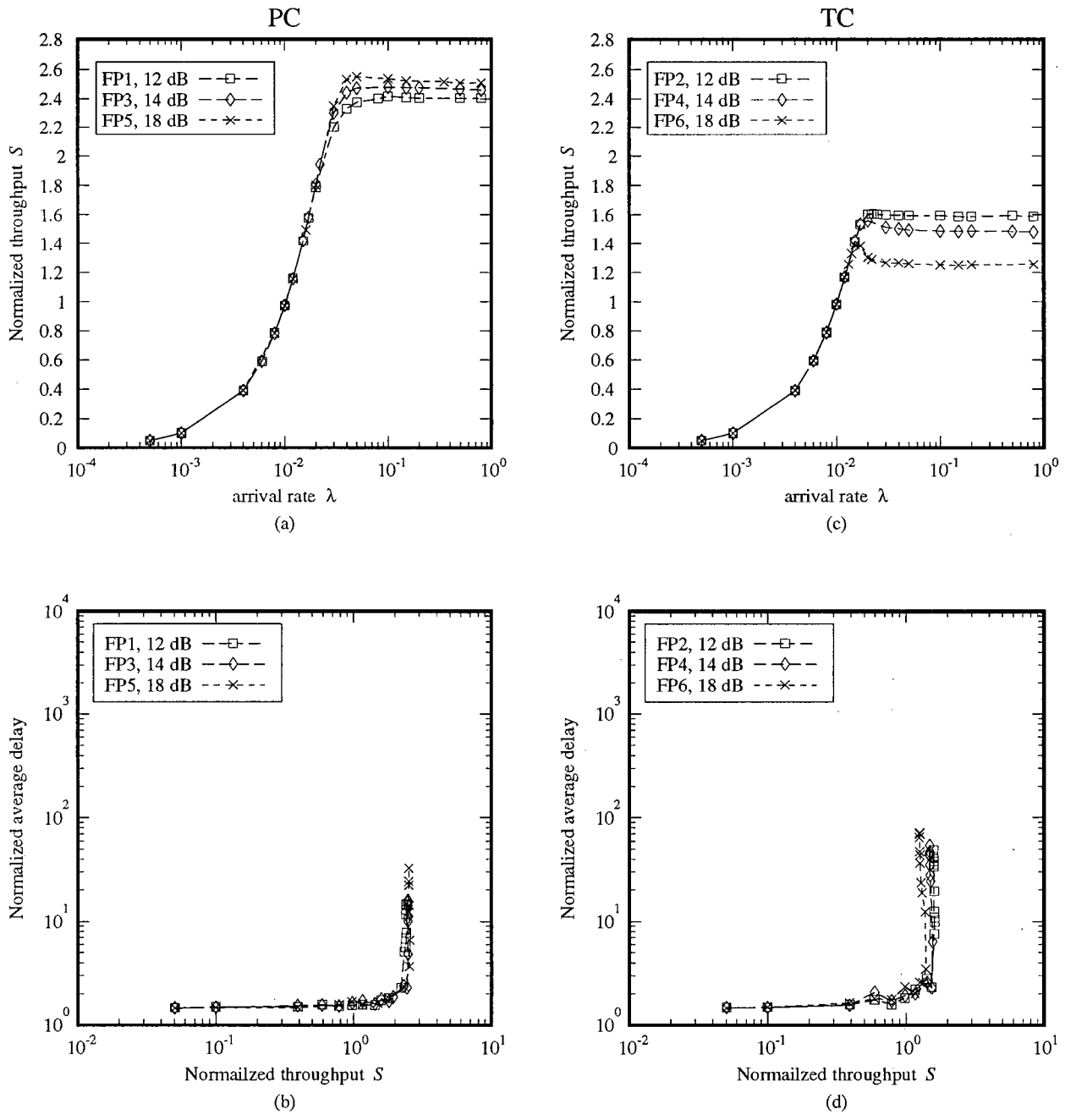

Figure 4.6 Throughput and delay for system parameters in table 4.5, 5 RBs

From the results shown in this chapter, the selection of the number of RBs and *THSNR* is crucial to the system performance. Increasing the number of RBs will increase the throughput.

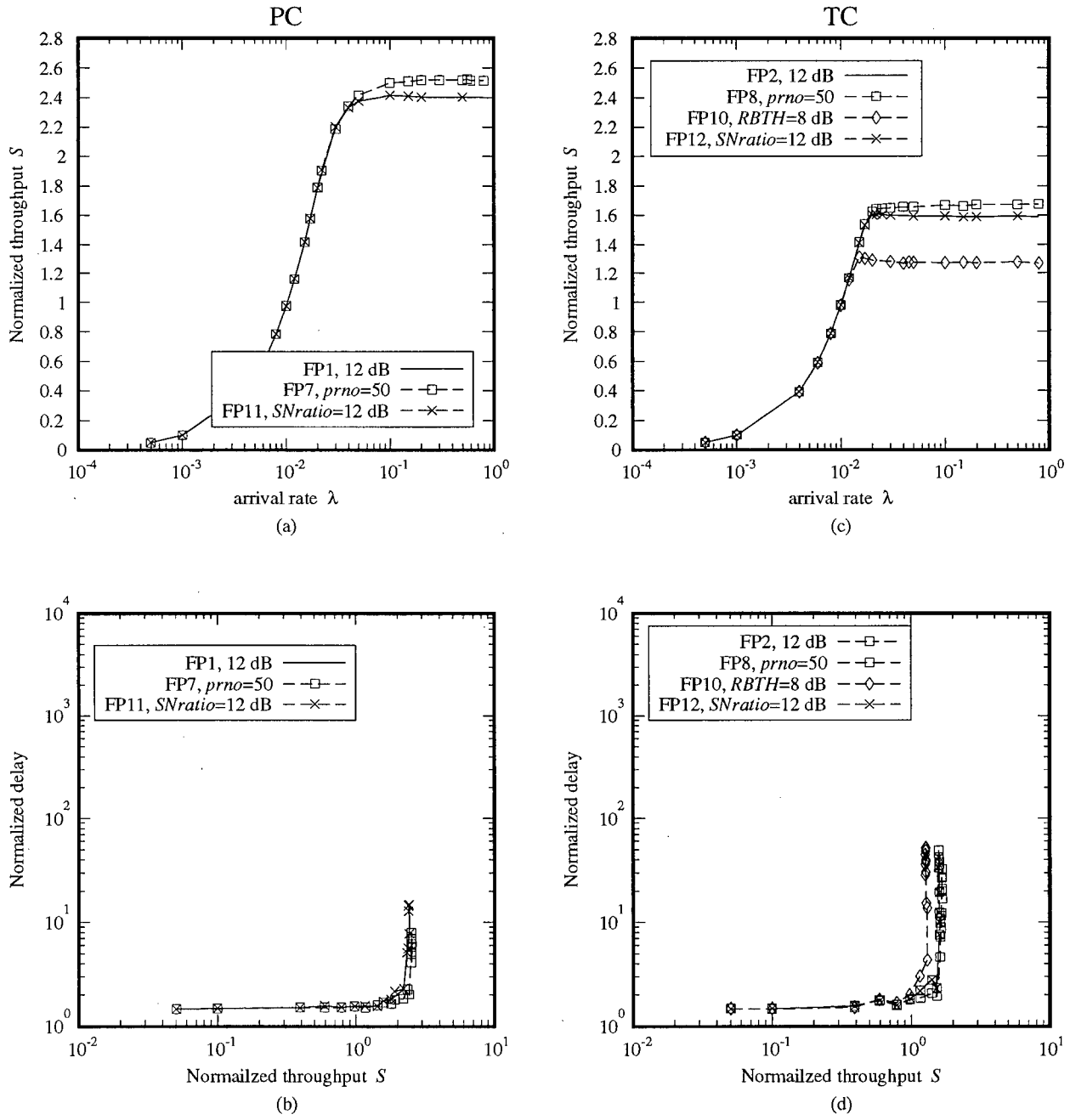

Figure 4.7 Throughput and delay for system parameters in table 4.6, 5 RBs

Increasing *THSNR* will increase the throughput, provided that the channel is not saturated, so that multiple packet receptions can occur. A larger *prno* = 50 improves the throughput for all the cases shown. Using a *RBTH* with a lower value than *SNratio* is not advisable. It only causes a RB to lock onto a weaker packet. A higher *SNratio* has no effect on *S* with the FP method but it gives a higher maximum *S* with the AP method.

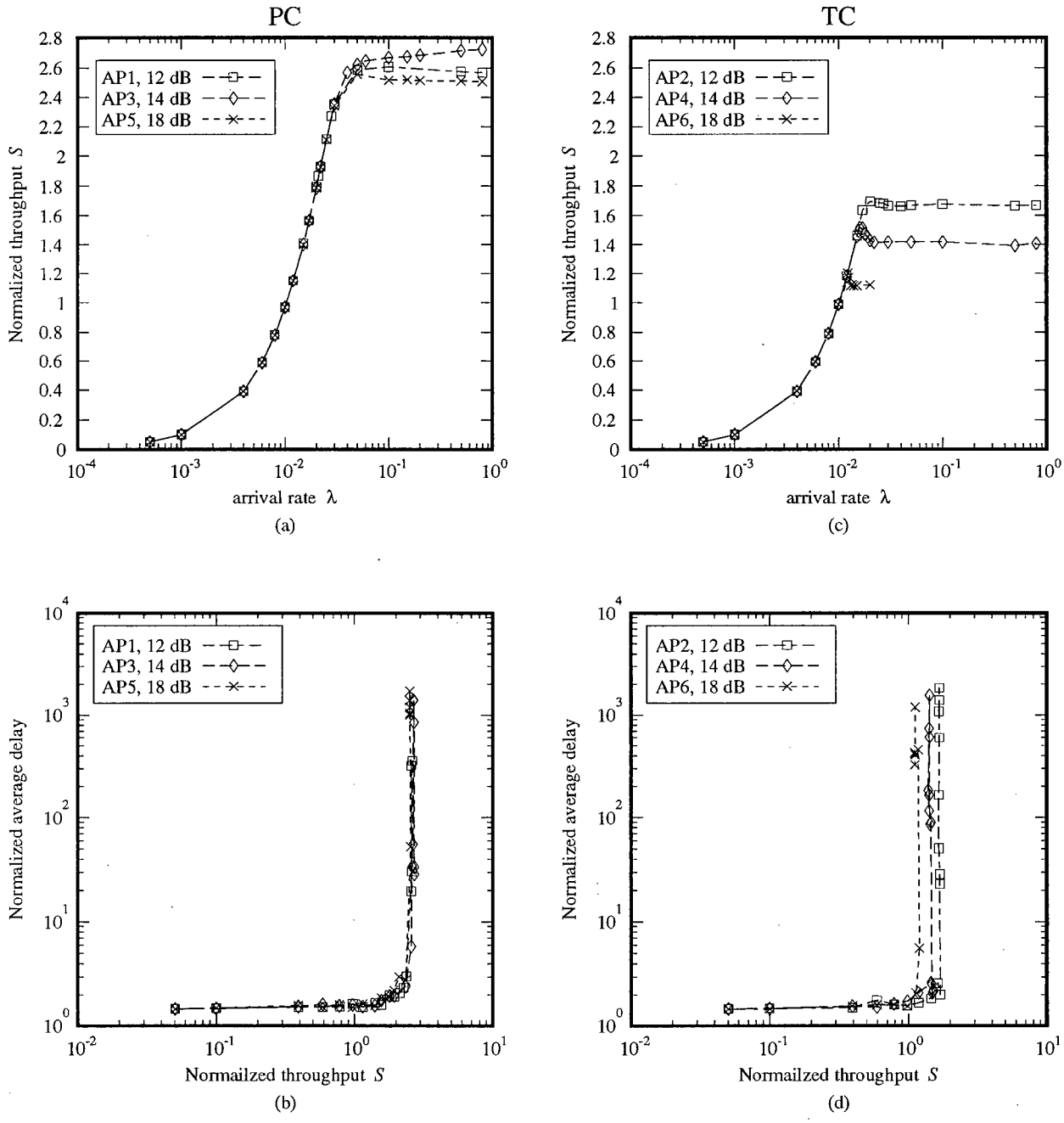

Figure 4.8 Throughput and delay for system parameters in table 4.7, 5 RBs

Among the power control methods and capture schemes, it seems that the AP method, which gives a fair chance of channel access to terminals, and the PC scheme, which improves S in various comparisons, are preferred for the uplink multiple access.

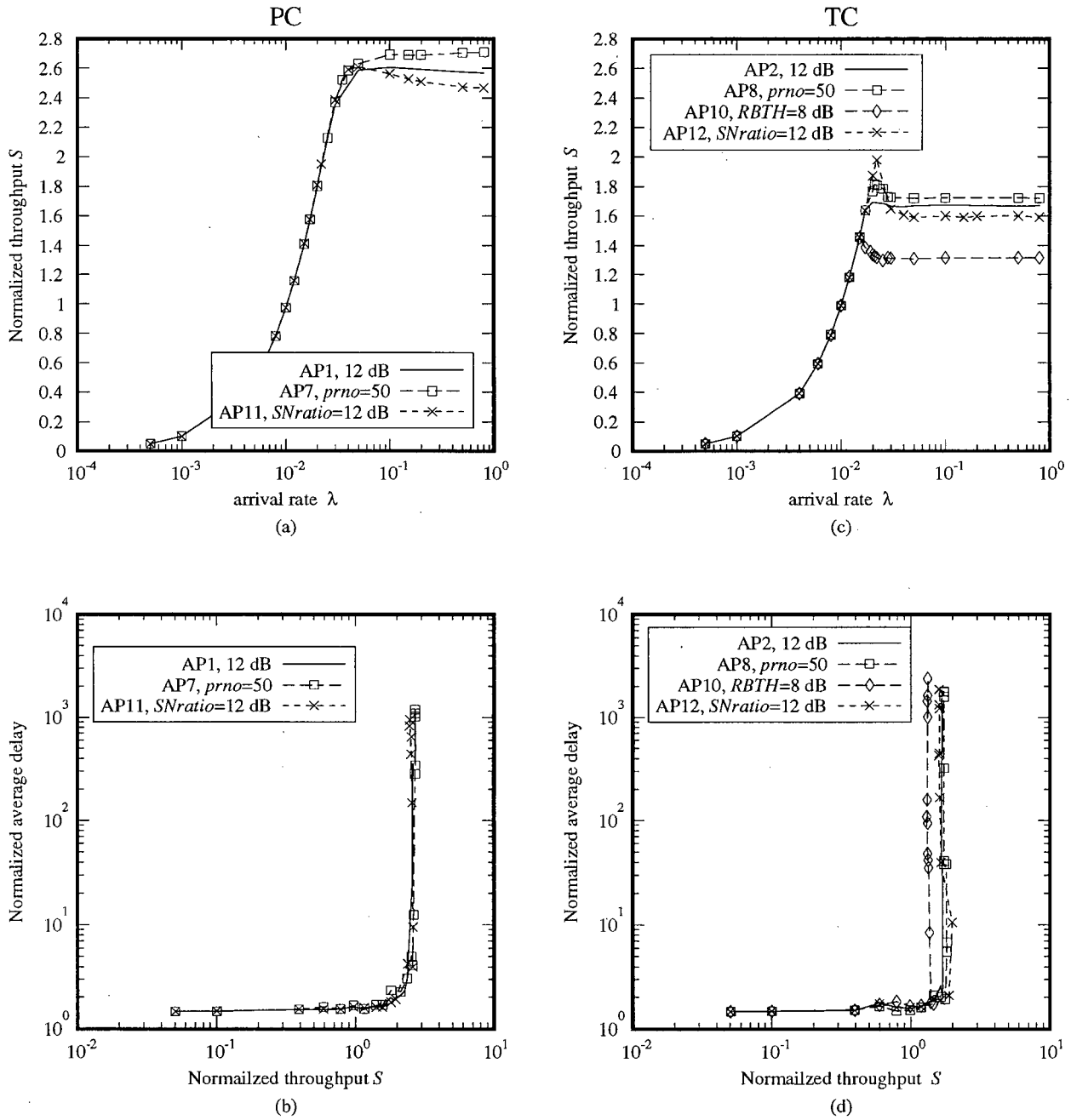

Figure 4.9 Throughput and delay for system parameters in table 4.8, 5 RBs

Chapter 5
Performance Analysis of Uplink and Downlink Sharing a Common Multiple Access Channel

Some WLANs use a common channel for both uplink and downlink traffic in order to gain the advantage of having maximum bandwidth available to the channel. Particularly in SS systems, a higher bandwidth means a higher *PG* can be used in the system, which enables better system performance. The performance of the uplink/downlink CSMA protocol is studied relative to different variable parameters in table 3.3.

5.1 Uplink/Downlink Protocol

In this section, the problem of 1–persistent CSMA being employed in an uplink/downlink system is presented, and a dual persistency CSMA protocol is presented as the solution to this problem.

5.1.1 Problem of 1–persistent CSMA

In a WLAN with separate channels for its uplink and downlink traffic, the downlink traffic does not suffer any interference from the uplink. However, in a WLAN sharing a common channel between the uplink and downlink, the downlink traffic is subject to the same multiple access interference as the uplink. Thus when the 1–persistent CSMA protocol is used in a system with both uplink/downlink traffic using a common channel, the downlink traffic has much less throughput than the uplink traffic. Ideally, every successful packet transmission in the uplink should be balanced by a successful packet transmission in the downlink. In the distributed WLAN, there are 100 stations and the number of RBs may vary from 1 to 5. However, with more terminals than the RBs competing for channel access, RBs' downlink transmissions are usually backlogged by a busy channel due to the vast amount of uplink traffic. The results of uneven channel access for $THSNR$ = 12 dB using five, two, and one

RBs are shown in figures 5.1 to 5.3. These results are based on a 1–persistent CSMA model for both uplink and downlink traffic. Other default values are shown in tables 3.2 and 3.3.

From figure 5.1, we can see in region A that the uplink and downlink throughput curves follow each other closely at low channel traffic, and throughput increases with total channel traffic. In region B, the two throughput curves start to diverge, and the uplink throughput continues to rise at a faster rate than downlink throughput. This happens when more stations are sending packets to the RBs and the RBs start to have less access to the channel. While the channel traffic, as well as the uplink throughput, continues to rise further in region C, the downlink throughput drops. This is the region in which the RBs have difficulty sensing the channel idle, which prevents their transmissions. Eventually, the traffic becomes so high in region D that the throughput of both uplink and downlink drop due to severe multiuser interference.

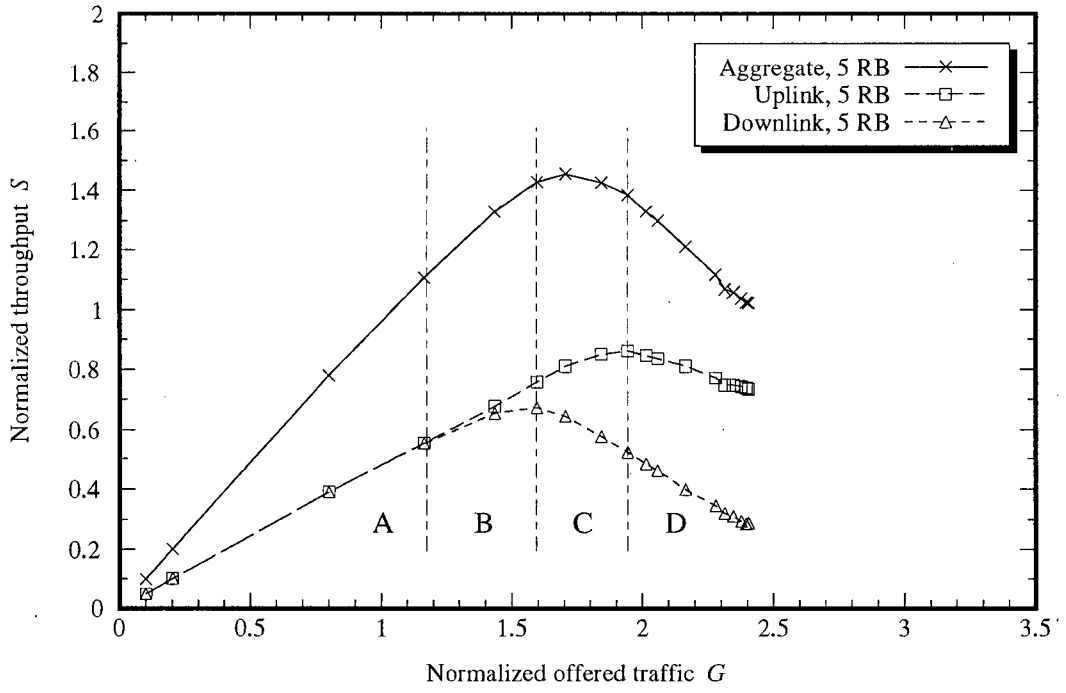

Figure 5.1 Aggregate, uplink and downlink throughput for 5 RBs, *THSNR* = 12 dB, *prno* = 9

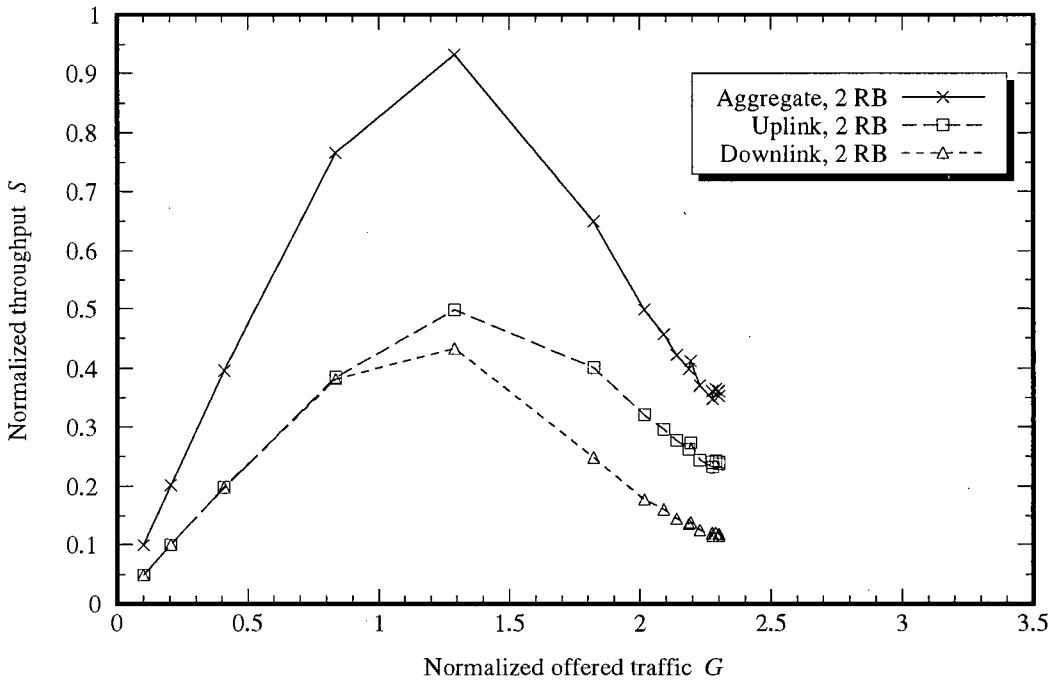

Figure 5.2 Aggregate, uplink and downlink throughput for 2 RBs, *THSNR* = 12 dB, *prno* = 9

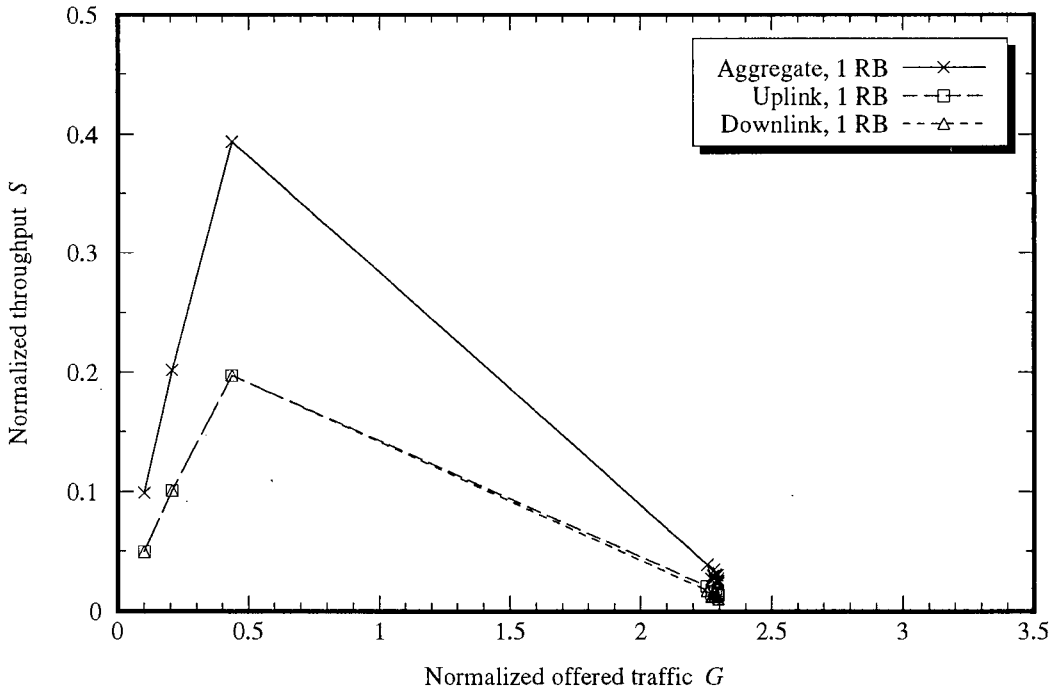

Figure 5.3 Aggregate, uplink and downlink throughput for 1 RB, *THSNR* = 12 dB, *prno* = 9

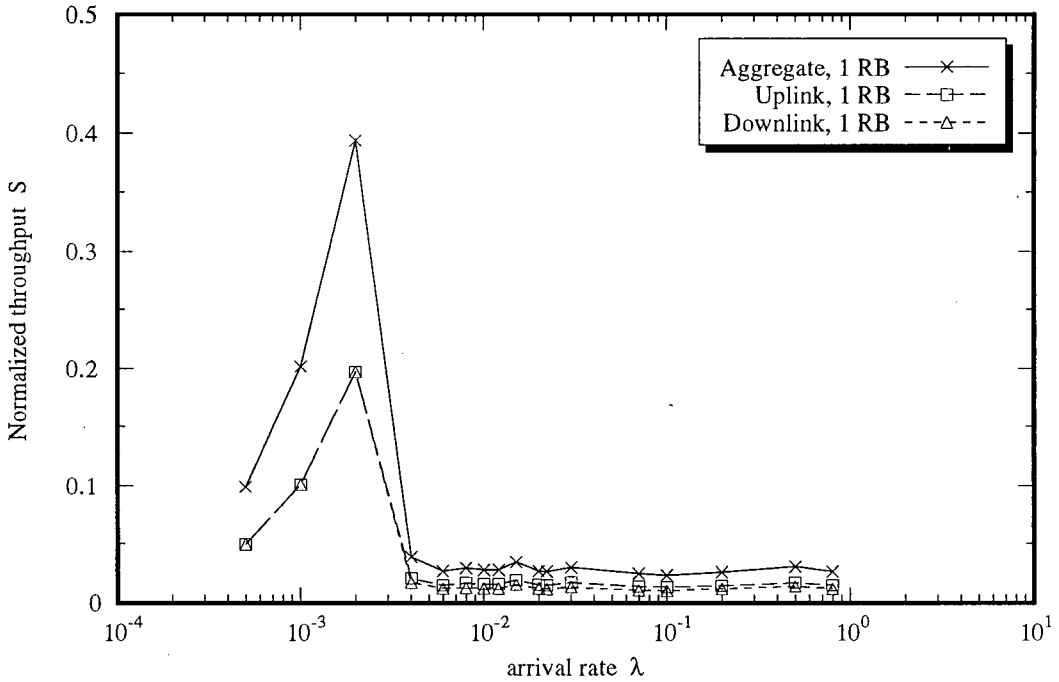

Figure 5.4 Aggregate, uplink and downlink throughput
for 1 RB, S-vs.-λ, $THSNR$ = 12 dB, $prno$ = 9

Although the four regions are not drawn in figures 5.2 and 5.3, and some of the regions are too small to visualize, the same argument still applies. If fewer RBs are used, the throughput becomes worse. In the 1 RB case, once G has exceeded 0.5 the throughput approaches zero. This is more obvious in figure 5.4, where the throughput, S, versus arrival rate, λ, is plotted. Figures 5.3 and 5.4 come from the same set of simulation results but they are plotted with different parameters on the abscissa.

5.1.2 Dual Persistency CSMA Solution

The uneven channel access for the downlink traffic is solved by a dual persistency CSMA protocol. This protocol is useful when the number of stations and RBs accessing the uplink and downlink differ by several times. In our model, the ratios range from 100 terminals : 1 RB to 49 terminals : 5 RBs. The protocol utilizes two different types of access persistency for the CSMA. For the uplink, where a large number of terminals are competing for channel access, the non-persistent CSMA protocol is employed. For the downlink, where a few

RBs are accessing the channel, the 1–persistent CSMA protocol is used. The non-persistent CSMA protocol operates as follows :

1. When a terminal has a packet ready to transmit, it senses the state of the channel. If the channel is idle, the packet is transmitted.
2. Otherwise, if the channel is sensed busy, the terminal backoffs its transmission to some later time, according to the retransmission delay distribution. At the new point in time, it senses the channel and repeats these steps.

The operation of 1–persistent CSMA for the RBs is the same as the one described in section 4.1. Note the difference between the two types of CSMA mentioned here. In 1–persistent CSMA, a ready terminal, upon sensing the channel busy, continues to monitor the status of the channel until it becomes idle; then the terminal transmits right away. In non-persistent CSMA, a backoff terminal senses the channel only at some time in future and hence the terminal does not persist on transmitting.

An acknowledgment is generated when a station or an RB has successfully received a packet. Figure 5.5 shows the relationships among the terminal, the RB, the uplink/downlink data packets, and the uplink/downlink ack packets. In figure 5.6, a pictorial version of the protocol is shown. A detailed description of the simulation model for the dual persistency CSMA protocol is described in appendix A.

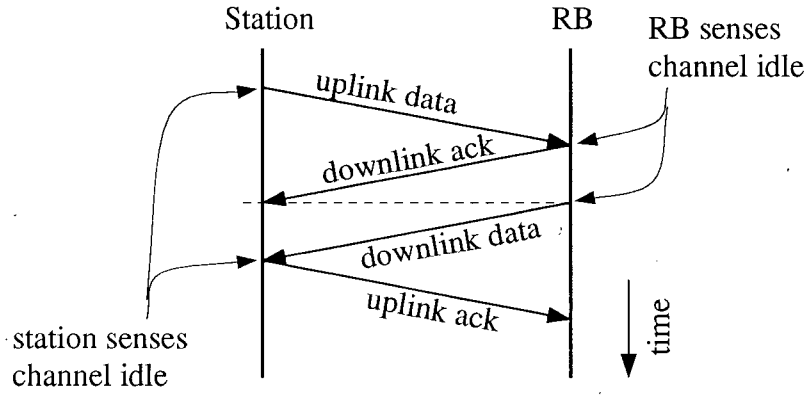

Figure 5.5 Uplink/Downlink data and acknowledgment relationships

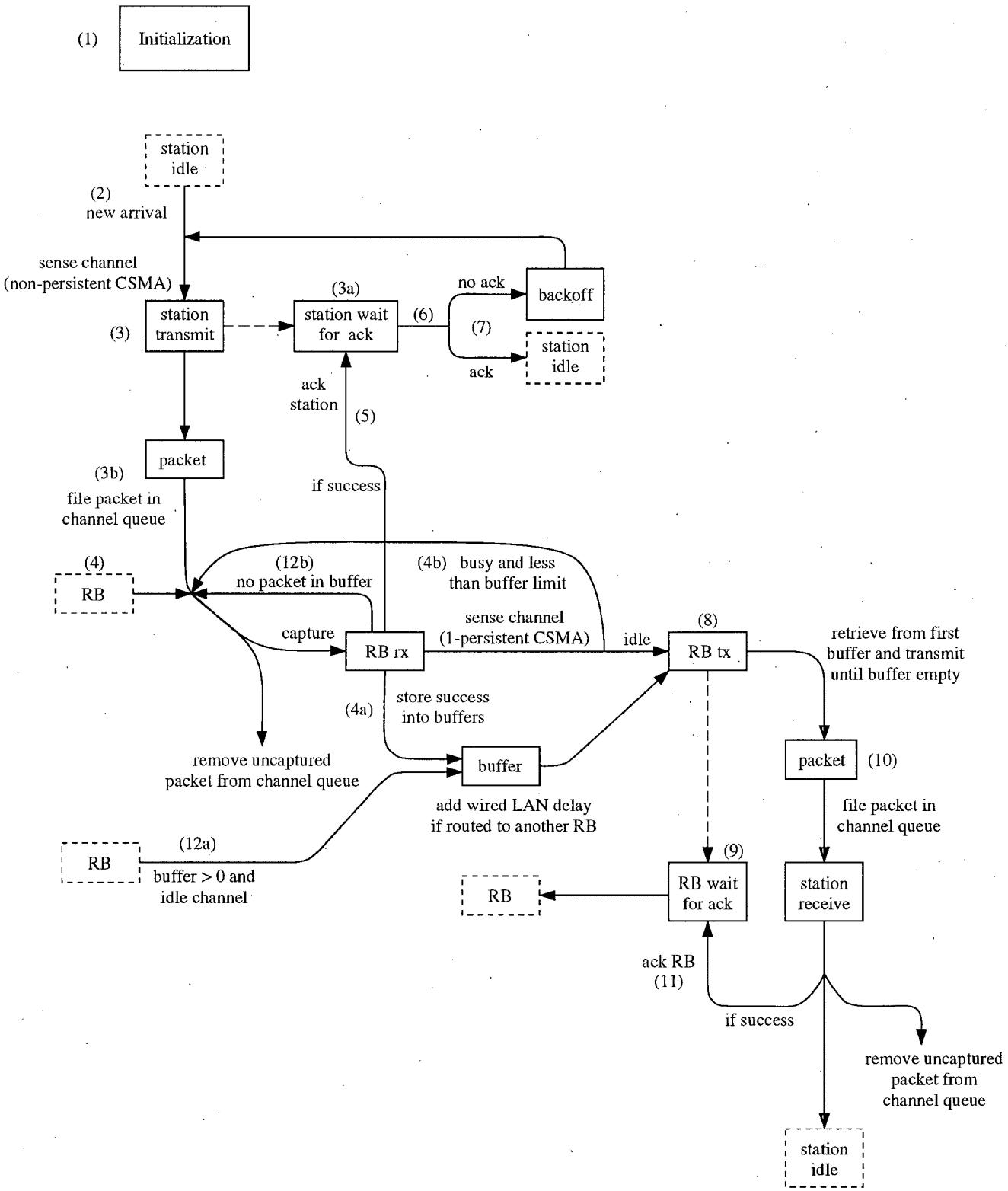

Figure 5.6 WLAN dual persistency CSMA MAC protocol model

5.1.3 Improvement from Dual Persistency CSMA

Figure 5.7 depicts the results of dual persistency CSMA on the uplink and downlink traffic, with FP method, TC scheme, *THSNR* = 12 dB, RB = {1, 2, 3, 4, 5}, and *prno* = 9. Table 5.10 shows the values of aggregate, uplink and downlink throughput with $\lambda = 0.01$ for various numbers of RBs. We can see the throughput on the downlink is improved in such a way that uplink and downlink S are almost equal, with slightly higher uplink throughput than the downlink. However this difference is not noticeable from the graph. Therefore this protocol is shown to balance the amount of uplink and downlink throughput.

Table 5.10 Comparison of aggregate, uplink and downlink throughput of dual persistency CSMA at $\lambda = 0.01$

	S		
Number of RB	Aggregate	Uplink	Downlink
1	0.46962	0.23483	0.23480
2	0.94100	0.47051	0.47049
3	1.10634	0.55337	0.55297
4	1.18703	0.59355	0.59347
5	1.17702	0.58864	0.58838

A balanced throughput is necessary in this common uplink/downlink channel model. Higher uplink throughput than the downlink will cause packets loss at the RBs since the RBs have limited buffers and it is more difficult for the RBs to access the channel to transmit the packets in the buffers.

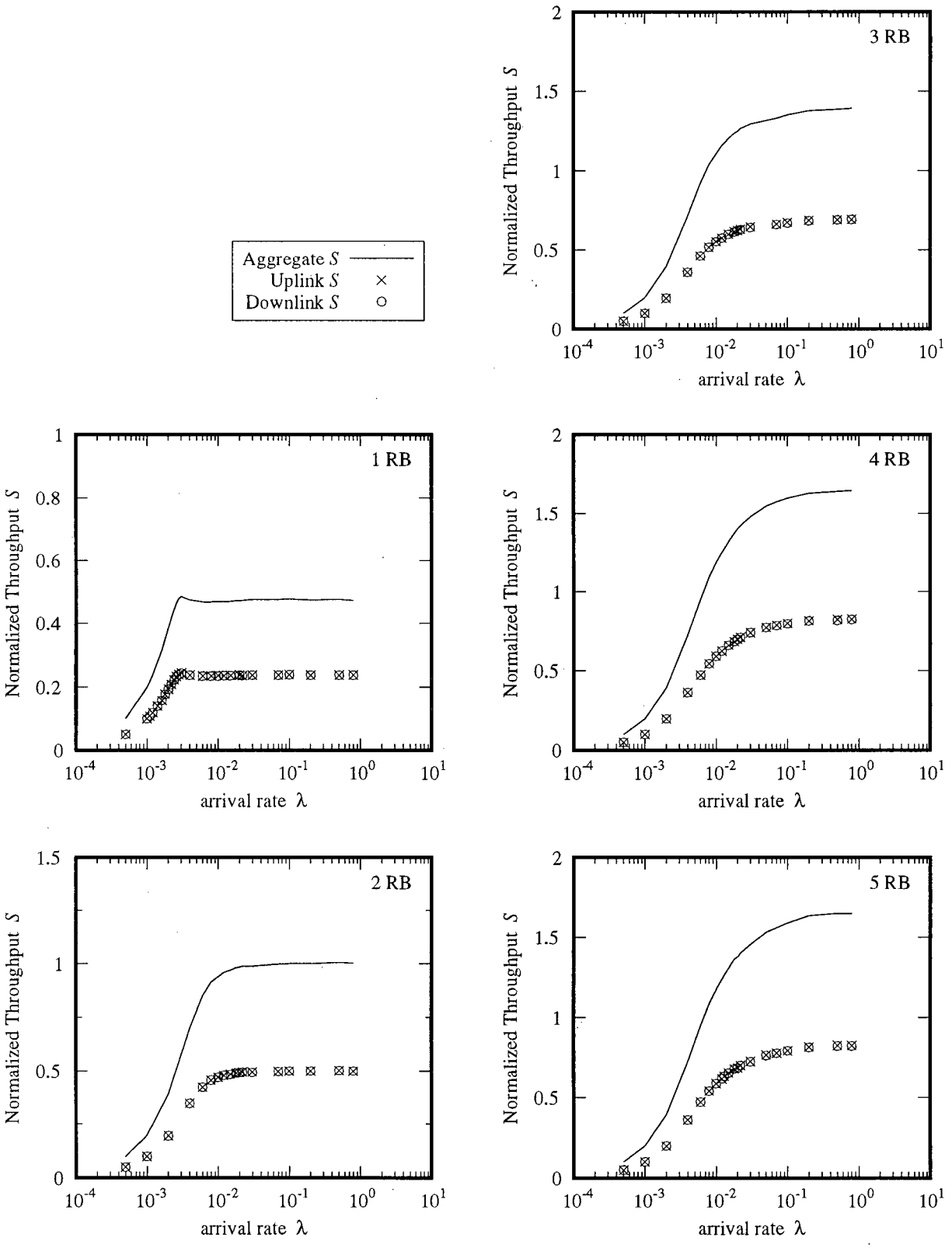

Figure 5.7 Uplink and downlink S of dual persistency CSMA with FP, TC, *THSNR* = 12 dB, RB = {1, 2, 3, 4, 5}, *prno* = 9

5.2 Results and Discussion

The followings are the major results of the complete dual persistency CSMA system. Specifically, the effects of various parameters that may affect the system design are examined. If not otherwise specified, the default parameters are : FP method, TC scheme, *THSNR* = 12 dB, *prno* = 9, and *mdatatime* = 4 for the PC scheme.

5.2.1 Effect of Number of RBs

The effect of different number of RBs at *THSNR* = {12, 14, 18} are shown in figure 5.8. The three sub-figures have some similarities such as :

1. Little throughput difference for different number of RBs when λ (or G) are small.
2. The throughput of each RB starts to diverge once the value of λ has saturated the system and the system saturates at smaller λ when there are fewer RBs.
3. For 1 RB, the throughput reaches a certain peak as λ increases to a point where $G \sim 1$. Thereafter, the throughput drops slightly and stays at a certain value. The same phenomenon happens to 1 and 2 RBs at *THSNR* = 14 dB and to 1 – 3 RBs at *THSNR* = 18 dB.
4. Throughput in RB = {4, 5} continue to increase as λ approaches the upper limit considered in the simulations.
5. An increase from 1 to 2 RBs gives the most significant increase in throughput, while an increase from 4 to 5 RBs has little or no effect on the throughput.

There is little throughput difference at small values of λ for different number of RBs because when channel traffic is low, few collisions occur and $S = 2 \times N \times \lambda$. As λ increases, there are too many transmissions and 1 RB is flooded with packets. In this case the RB's capacity is saturated and collisions occur. The slight drop in throughput after the peak in the three graphs is due to multiuser interference. However, throughput is maintained at a steady value because of the capture effect in spread spectrum. Hereafter, this steady value of the throughput is referred as the saturated throughput.

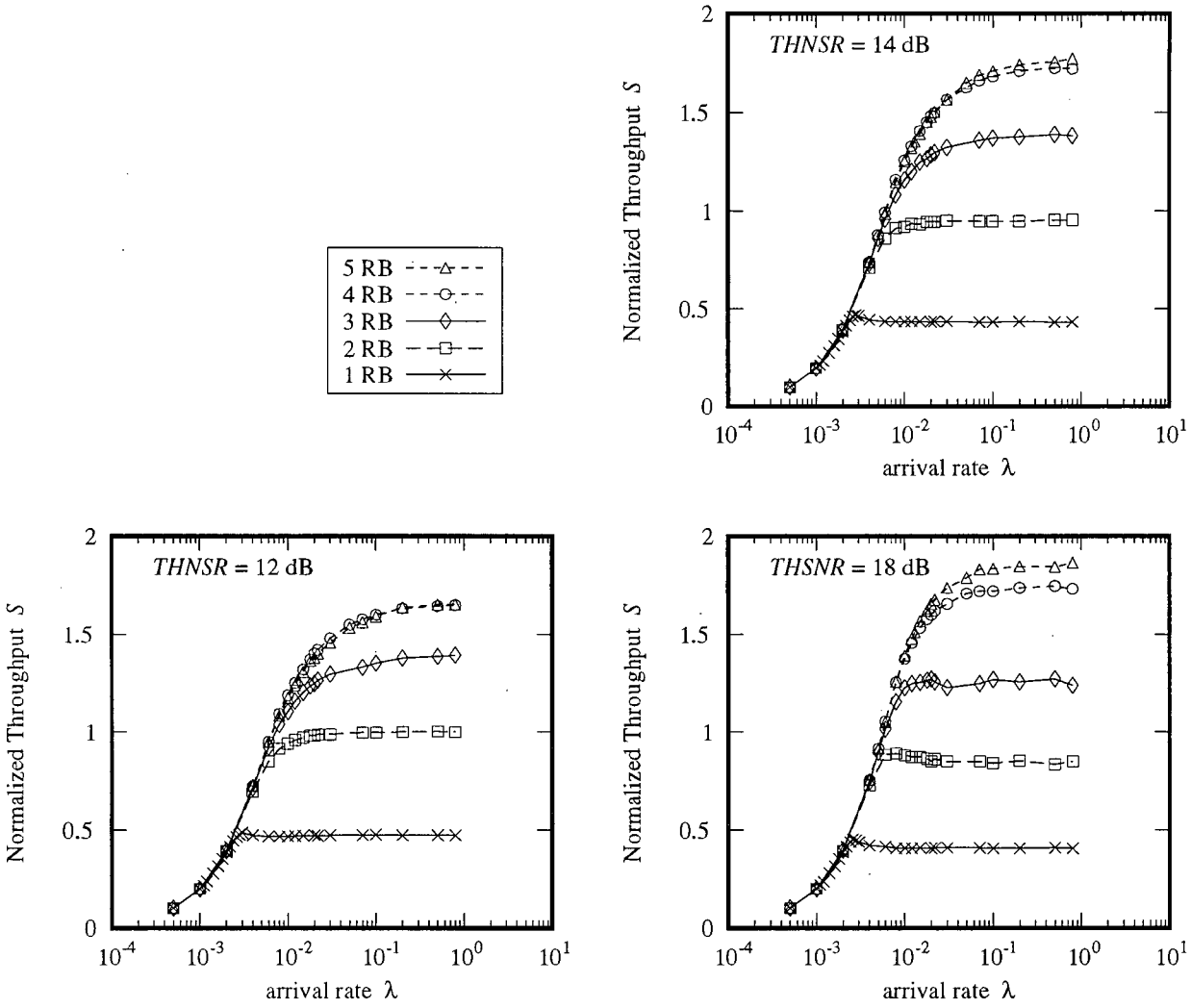

Figure 5.8 Effect of number of RBs with FP, TC, *THSNR* = {12, 14, 18} dB

It is necessary to explain why saturated throughput occurs. For a given value of *THSNR*, a certain number of packets can be transmitted to the channel. With fewer RBs, the chances of receiving a packet decrease. Excessive traffic causes collisions at the RBs and thus in figure 5.9 we see a small drop in the throughput of RB = {1, 2}. This is referred as saturation in channel capacity. As more RBs become available, a packet may be considered as an interferer at an RB but at the same time may contribute a successful transmission at another RB. This is why there is no saturated throughput in figure 5.9 when RB = {3, 4, 5} with *THSNR* = 12 dB.

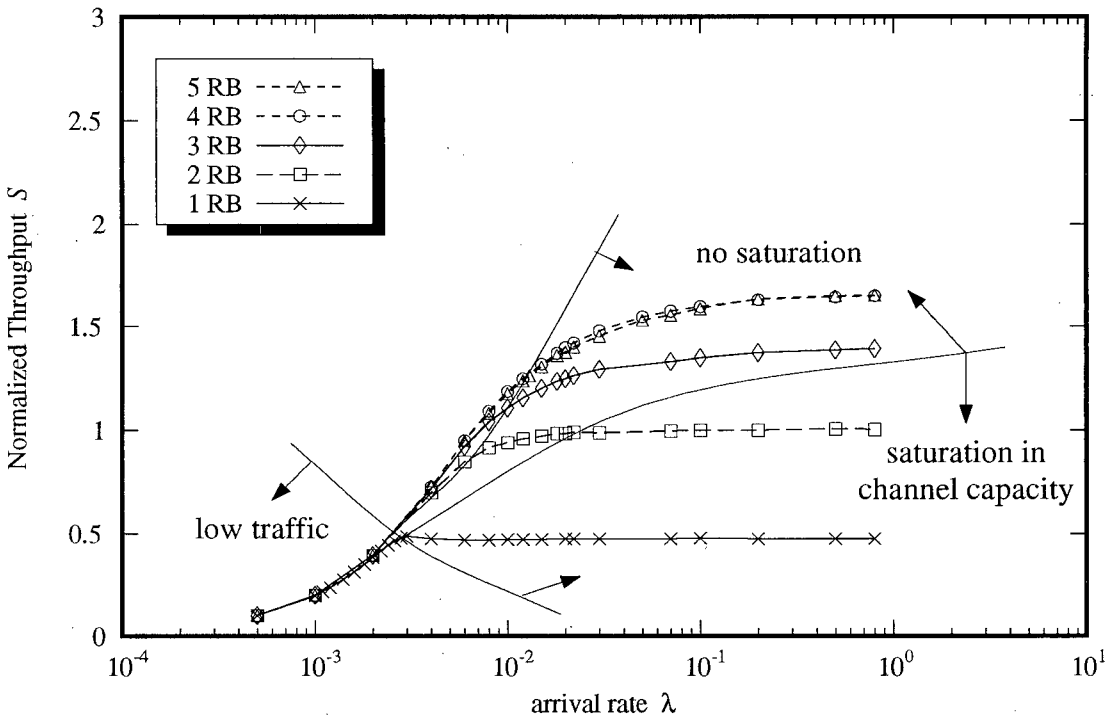

Figure 5.9 Saturation regions with FP, TC, *THSNR* = 12 dB

When the number of RBs increases from 4 to 5, the gain in throughput is not as significant as with an increase from 1 to 2 RBs for $\lambda > 0.002$. In fact, there is virtually no difference in figure 5.8, *THSNR* = 12 dB and only slight improvement with 5 RBs in the *THSNR* = 14 dB case of the same figure. When *THSNR* = 18 dB, 5 RBs the greatest improvement is seen when the number of RBs is increased from 4 to 5. This is because the effective range of carrier sensing has shrunk and there are more hidden terminals in the *THSNR* = 18 case than in the other cases. With all these packets present in the channel, an extra available RB improves the chances of receiving a packet for two reasons. First, an extra RB reduces the average distance between any pair of RB and station and thus there will be a higher SNR at the receiver. Second, an additional RB can increase the number of multiple packet receptions, and hence there will be a higher number of successful packet receptions per each packet transmission time.

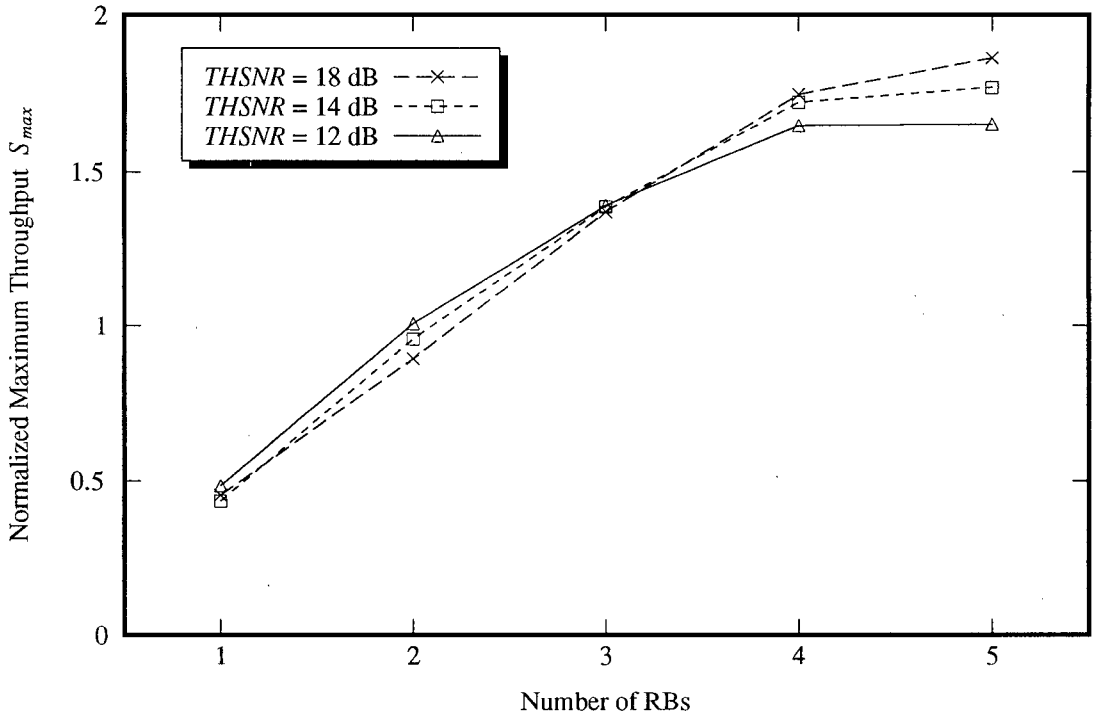

Figure 5.10 Effect of number of RBs on maximum S for different *THSNR*

It is also desirable to look at the throughput as a function of number of RBs. This is shown in figure 5.10 for the three different values of *THSNR*. An arrival rate of 0.01 is chosen for the plots. From this figure, we notice that the addition of an RB to a 1 RB system gives the highest gain in S and the gain gradually decreases with each succeeding increment of RB. However for *THSNR* = 12 dB, an increase from 4 to 5 RBs does not produce a gain in S. The reason is that a smaller *THSNR* reduces the number of hidden terminals and therefore fewer simultaneous transmissions may take place. Use of the fifth RB in *THSNR* = 12 dB only results in duplicated packet receptions. The fifth RB does provide extra S in a system with higher *THSNR* since more packets are simultaneously transmitted over the channel.

Besides the aggregate throughput, the normalized delay is another measure of system performance. The delay measured on this uplink/downlink model is the same as the one described in section 3.4.1. The three graphs in figure 5.11 show the results of normalized delay as a function of the aggregate throughput at *THSNR* = {12, 14, 18} dB. The general observations from these three graphs are as follows :

1. For all *THSNR*, as *S* increases the delay of a system that has fewer RBs rises faster than the one with more RBs . When *S* has reached its peak, it drops slightly as traffic continues to increase but the delay becomes very high.
2. Increasing the number of RBs improves the throughput/delay characteristics of the system but with diminishing return.
3. For all values of *THSNR*, the difference in delay between systems with 4 and 5 RBs is not obvious.

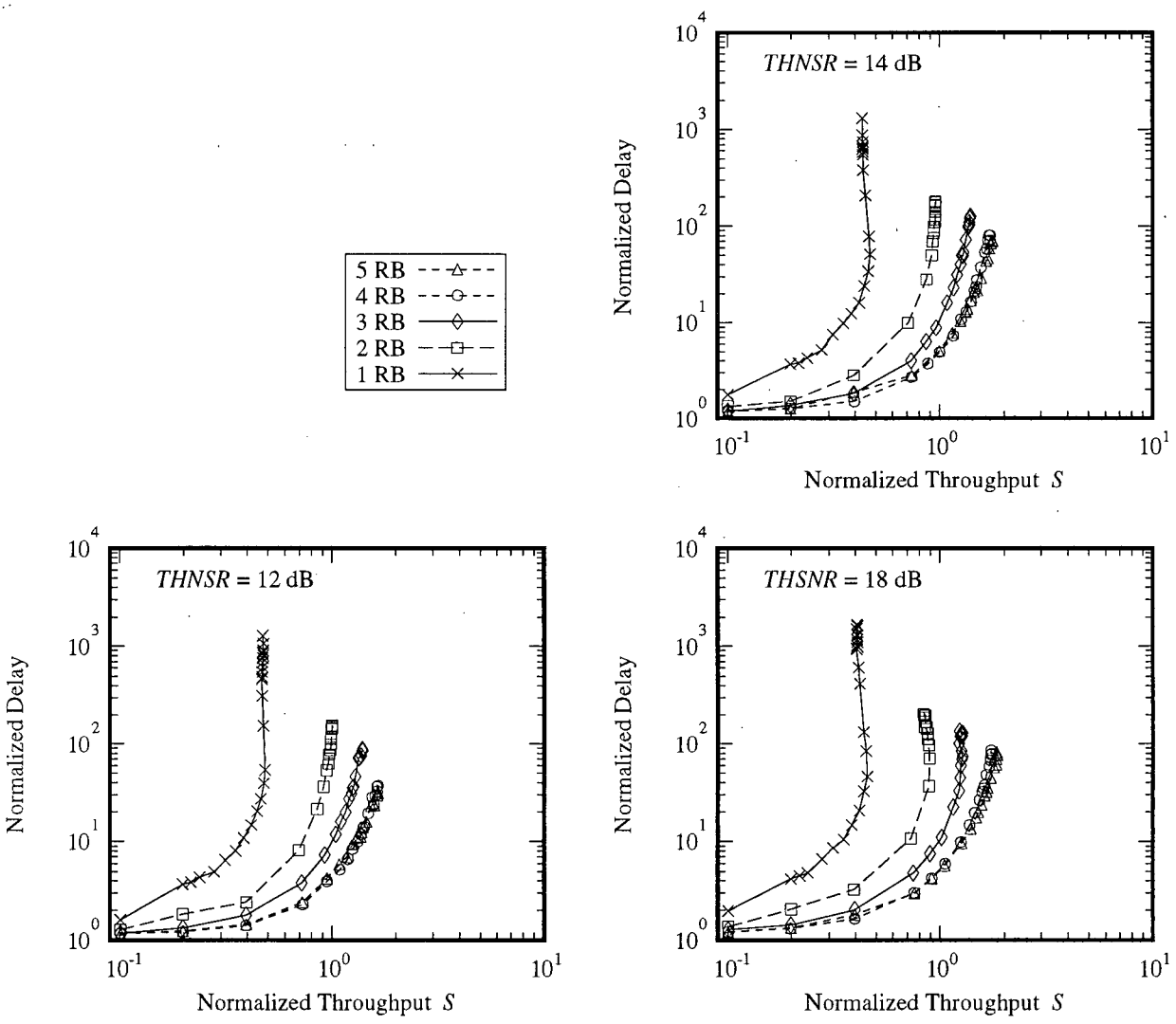

Figure 5.11 Delay-vs.-throughput with *THSNR* = {12, 14, 18} dB

Figure 5.12 presents the effect of number of RBs on delay for different *THSNR* at λ = 0.01. For 1 to 4 RBs, every additional RB reduces the delay experienced by the system. However, an increase from 4 to 5 RBs does not reduce the delay at λ = 0.01.

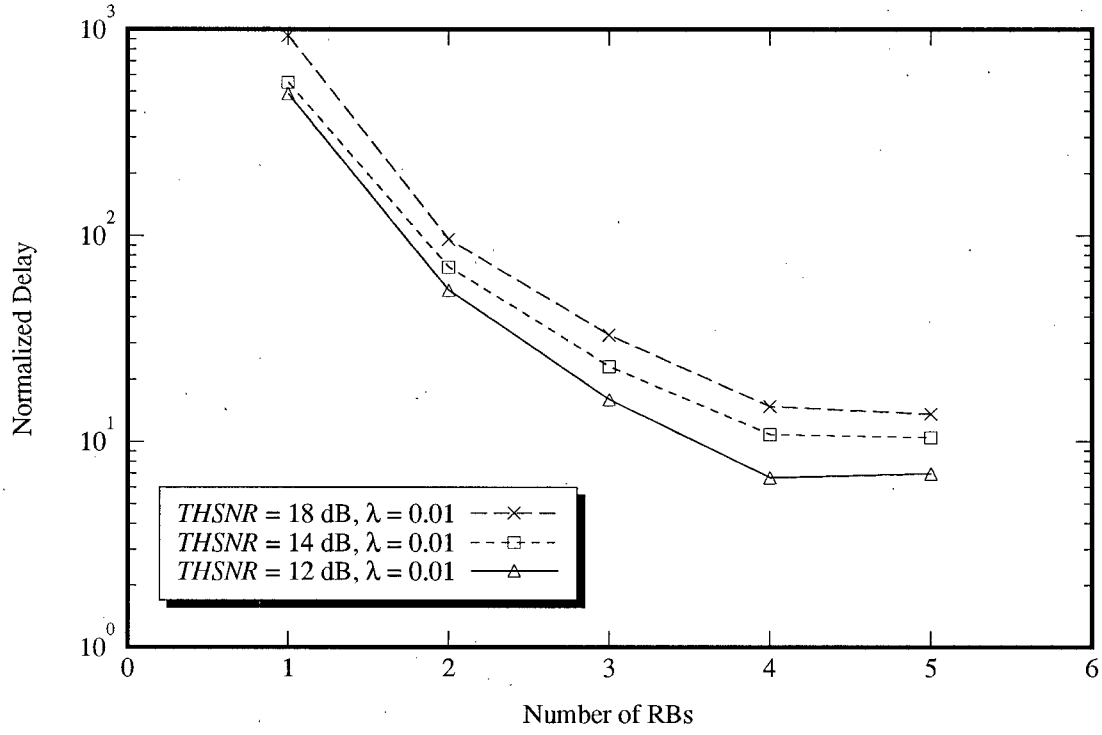

Figure 5.12 Effect of number of RBs on delay for different *THSNR* at λ = 0.01

To summarize the effect of number of RBs, the addition of an RB to a 1 RB system produces the most significant improvement in throughput and delay, while the addition of an RB to a 4 RBs system has little effect due to duplicated packet receptions. Multiple RBs can help to reduce the saturation problem.

5.2.2 Effect of *THSNR*

The sensing threshold, *THSNR*, can be thought of as a parameter controlling the number of hidden terminals with respect to a particular station in the system. For CSMA protocols in general, a system with no hidden terminal is desirable. However, in this spread spectrum capturing model, we may want to have a few extra transmissions so that the capturing of different packets by different RBs is possible.

Figure 5.13 depicts the effect of *THSNR* on the system throughput at different values of λ. For a 1 RB system, increasing λ causes the throughput to diverge for different values of *THSNR*, with *THSNR* = 8 dB yielding the highest saturated throughput. Higher values of *THSNR* decrease the saturated throughput, with *THSNR* = 18 dB yielding the lowest saturated throughput. In the 1 RB case, varying *THSNR* does not result in great variations in *S*. The maximum saturated throughput attainable in the *THSNR* = 8 dB case is 0.553, while the maximum saturated *S* in the *THSNR* = 18 dB case is 0.405.

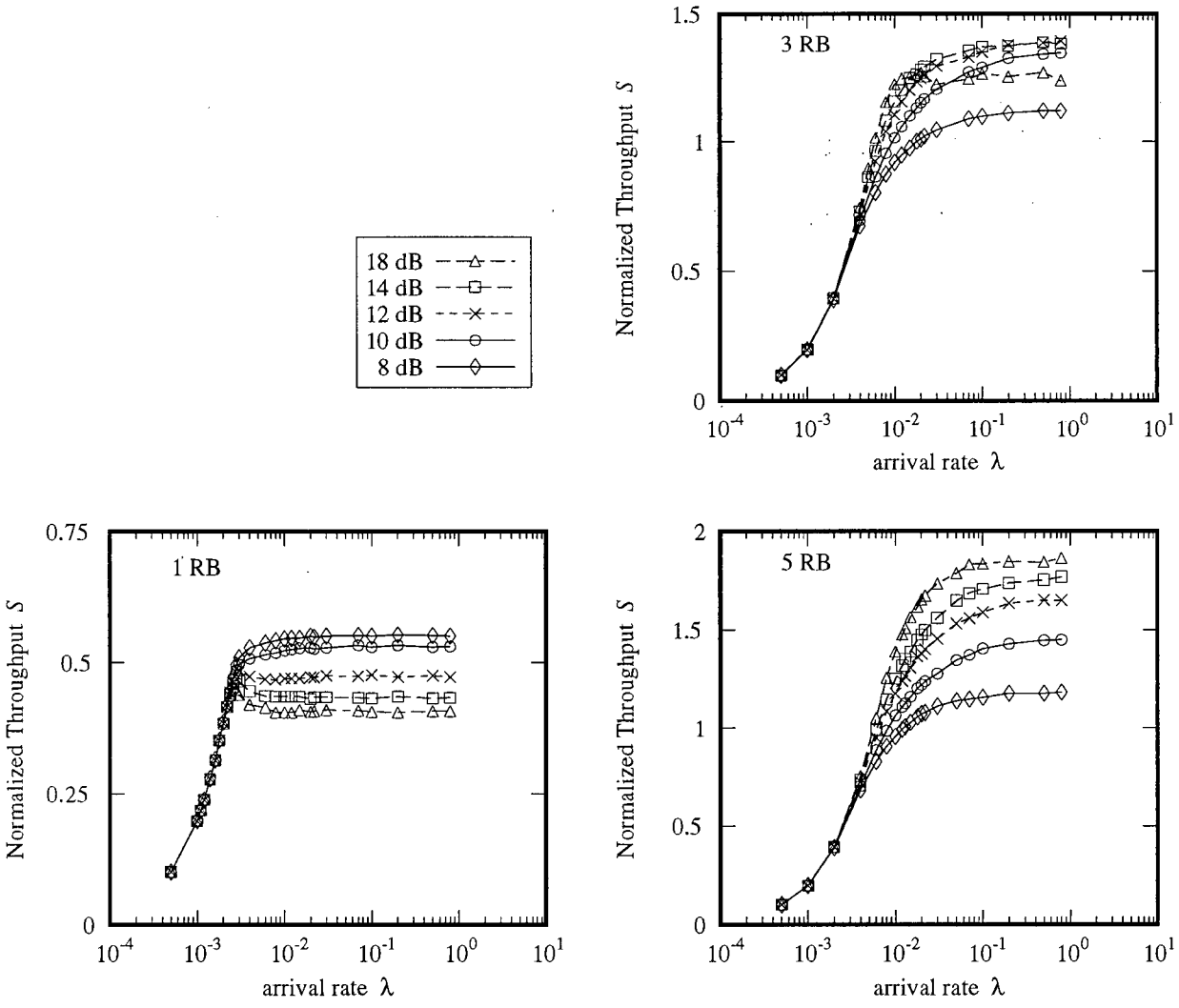

Figure 5.13 Effect of *THSNR* with RB = {1, 3, 5}

In figure 5.13, RB = {3, 5}, the effect of *THSNR* is more prominent. We first notice that *THSNR* = 8 dB has the lowest throughput, as opposed to the 1 RB case which has the highest throughput. When *THSNR* is increased to higher values, there is a significant gain in S. The gain in S occurs because there are more transmissions to the channel since more stations can now sense an 'idle' channel, and multiple packet receptions may occur. One might think of this as a reduction in the range of the carrier sensing circle. When *THSNR* = 18 dB is simulated with 3 RBs, different results are obtained. After a certain value of λ (or G) has been reached, the value of S declines as λ increases. This value of *THSNR* allows too many hidden terminals in the system and too many packets into the channel. These excessive packets do not contribute to the system throughput. Rather, they cause too much interference at the RBs, where a potentially correct reception is taking place.

All plots in figure 5.13, 5 RBs have an upward trend and no decline in S and thus the system does not have saturation in capacity for all values of *THSNR*. The largest gain occurs when *THSNR* is increased from 8 dB to 10 dB, for RB = {3, 5}.

Although the throughputs of RB = {3, 5} are not plotted together in the same graph, the S of 5 RBs is higher than the S of 3 RBs for all *THSNR*. This confirms the results from section 5.2.1 that more RBs can improve the system throughput even when another parameter is under investigation.

The effect of *THSNR* shown in figure 5.13 may not be very easy to see, especially in figure 5.13, 1 RB where the plots are clustered together. To see a more clear picture of its effect, the aggregate throughput is plotted against the variable *THSNR* for three different arrival rates, λ = 0.004, 0.01, 0.03. These three rates are chosen for the following reasons, respectively :

(i) throughput curves begin to diverge

(ii) $\lambda \times N = 1$

(iii) some λ larger than (ii) above

The plots in figure 5.14 illustrate the S-vs.-*THSNR* for RB = {1, 3, 5}. Along each plot in each graph, the gain or decline in throughput is caused by varying *THSNR* for a particular

λ. In figure 5.14 with 1 RB, the throughput begins with the highest value at *THSNR* = 8 dB and it drops as *THSNR* increases. Higher *THSNR* causes more interferences at the RBs and decreases the throughput.

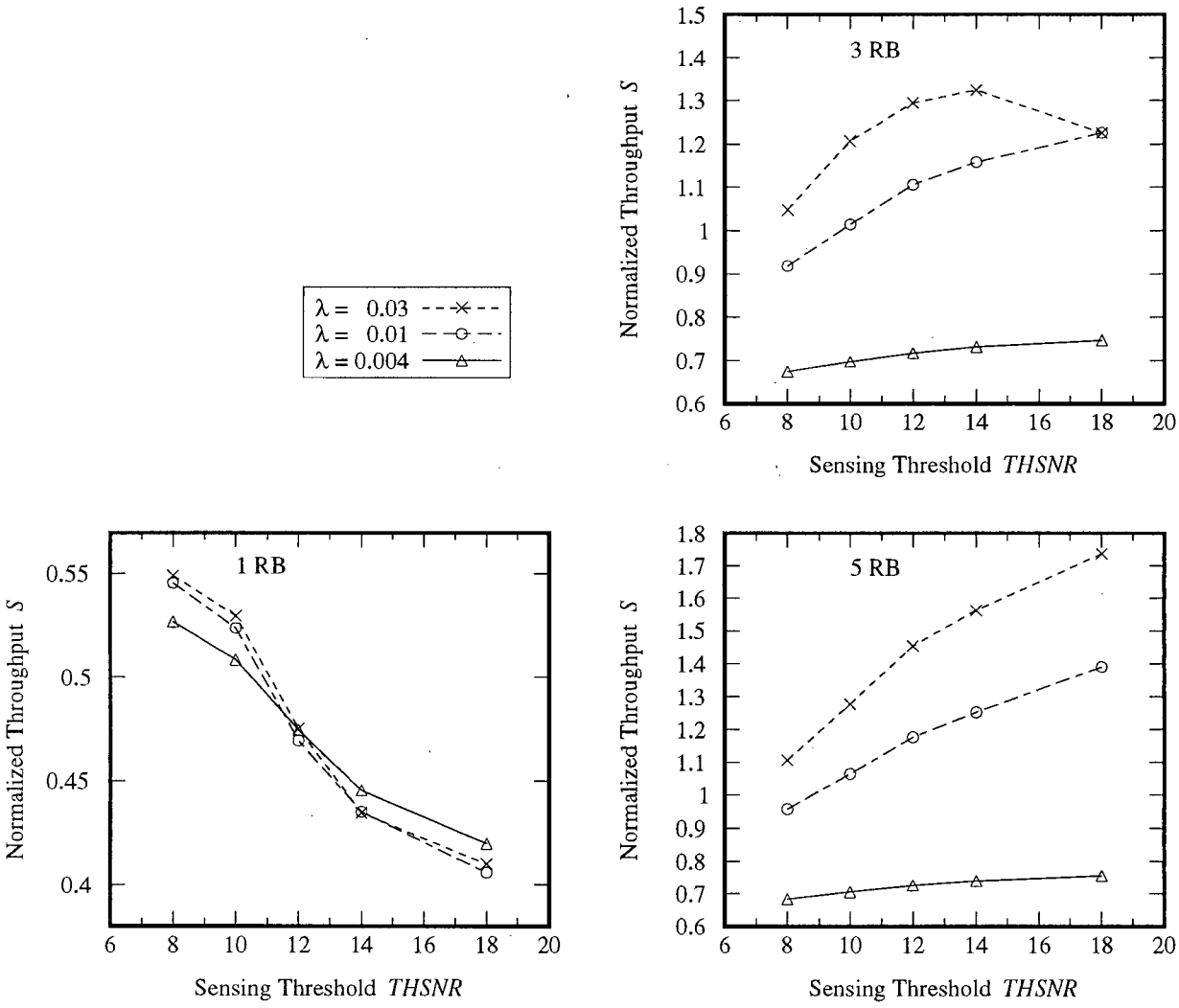

Figure 5.14 Effect of *THSNR* on *S* for different λ with RB = {1, 3, 5}

In figure 5.14 with 3 RBs, the throughput characteristics are completely different. First, in a system with λ = 0.004 and 0.01, the throughput shows a continuous upward trend. Second, for λ = 0.03, the throughput first increases and then drops when *THSNR* has reached 18 dB. The last part of figure 5.14 shows a 5 RBs case where only positive slope on *S*-vs.-*THSNR* plots can be seen.

It was previously assumed that higher *THSNR* would increase S due to multiple packet reception. We can justify this by looking at the gain in S between two different values of λ for a given *THSNR* in multiple RB cases. The only exception is in the case of 3 RBs, *THSNR* = {14, 18} dB and λ = 0.03 where S actually drops. Since both values of λ use the same number of RBs, duplicated packet receptions is less likely to occur when *THSNR* = 18 dB than 14 dB. Therefore, the drop in S in a system with 3 RBs is due to saturation in capacity.

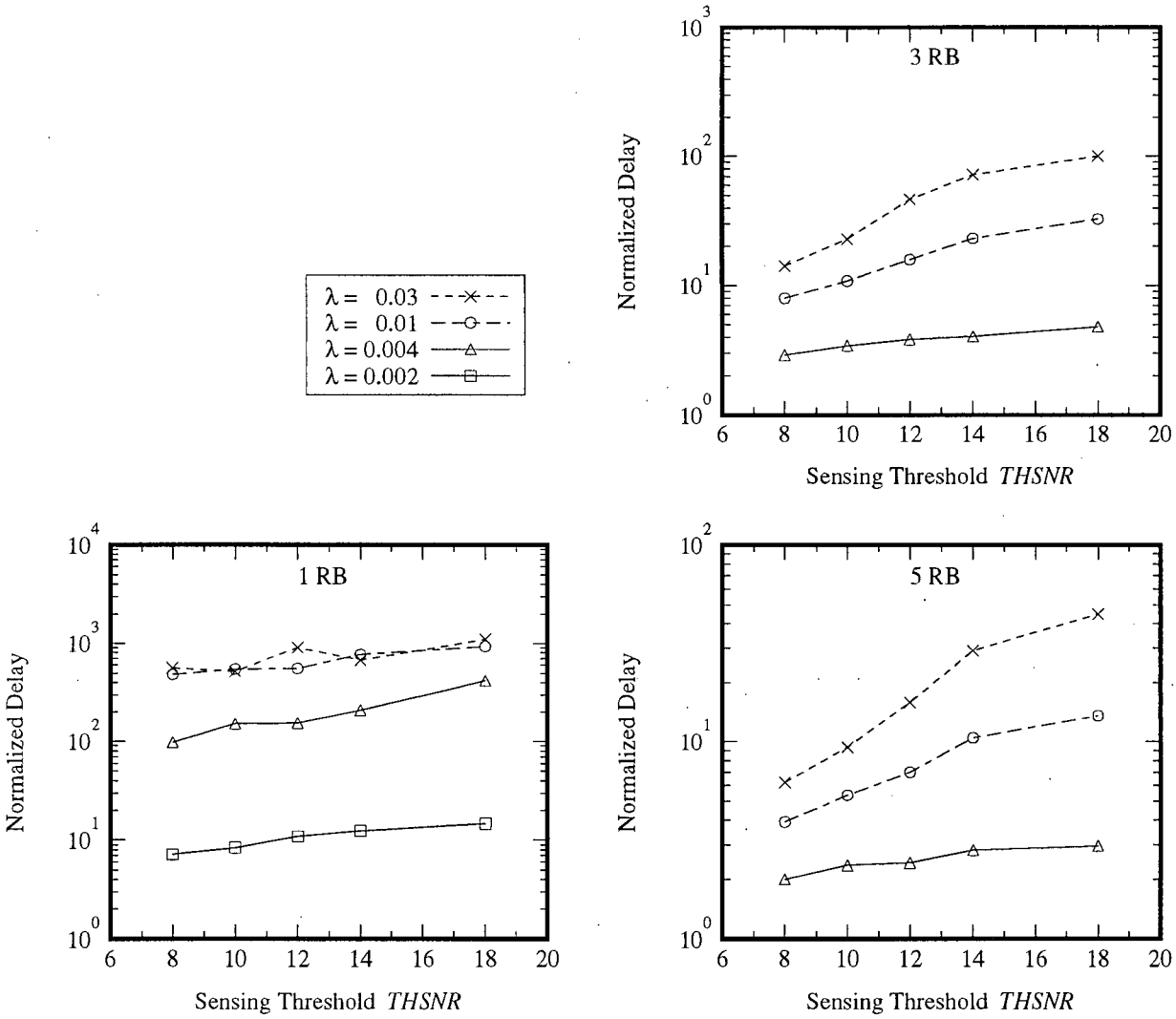

Figure 5.15 Effect of *THSNR* on delay for different λ with RB = {1, 3, 5}

The impact of *THSNR* on the delay of the system is shown in figure 5.15 where delay-vs.-*THSNR* increases with *THSNR*. At a low *THSNR* (low number of hidden terminals),

duplicated packet receptions occur more often. This means that if a packet fails at one RB, there is another chance for that packet to be correctly received by another RB. Therefore, at a low *THSNR* there is a smaller chance for that station to retransmit. At a high *THSNR*, multiple packet receptions are more likely to happen. However, higher *THSNR* values also mean that more packets are transmitted and collided and retransmissions are necessary.

5.2.3 Effect of Power Control Method

The power control method is aimed at reducing mutual interference among transmitting stations. Its effect is shown in figure 5.16 for 1–5 RBs. We analyze its effect on the system at *THSNR* = 10 dB. In figure 5.16, where the results of 1 RB are shown, we see two totally different throughput curves. With the FP method, the curve is identical to the 10 dB plot in figure 5.13, 1 RB, and it shows that saturation in capacity occurred at high values of λ. With the AP method, the throughput is the same as the FP method at low values of λ but it drops abruptly for $\lambda > 0.002$. The decline in throughput occurs for the following two reasons :

1. Smaller received power at the RB
2. Higher level of interference at the RB due to inaccurate sensing of the channel state

Smaller transmitted power and a larger number of contending transmissions cause a smaller SNR and a higher ISR at the receiver and thus smaller throughput.

Figure 5.16, 2 RBs, indicates a tremendous gain in S compared to the 1 RB case. The saturated throughput jumps from 0.08 to 0.88 (1100%) from 1 to 2 RBs when the AP method is employed. On the other hand, with the FP method, the gain in throughput is 196% (from 0.53 to 1.04).

By having more RBs, we see further improvements in the system throughput by employing the AP method. At some values of λ, the throughput curve using the AP method is greater than that of the FP method. Furthermore, the AP method outperforms the FP method at all λ values in figure 5.16, 5 RBs. So far, only the results of *THSNR* = 10 dB have been displayed. Other values of *THSNR* also have been considered in the simulations. Indeed, the results of *THSNR* = {12, 14, 18} dB are very similar to figure 5.16.

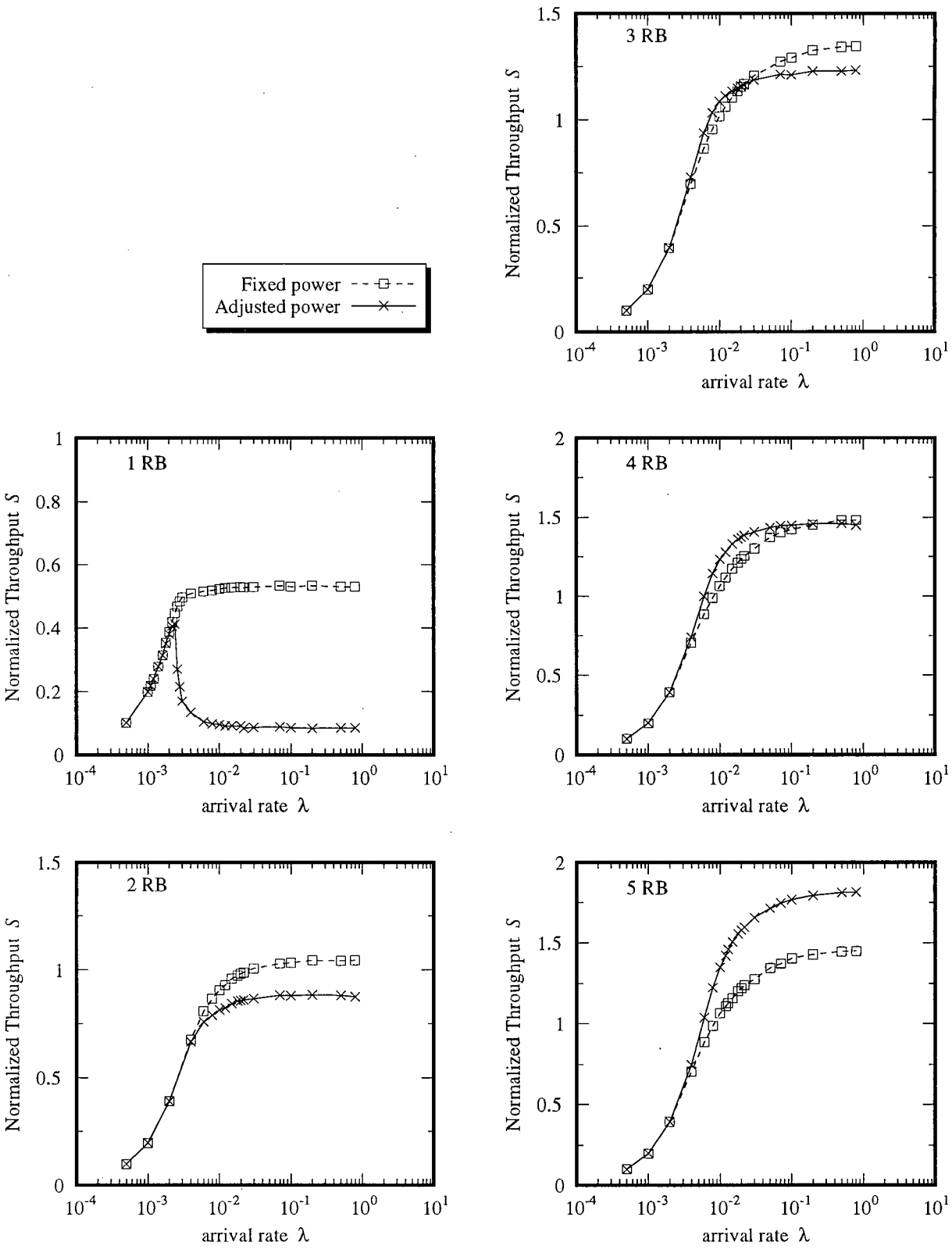

Figure 5.16 Effect of power control methods for different λ with *THSNR* = 10 dB and RB = {1, 2, 3, 4, 5}

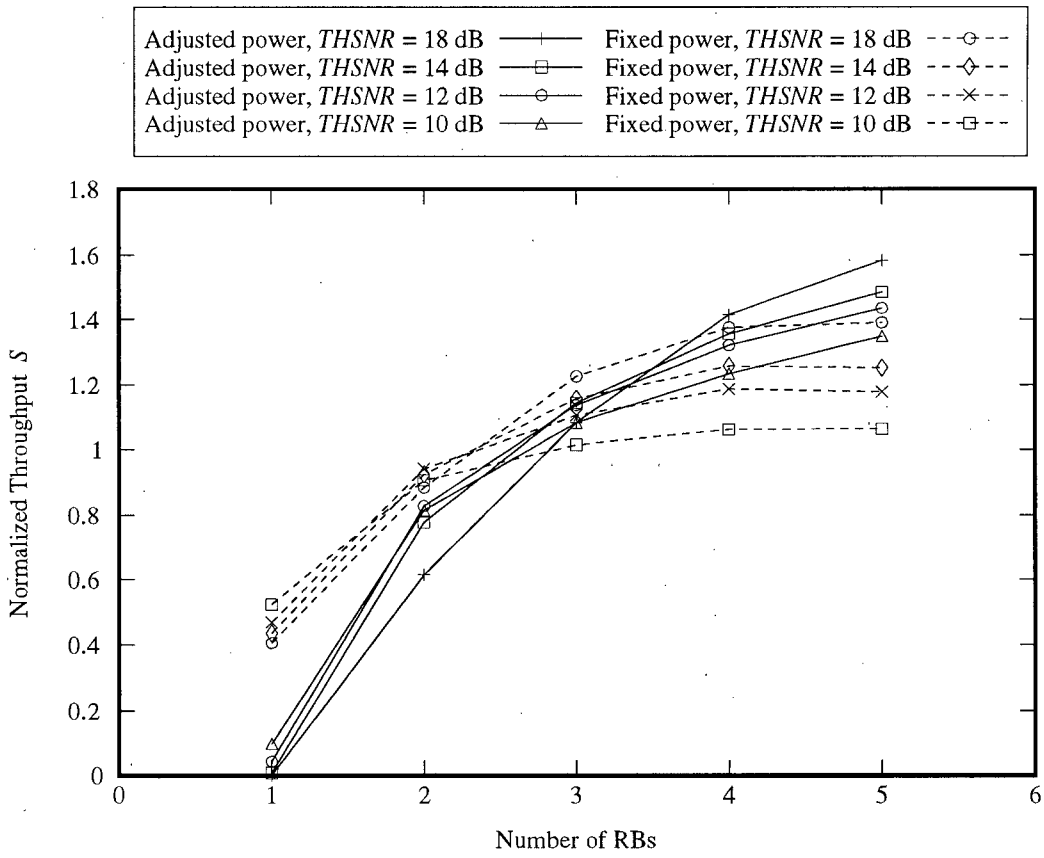

Figure 5.17 Effect of power control and effect of number of RBs on S for different *THSNR* with $\lambda = 0.01$

To see the effect of power control combined with the effect of number of RBs, a plot of S-vs.-number of RBs with different *THSNR* and different power control methods is necessary. The example chosen here is $\lambda = 0.01$ and it is shown in figure 5.17. First notice that with 1 RB, all *THSNR* that employ the AP method have very low throughput when compared to the corresponding *THSNR* using the FP method. At the other extreme, when 5 RBs are used, the AP method at various *THSNR* has higher throughput than the respective *THSNR* that use the FP method. Therefore, the AP method works better when multiple RBs are employed.

Besides throughput, we examined the delay experienced by the terminals. The results are shown in figure 5.18 where the delay is plotted against various number of RBs for *THSNR* = {10, 12, 14, 18} dB and for both types of power control methods. The observation from this figure is that, in most cases, the FP method has less delay compared to the AP method.

Also, in each power control method, larger *THSNR* causes longer delay since more hidden terminals are transmitting and causing collisions.

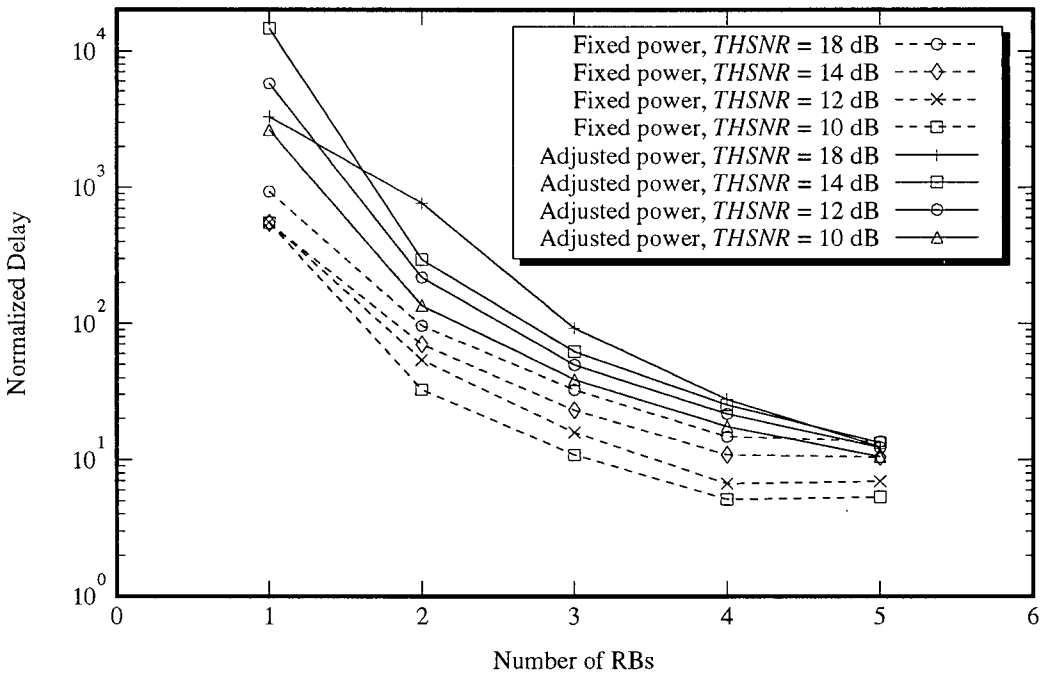

Figure 5.18 Effect of power control and effect of number of RBs on delay for different *THSNR* with λ = 0.01

However, in this figure, there is one point that does not seem to agree with the general trend of results. This point occurs at 1 RB and the an explanation for this abnormal behaviour is as follows. In the AP method , *THSNR* = 18 dB, 1 RB case, the delay experienced by the uplink stations seems to be much lower than the AP method, *THSNR* = 14 dB, 1 RB case. The normalized delay obtained is 3264. Theoretically, we expect the delay to increase as *THSNR* increases. The reason for the smaller delay is that low delay is achieved at the beginning of the simulation when the channel is not saturated. Then all terminals become backlogged and there are not many successful transmissions.

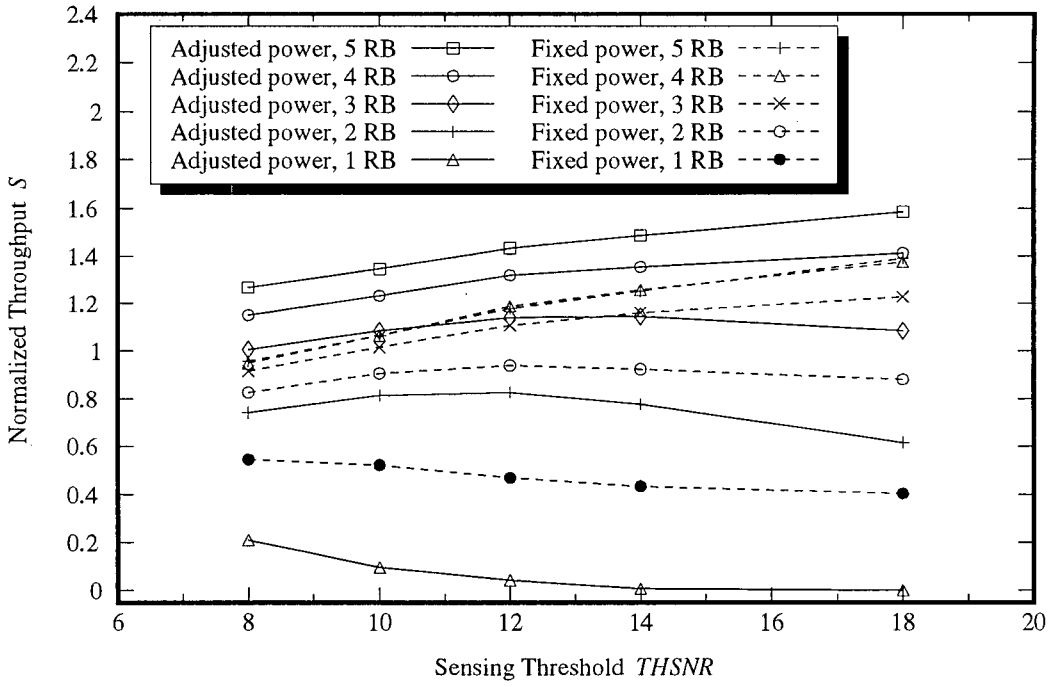

Figure 5.19 Effect of power control and effect of *THSNR* on S for different number of RBs with λ = 0.01, TC

While figures 5.17 and 5.18 emphasize the effect of number of RBs in the system, one may replot these two figures into figures 5.19 and 5.20 to see the effect of *THSNR*. The AP method with 1 RB's performance is much worse than its counterpart using the FP method for the same *THSNR*. Its extremely low throughput and extremely high delay indicate that the AP method is not an appropriate method to employ in a 1 RB system. By comparing the two power control methods in 1 RB and 2 RBs case, the difference in S in the 2 RBs case is greatly reduced.

Next, when 3 RBs are used, the effect of power control causes the throughput curves to cross over. At low *THSNR*, sensing is more sensitive and hence transmission is not easy to commence. As *THSNR* rises, the FP method becomes more inefficient than the AP method because the FP method results in higher interference and hence increases the ISR at the receiver. The crossover point for 3 RBs is at *THSNR* = 13.5 dB. When there are 4 or 5 RBs, it can be seen that the AP method outperforms the FP method for all values of *THSNR* considered. Also note that when the RBs are increased from 4 to 5, there is virtually no

gain in S using the FP method. On the other hand, increasing the number of RBs from 4 to 5 using the AP method produces a higher S. From the discussion above, the AP method is more suitable in a distributed architecture because multiple packets can be received at different RBs with less interference

Turning to figure 5.20, where the delay-vs.-*THSNR* is shown, the effect of *THSNR* is that higher values of *THSNR* induce higher delay. However, for the *THSNR* = 18 dB, 1 RB, and AP method case, a steady state is not achieved since most of the terminals are backlogged. No packet is transmitted and the delay is not accumulated.

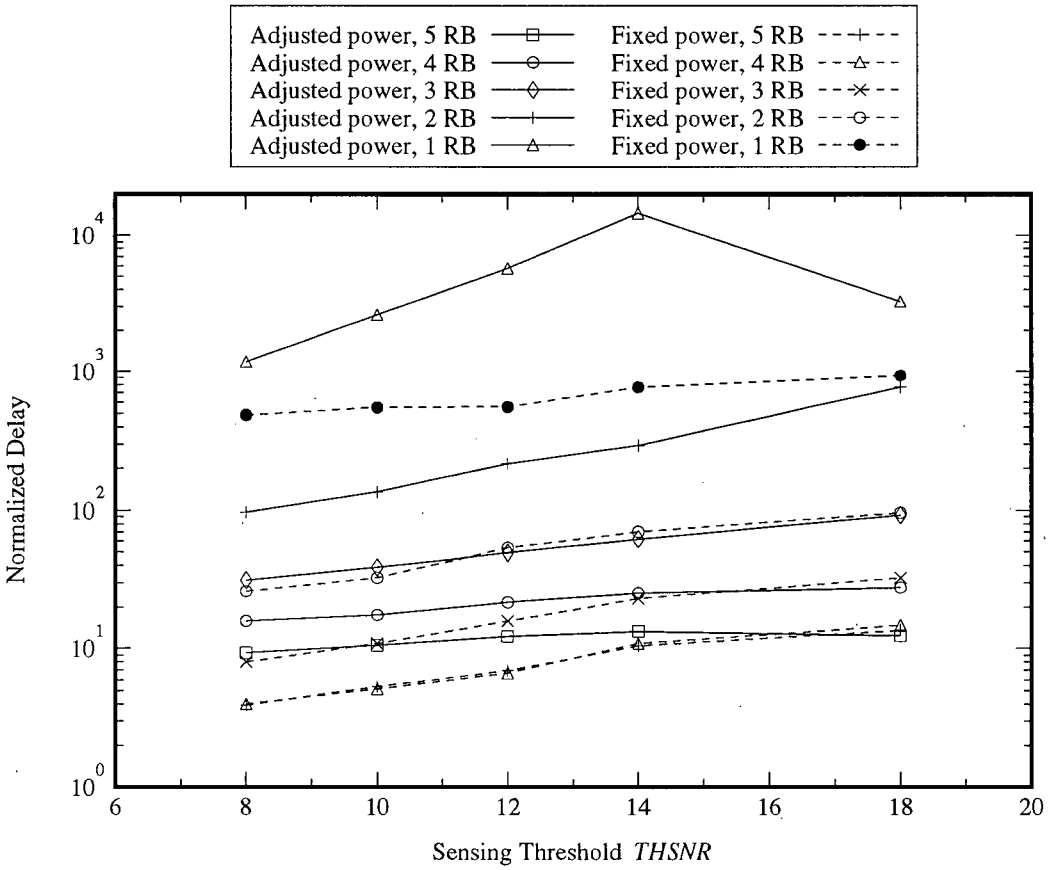

Figure 5.20 Effect of power control and effect of *THSNR* on delay for different number of RBs with λ = 0.01, TC

5.2.4 Effect of Capture Scheme

The two capture schemes described in chapter 3.2.4 are considered to investigate the capturing probability of the stations in the model. If the throughput-vs.-arrival rate analysis is employed, then the plots of power capture scheme (PC) and time capture scheme (TC) will overlap each other for all values of λ, and likewise for other values of *THSNR*. It would not be very interesting to see a series of graphs in which the results are identical. Therefore, we resort to measure the capturing probability, Pr_C, of the individual stations.

We first compare the Pr_C of a system under the two capturing schemes with *THSNR* = 12 dB, RB = {1, 3, 5}. These are plotted in figures 5.21 and 5.22 for the FP and AP methods respectively. In each of the two figures, the first column (a, b, c) shows the 3–D representation of Pr_C in the power capture scheme, and the second column (d, e, f) shows the results of the time capture scheme. We can see from figure 5.21 that there is not a very significant difference between the two capture schemes when the number of RBs are equal. This is true in figure 5.22 as well.

Indeed, figures 5.21 and 5.22 are more useful for investigating the effect of power control, the effect of number of RBs and also the effect of *THSNR* on the Pr_C of individual stations. When a system has only 1 RB, power control means that every station adjusts its transmission power to the RB with the value *SNratio*. Therefore all transmitted packets appear to have the same signal strength at the RB. Packets that have equal received power make it difficult for the RB to capture a packet using the PC scheme. The results are shown in figure 5.22 (a, d) where extremely low Pr_C is obtained.

In figure 5.21 (b, e), 3 RBs, we see that Pr_C is lower at (1, 10) since there is only one RB located at the far side of the room. Also, in (b, c, e, f) of the same figure, the FP method favours the centre stations, as indicated in the highest Pr_C near the room centre.

On the other hand, in figure 5.22 (b, c, e, f), the roughness of 3–D plot tells us that Pr_C varies from one station to another station. Stations that are next to each other can have a large variation in Pr_C. Moreover, the hollow of the 3–D plot at the centre actually shows that the AP method does not favour the centre stations. We see much higher Pr_C of the

near-wall and corner stations in figure 5.21.

In terms of fairness, Pr_C in figure 5.21 (c, f) shows that stations that are further away from the room centre have less Pr_C. Therefore, the FP method is unfair to those stations. In contrast, the AP method gives fairer access to those stations near the walls or at the corners because a flat Pr_C contour is seen for those stations. Stations that are under the RBs have higher Pr_C than the rest of the stations.

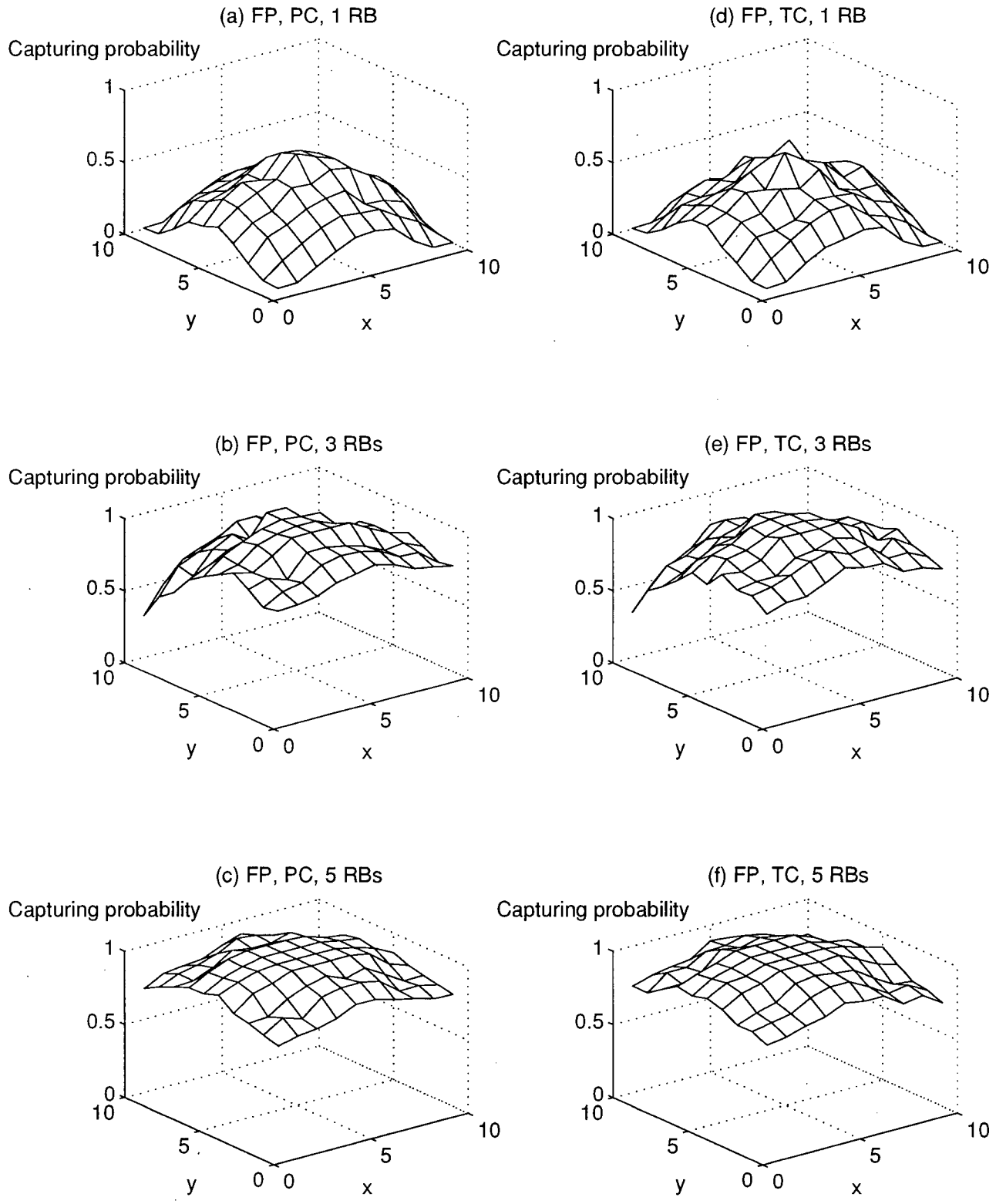

Figure 5.21 3–D plot Pr_C with $THSNR$ = 12 dB, FP, RB = {1, 3, 5} and λ = 0.01

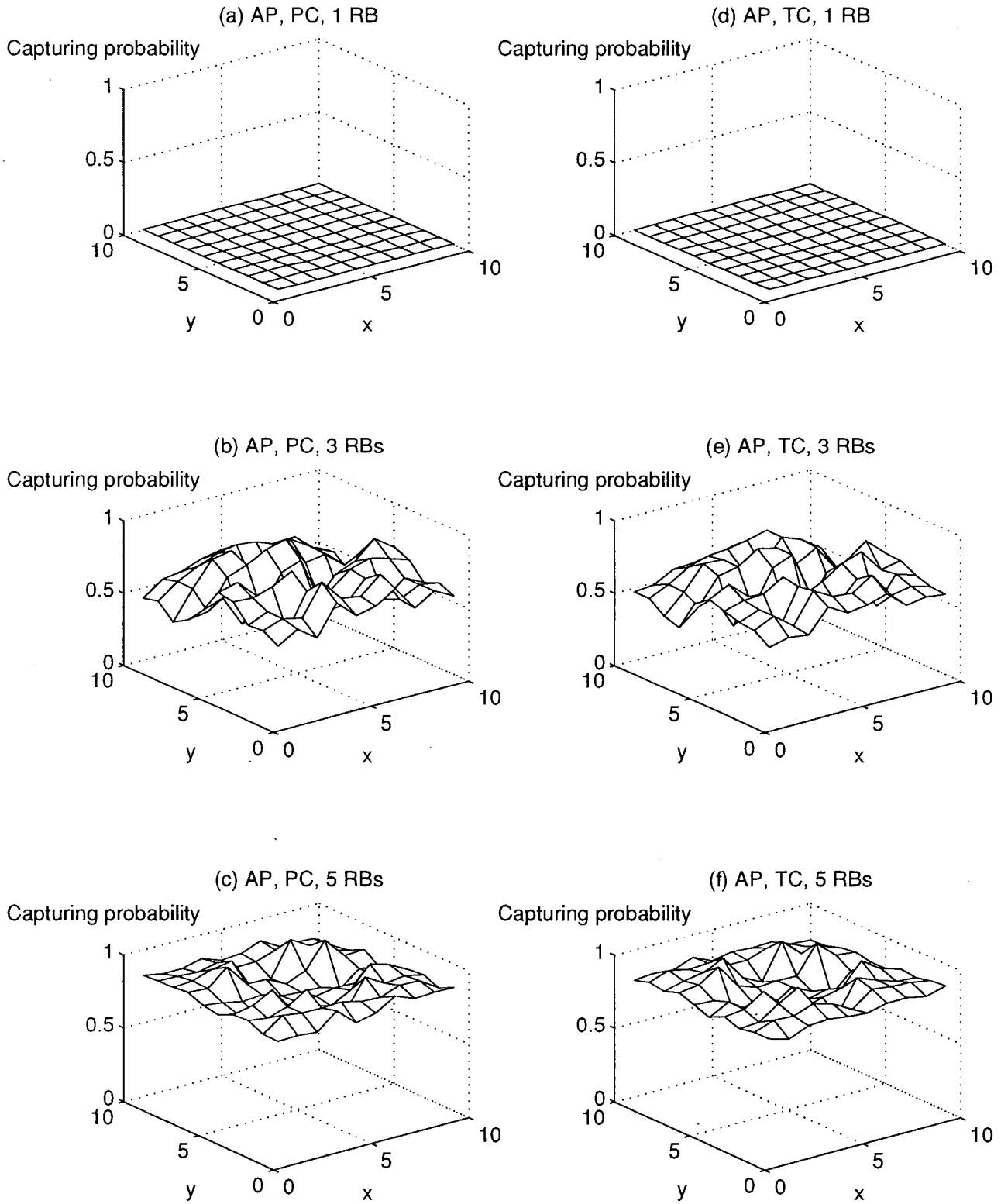

Figure 5.22 3–D plot Pr_C with $THSNR$ = 12 dB, AP, RB = {1, 3, 5} and λ = 0.01

Since the 3–D plots of Pr_C are difficult to comprehend, another approach to examine the effects of the two capture schemes is necessary. The average capturing probability, $\overline{Pr_C}$-vs.-distance analysis gives us a measure of the stations' uplink transmission success probability as a function of distance from the centre of the room (20m, 20m). Since all stations are placed at discrete locations, the distances measured from the room centre to the stations are also discrete. Thus the $\overline{Pr_C}$-vs.-distance plots also occur at discrete points. The average capturing probability is calculated from a set of stations that are of equal distance from the room centre. For example, two possible sets are {1, 10, 91, 100} and {45, 46, 55, 56}. In figure 5.23, there are 14 unique distance points from the centre and therefore there are 14 different sets. Using the method described above, the 14 sets of $\overline{Pr_C}$ are calculated and plotted against the discrete distance points.

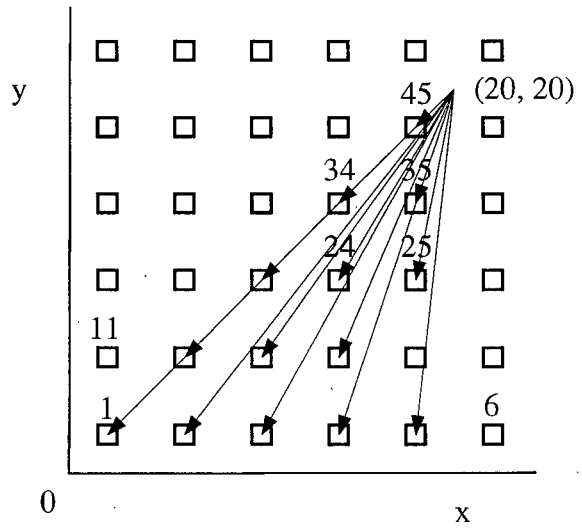

Figure 5.23 $\overline{Pr_C}$ at discrete distance point from the room centre

The effects of the two capture schemes are contrasted in figure 5.24 using different number of RBs and the two power control methods, at $THSNR$ = 12 dB. They show the average capturing probability at various distances from the centre. In each sub-figure, the lower two plots use the AP method and the upper two plots employ the FP method. When there is only 1 RB, the AP method is not suitable since most of the transmitted packets end up in collisions. With the FP method, the TC scheme has slightly lower $\overline{Pr_C}$ than the PC

scheme. $\overline{Pr_C}$ declines when stations are further away from the centre. The PC scheme gives a better $\overline{Pr_C}$ because it selects a signal with higher SNR, which is critical to the system when there is only 1 RB.

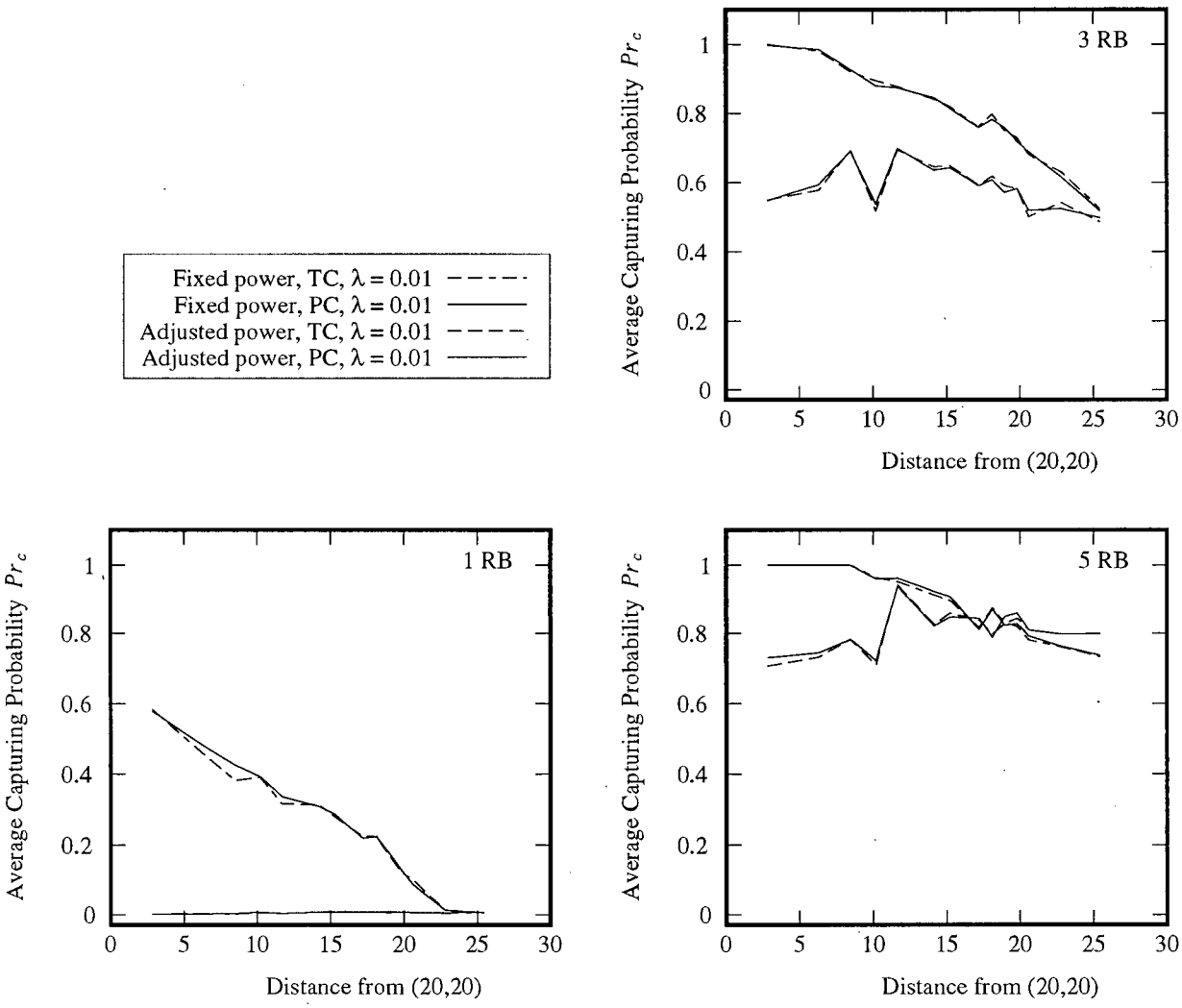

Figure 5.24 $\overline{Pr_C}$-vs.-distance from (20, 20) with *THSNR* = 12 dB and RB = {1, 3, 5}

In figure 5.24, 3 RBs, $\overline{Pr_C}$ using the AP method fluctuates in the distance range of 6 to 12 m. These fluctuations actually represents a change in *THSNR* coverage area and number of RBs linkage. In the 3 RBs case, two equal distance stations may not have the same number of RBs linkage. This movement from 6 to 12 m causes a change in SNR at the RBs. Table 5.11 summarizes the SNR in dB at the nearest RB of the five nearest stations (the first

five points in figure 5.24, 3 RBs) from the centre of a 3 RBs model. The change in the values of SNR at RB 1 due to a change in distance from the room centre closely resembles the fluctuations of $\overline{Pr_C}$ in figure 5.24, 3 RBs and this explains why $\overline{Pr_C}$ fluctuates. The AP method, 5 RBs system also has such fluctuations for the same reason.

Table 5.11 SNR of the nearest 5 stations from the room center at different RBs, 3 RBs model

Station no.	Distance (m)	RB 1	RB 2	RB 3
45	2.83	11.22	7.11	10.00
35	6.32	15.81	10.00	5.86
34	8.49	27.69	10.00	9.39
25	10.20	16.76	10.00	1.19
24	11.66	32.27	10.00	5.43

The effect of capture scheme is that the PC scheme works slightly better than the TC scheme in the AP method. Conversely, the TC scheme works marginally better than the PC scheme in the FP method. However, the difference in these two schemes is so small that the gain in $\overline{Pr_C}$ is considered insignificant in a CSMA system.

5.2.5 Effect of *mdatatime*

Mdatatime's effect is examined under the TC scheme with RB = {1, 3, 5} and with the two power control methods. The results shown in this section are simulated at *mdatatime* = {2, 4, 6} with *THSNR* = 14 dB.

Figure 5.25 shows that a system with 1 RB is not affected by the change in *mdatatime* for either power control methods. Therefore, we see a flat straight line spanning from 2 to 6 in *mdatatime*. With more RBs, increasing *mdatatime* from 2 to 4 does not change the value of *S* at all. Nonetheless, we see a decrease in *S* when *mdatatime* is increased from 4 to 6 with RB = {3, 5}. Larger *mdatatime* creates a larger time frame for arrivals at an RB. However, this also causes an extended period of interference.

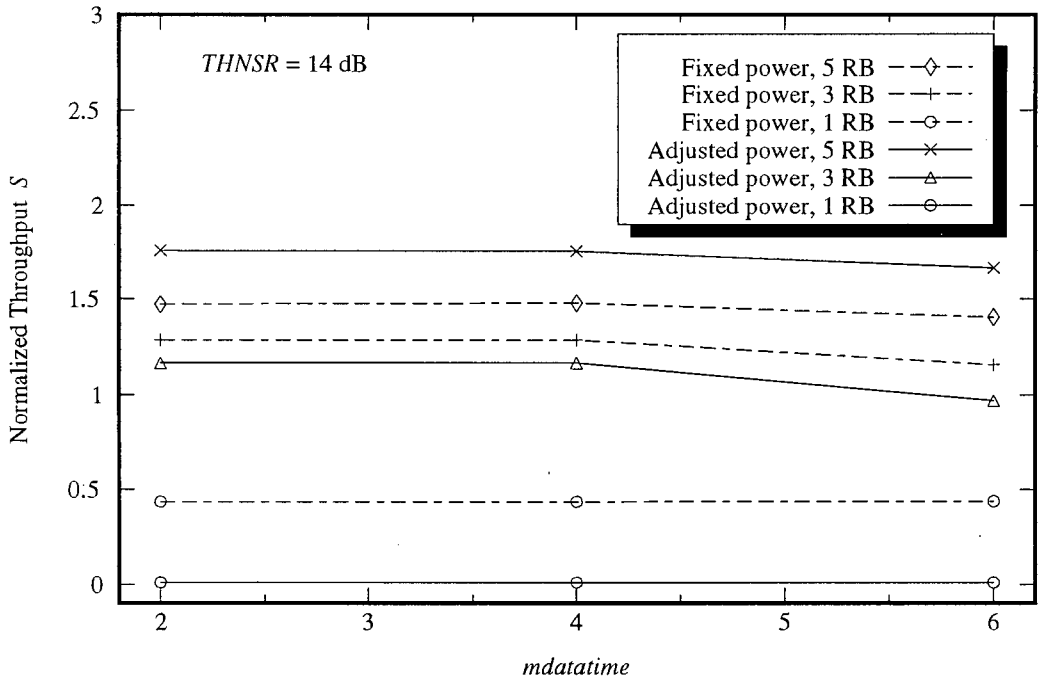

Figure 5.25 Effect of *mdatatime* on S with *THSNR* = 14 dB, RB = {1, 3, 5}, λ = 0.02

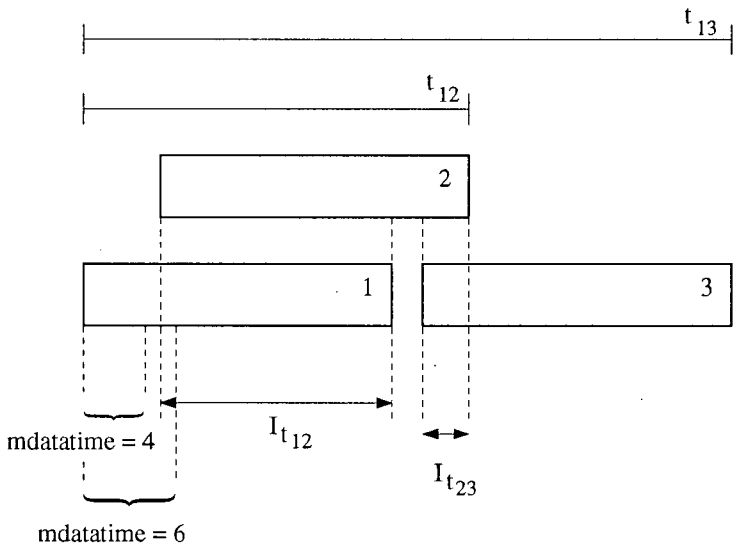

Figure 5.26 Extended period of interference

This extended period of interference is illustrated by an example. In figure 5.26, packet1 is captured because packet2 appears after the time frame *mdatatime* = 4. Packet2 is considered

as interference and its interfering power is suppressed by the *PG*. Packet3 has no effect on the reception of packet1. Next, consider a case with *mdatatime* = 6 such that packet2's received power happens to be higher than packet1. In this case, the RB locks onto packet2 if the PC scheme is used. However, packet3 interferes with the rear end of packet2. The interfering period between packets 1 and 2 is mutual and it is denoted as I_{t12}. Similarly the interfering period between packets 2 and 3 is denoted as I_{t23}. In the first case with *mdatatime* = 4, I_{t12} is the only interfering period that exists. However, in the second case, the total interfering period is $I_{t12} + I_{t23} \geq I_{t12}$. If the power of packet3 is similar to that of packet2, the extended interfering period (I_{t23}) could result in no packet being captured over the period t_{13}. Therefore, higher *mdatatime* decreases the throughput per busy period. The first case has one successful packet per t_{12} while the second case has no successful packet per t_{13}.

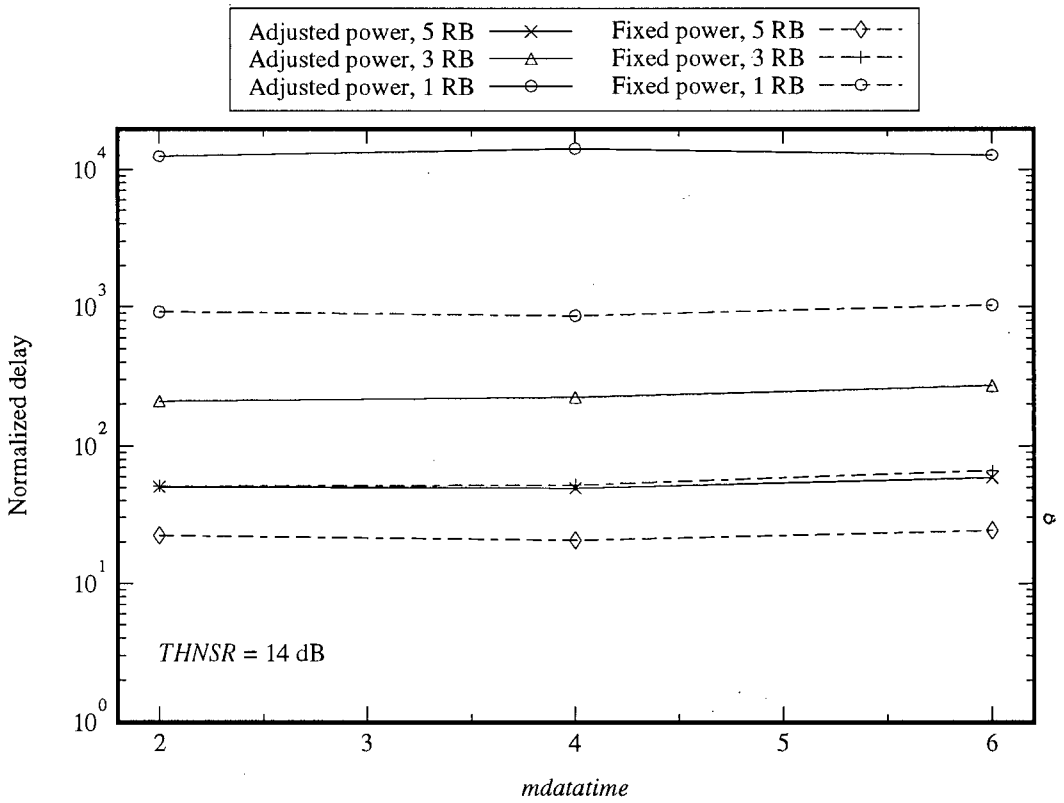

Figure 5.27 Effect of *mdatatime* on delay with *THSNR* = 14 dB and RB = {1, 3, 5}, λ = 0.02

In figure 5.27, the effect on delay is shown. For most cases, we see that the trend of higher *mdatatime* causes longer delay. However, the amount of additional delay is quite

small and is not considered significant.

The overall effect of *mdatatime* on the system is not as influential as some of other previously mentioned parameters. Its effect is more pronounced if the value of *THSNR* is high. When *THSNR* is small and the sensing range of each station encompasses many stations, the effect of *mdatatime* on the system performance is not obvious.

5.2.6 Effect of *prno*

It was previously mentioned in section 3.3.3 that the purpose of *prno* is to smooth out the number of retransmissions over the period of 1 + *prno* after a collision. We look at the effect of *prno* on *S* for *THSNR* = 18 dB. It is expected that a larger value of *prno* will give a better performance to the system.

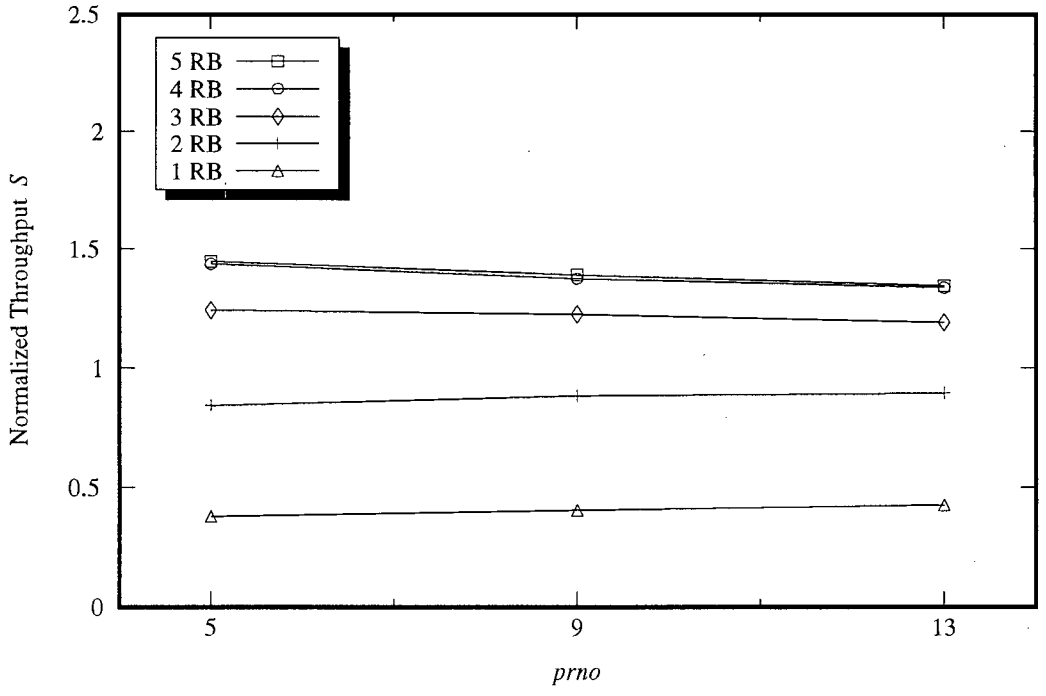

Figure 5.28 Effect of *prno* on *S* with *THSNR* = 18 dB and RB = {1, 2, 3, 4, 5}, λ = 0.01

Figure 5.28 shows how the system *S* behaviour varies with different values of *prno*. For RB = {1, 2}, *S* is increased slightly when *prno* is increased from 5 to 13. For RB = {3, 4, 5}, *S* is decreased when *prno* is increased from 5 to 13. Thus larger *prno* improves a system with

a small number of RBs (i.e., a system in saturation) but it is counter productive to a system with more RBs (i.e., a system is not saturated). Larger *prno* simply delays a retransmission for an extended amount of time and does not fully utilize the capacity of multiple RBs.

The results of delay analysis on the effect of *prno* are shown in figure 5.29. For RB = {4, 5}, larger *prno* actually causes longer system uplink delay. This is because with a high number of RBs, a station suffering from multiple collisions is less likely to happen than in a system with small number of RBs. Hence a larger *prno* actually puts a packet to backoff for some unnecessary delay. For RB = {1, 2}, larger *prno* helps to randomize the number of retransmissions over the period of 1 + *prno*. Thus, a packet may get through the channel successfully more easily if it is backoff once with *prno* = 13 than if it is backoff for several collisions with *prno* = 5. This gives the reason why we see a drop in delay when RB = {1, 2} even when a larger *prno* is used. A change in *prno* does not have an effect on 3 RBs at *THSNR* = 18 dB.

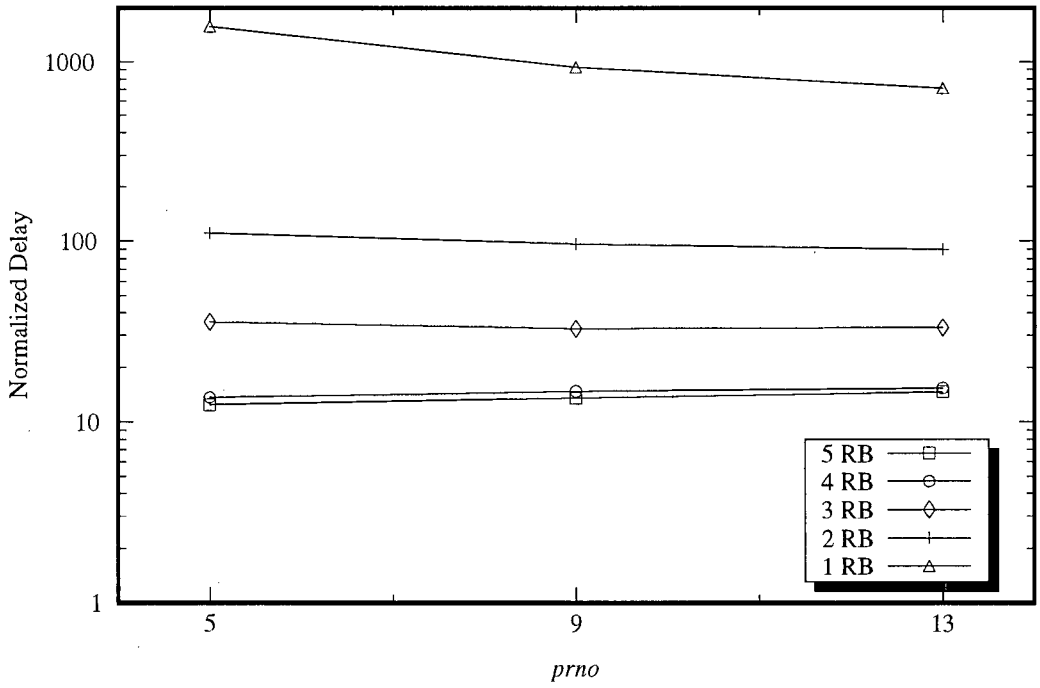

Figure 5.29 Effect of *prno* on delay with *THSNR* = 18 dB and RB = {1, 2, 3, 4, 5}, λ = 0.01

5.2.7 Effect of Network Size

To study the effect of network size, N, on the system, stations of $N = \{25, 49, 100\}$ have been simulated with *THSNR* = {12, 18} dB. Figure 5.30 depicts the normalized S-vs.-λ for RB = {1, 5} with *THSNR* = 12 dB. Note that the total arrival rate = $N \times \lambda$ and different values of N will have different numbers of hidden terminals outside the *THSNR* = 12 dB sensing circle. Therefore, S increases with N when the network is not saturated, whereas throughput levels out when the network becomes saturated. This can be observed from figure 5.30 where the 1 RB system saturates when λ becomes large and the throughput curves level out and overlap each other.

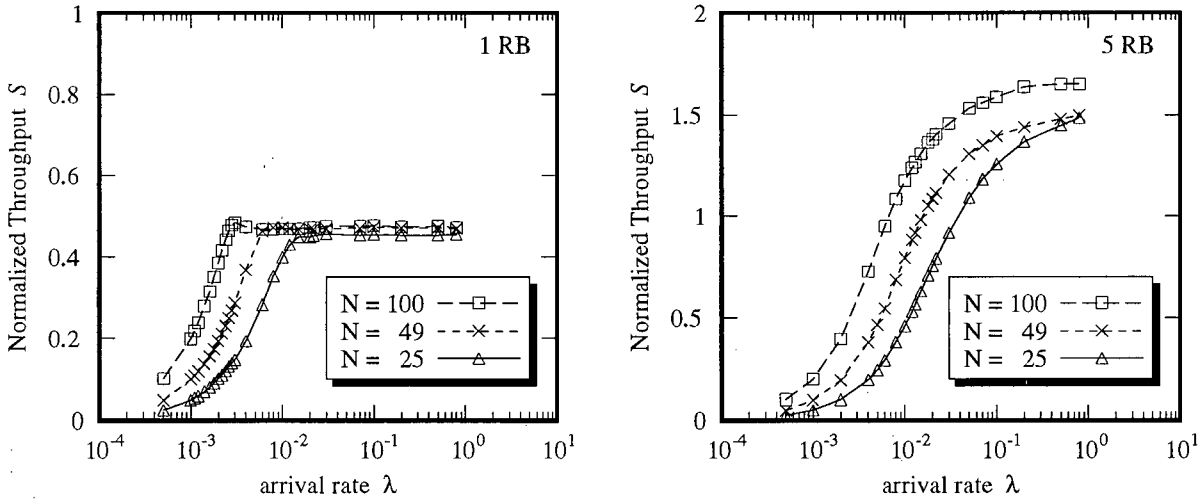

Figure 5.30 Effect of network size with *THSNR* = 12 dB and RB = {1, 5}

Figure 5.31 shows the effect of network size on throughput for 1 – 5 RBs and for *THSNR* = {12, 18} dB. A larger network size tends to increase the system throughput only if the network is not saturated. A larger network size also increases the number of hidden terminals in the model. Thus in the figure, there is a significant increase in S for multiple RBs systems.

In figure 5.32, the delay is plotted against the network size with $\lambda = 0.01$ and *THSNR* = {12, 18} dB. Generally, a larger network size causes a longer delay for a terminal to deliver a packet since more terminals are competing for the channel. The difference in delay between 4 and 5 RBs is minimal at this value of λ.

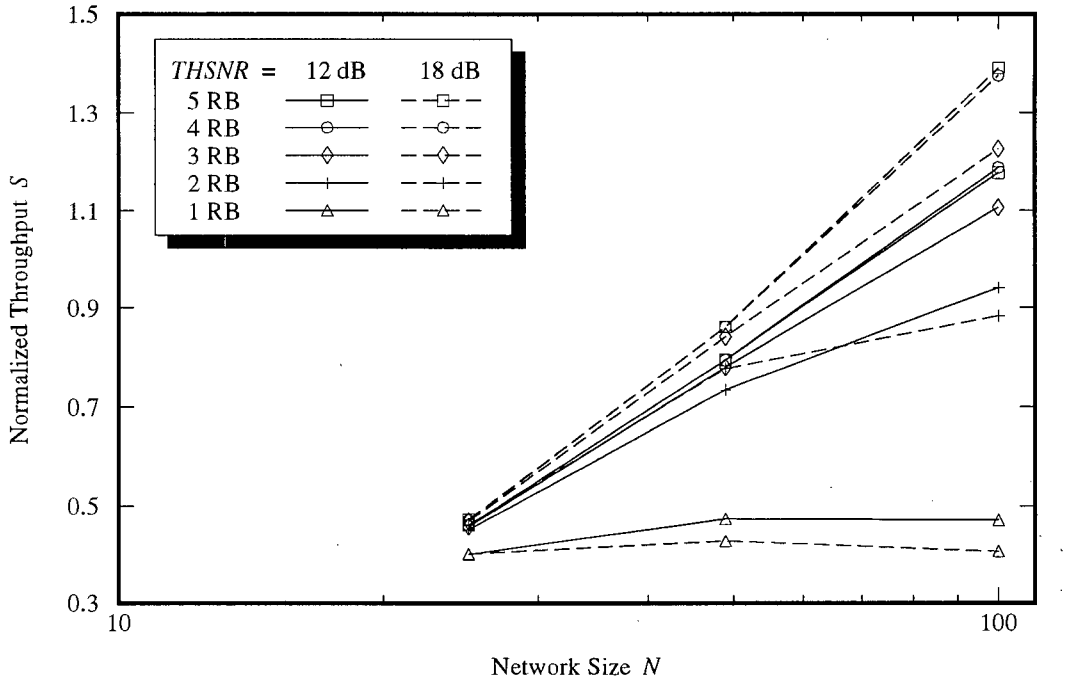

Figure 5.31 Effect of network size on throughput for different *THSNR* and RBs with $\lambda = 0.01$

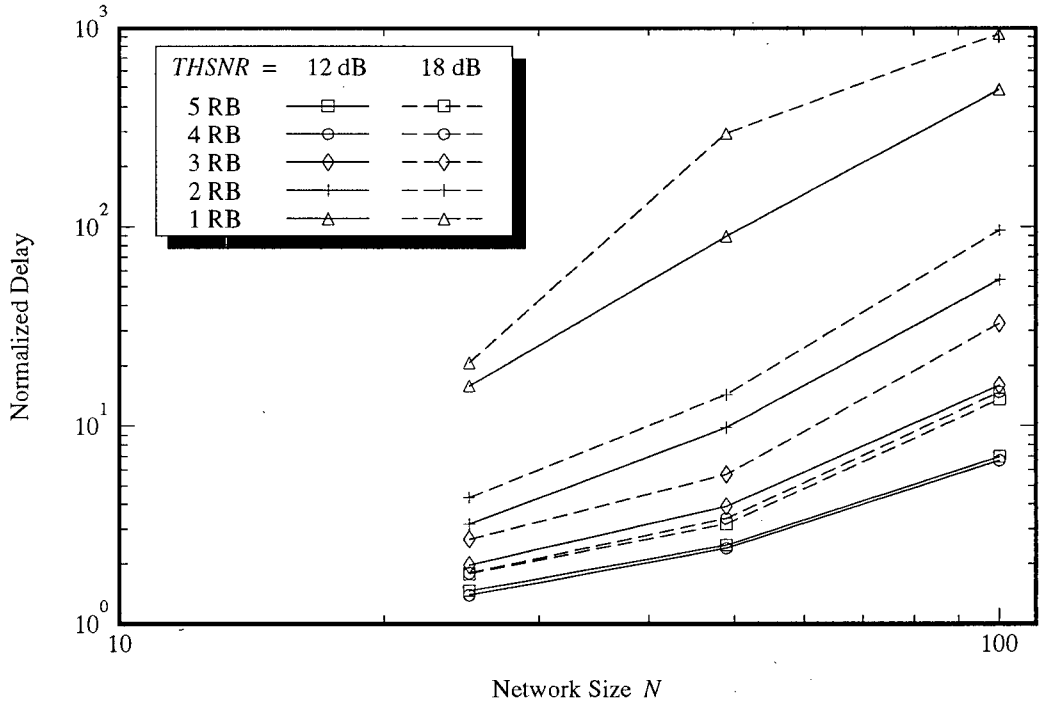

Figure 5.32 Effect of network size on delay for different *THSNR* and RBs with $\lambda = 0.01$

Thus changing N effectively changes the number of hidden terminals in the system, which in turn affects the number of multipacket receptions. However, this does not imply that we can increase the network size without bound to achieve a higher throughput. If the amount of traffic is over the capacity, terminals are either always backlogged or always in collisions.

5.2.8 Effect of Room Dimension

This section discusses the effect of room dimension on the system. Three room sizes = {40, 60, 80} m^2 are simulated. The initial design for the system is 40 m^2. Then the size of the room is enlarged and the positions of the stations are moved accordingly to preserve a uniform distribution within the room. When the AP method is used, the same $SNratio$ = 10 dB is employed. Enlarging the room size results in more hidden terminals. A system that employs the FP method uses the same transmitting power as in the 40 m^2 model.

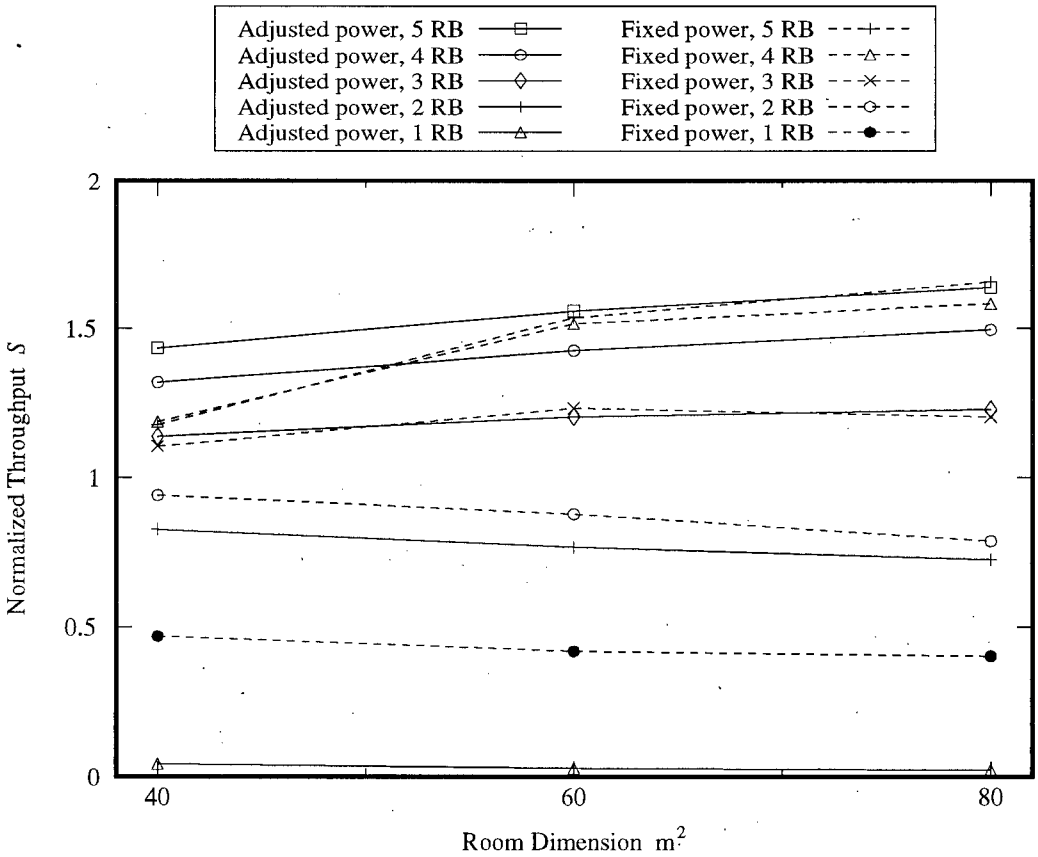

Figure 5.33 Effect of room dimension on S with $THSNR$ = 12 dB, λ = 0.01

Again, we use the method of plotting S versus the parameter under investigation to demonstrate its effect. Figure 5.33 is a plot of S-vs.-room dimension at $\lambda = 0.01$. The slight downward trend for RB = {1, 2} indicates that S decreases because of the increased number of hidden terminals in the system and thus higher ISR at the receivers. A noticeable increase in S is seen for RB = {4, 5} from 40 m^2 to 60 m^2. Since in this case the system is not saturated with packets, the increased number of hidden terminals provides a higher chance for multipacket receptions.

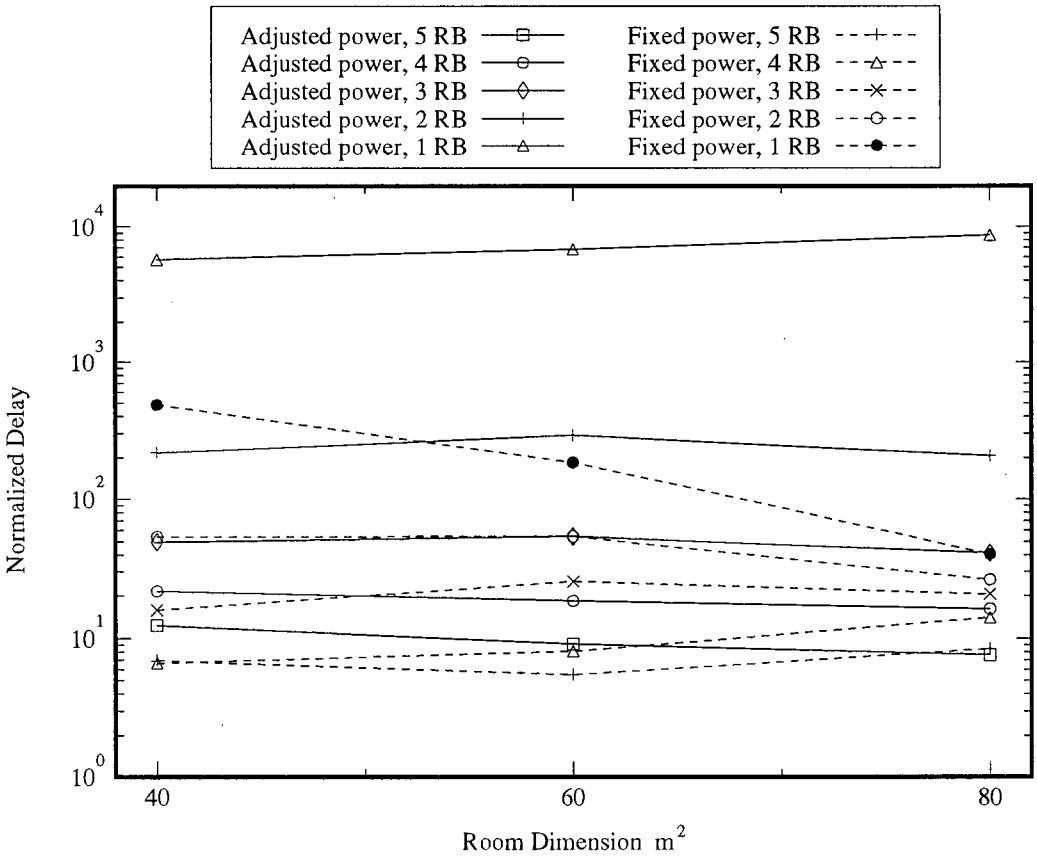

Figure 5.34 Effect of room dimension on delay with *THSNR* = 12 dB, $\lambda = 0.01$

Delay variation as a function of room dimension is shown in figure 5.34. In most cases, delay does not vary as much as the other parameters. Therefore, we see most of the curves do not have very steep slopes. The only exception occurs in the case of FP method with 1 RB. The decrease in delay occurs because more hidden terminals and lower received power at the

RB due to increased separation have caused distant stations to go into the backlogged state. Thus only those stations that are closer to the RB can transmit their packets successfully. In the 80 m^2, 1 RB, AP method model, stations that are near the RB have much less Pr_C than those stations in the FP method model. Therefore, long delay exists in the AP model. For the FP method model, most of the transmissions from distant stations are unsuccessful. Only the center stations can deliver packets and the delays of these center stations are much shorter than those center stations in the AP method.

5.3 Summary of Effects of Various Parameters

Table 5.12 summarizes the qualitative effects of different parameters on the system throughput. These observations are true for the sets of conditions and parameters specified in the previous sections of this chapter.

Table 5.12 Summary of effects of different parameters

		Scheme 1	**Scheme 2**	**Condition**
Increase number of RB	Fixed power	Improved	Improved	Fixed *THSNR*
	Adjusted power	Improved	Improved	
		1 RB	**4-5 RBs**	
Increase *THSNR*	Fixed power	Worsen	Worsen	TC scheme
	Adjusted power	Worsen	Improved	
Power Transmission Method	Fixed power	Better than adjusted power in low number of RBs. Little gain between 4 and 5 RBs		TC scheme
	Adjusted power	Better than fixed power when the number of RBs are high. Does not work in 1 RB case.		
Capture Scheme	Power capture	Slightly better than time capture with fixed power		
	Time capture	Slightly better than power capture with adjusted power		
		Fixed power	**Adjusted power**	
Increase *mdatatime*	Power capture	Worsen	Worsen	
		1-2 RBs	**4-5 RBs**	
Increase *prno*	Fixed power	Improved	Worsen	TC scheme
		Not in saturation	**In saturation**	
Increase Network size	Fixed power	Improved	Worsen	TC scheme
		1-2 RBs	**4-5 RBs**	
Increase Room dimension	Fixed power	Worsen	Improved	TC scheme
	Adjusted power	Worsen (does not work in 1 RB case)	Improved	

Chapter 6
Conclusion

6.1 Concluding Remarks

The interest in WLANs for indoor wireless communications is motivated by their terminals portability and network flexibility. A novel distributed architecture WLAN model employing multiple RBs, direct sequence spread spectrum signaling and CSMA multiple access is proposed. Simulation results are obtained to examine the performance of the multiple access protocol and other various aspects of WLANs, under two different types of channel traffic : uplink only and uplink/downlink.

The throughput, delay and capturing probability performance of the 1–persistent CSMA protocol are simulated in an uplink only WLAN model. The results show that a maximum throughput of 2.62 is achievable when 5 RBs are used in the system. This value of maximum throughput occurs when a moderate *THSNR*, the AP method and the PC scheme are used. The average delay experienced by the system is low as long as the system is not in saturation. Capturing probabilities of the corner and near wall stations are improved when the AP method is used. Other significant parameters that have been evaluated in the uplink only model are the number of RBs, *THSNR* and *prno*. From the results, increasing the number of RBs improves the system performance when the channel is in saturation. By varying *THSNR*, the tradeoff between hidden terminals and multiple packet receptions can be observed, with different power control methods and different capture schemes. A higher *prno* increases throughput in a 5 RBs system, for all power control methods and capture schemes. With these results, the conclusion is that the AP method, the PC scheme, a moderate *THSNR* and a high *prno* are preferred in the uplink only model.

After examining the uplink only WLAN, the 1–persistent CSMA protocol is employed in the uplink/downlink channel model. A problem found in this combination of the protocol and the channel is that uplink transmissions obtained most of the channel access, leaving the

downlink with much less throughput. A dual persistency CSMA protocol, where the uplink uses non-persistent CSMA and the downlink utilizes 1–persistent CSMA, is introduced to solved this problem. From the simulation results, the dual persistent CSMA protocol is shown to balance the uplink and downlink traffic. This balanced throughput is necessary in this common uplink/downlink channel model.

Various design parameters are studied in the uplink/downlink model. Increasing the number of RBs improves the throughput. In distributed WLANs, a tradeoff exists between duplicated packet receptions and multiple packet receptions for a given number of RBs as λ increases. From the results in this thesis, the tradeoff is found to be affected by the number of packets transmitted, *RBTH*, transmitting power, *THSNR* and the required SNR.

When the number of RBs is large, a higher *THSNR* is desirable because it allows more hidden terminals to exist so that multipacket receptions are possible. However, if the channel is saturated or if the number of RBs is small, a smaller *THSNR* is desirable. The adverse effect of hidden terminals being counter-balanced by the positive effect of multipacket reception is an unique property of the distributed WLAN. This property is greatly affected by the *THSNR*, required SNR, power control methods, room dimension, location of RBs and location of terminals.

From the results in this thesis, the AP method is found to be effective in raising the Pr_C of the corner stations to values comparable to those of their neighbours. This indicates that the near-far effect is reduced. However, the FP method performs better in a system with a smaller number of RBs.

In conclusion, the design of a distributed WLAN sharing a common uplink/downlink channel should employ a high number of RBs, a moderate *THSNR*, adjusted power transmission, power capture scheme, a small *prno* and a small *mdatatime*.

6.2 Future Research Work

Some areas in which further investigations are of interest are as follows :

1. The power control method considered in this thesis adjusts the transmitting power with respect to the second nearest RB. It may be worthwhile to examine more complicated power control methods to achieve higher channel utilization. A possible example is to adjust the transmit power until a certain value of Pr_C is maintained.
2. In the multiple RBs model, it is assumed that duplicated copies of a packet received by several RBs will be eliminated. The internetworking problem unique to the distributed architecture has not been investigated. Thus future research may consider the design of an internetworking protocol which harmonizes the protocols of the WLAN and wired LAN.
3. A draft standard for WLAN, IEEE 802.11, is now being balloted for possible official adoption in 1996. This standard uses a protocol called CSMA/CA, where CA stands for collision avoidance. It would be interesting to compare the performance of the CSMA/CA with that of the dual persistency CSMA protocol.

Bibliography

[1] C. Rees, "Building LAN's without cable," *Canadian Datasystems*, vol. 18, pp. 65–66, May 1986.

[2] John R. Barry, Joseph M. Kahn, Edward A. Lee, David G. Messerschmitt, "High-Speed Nondirective Optical Communication for Wireless Networks," *IEEE Network Magazine*, vol. 5, pp. 44–54, Nov. 1991.

[3] Roger Dettmer, "Local Network Radio the Wireless LAN," *IEE Review*, vol. 39, Issue 3, pp. 127–131, May 1993.

[4] IEEE 802.11 Working Group, *Draft Standard D2.0 Wireless MAC and PHY Specifications*. IEEE, D2.0 ed., 1994.

[5] Ahmed H. Abdelmonem, Tarek N. Saadawi, "Performance Analysis of Spread Spectrum Packet Radio Network with Channel Load Sensing," *IEEE Journal on Selected Areas in Communications*, vol. 7, no. 1, pp. 161–166, Jan. 1989.

[6] James E. Mitzlaff, "Radio Propagation and Anti-Multipath Techniques in the WIN Environment," *IEEE Network Magazine*, vol. 5, pp. 21–26, Nov. 1991.

[7] Dole Buchholz, Paul Odlyzko, Mark Taylor, Richard White, "Wireless In-Building Network Architecture and Protocols," *IEEE Network Magazine*, vol. 5, pp. 31–38, Nov. 1991.

[8] Bryan Munro-Smith, Keyvan Farhangian, "The Performance of Evaluation of Wireless LAN Systems," in *IEE Collquium on 'The Cordless Offoce' (Digest No. 1993/172)*, (London, UK), pp. 1/1–12, Oct. 1993.

[9] Leonard Kleinrock, Fouad A. Tobagi, "Packet Switching in Radio Channels : Part I - Carrier Sense Multiple-Access Modes and their Throughput-Delay Characteristics," *IEEE Transactions on Communications*, vol. COM-23, no. 12, pp. 1400–1416, Dec. 1975.

[10] Fouad A. Tobagi, "Analysis of Two Hop Centralized Packet Radio Network Part II : Carrier Sensing Multiple Access," *IEEE Transcations on Communications*, vol. COM-28, no. 2, pp. 208–216, Feb. 1980.

[11] Hideaki Takagi, Leonard Kleinrock, "Throughput Analysis for Persistent CSMA Systems," *IEEE Transcations on Communications*, vol. COM-33, no. 7, pp. 727–638, Jul. 1985.

[12] Hideaki Takagi, Leonard Kleinrock, "Correction to 'Throughput Analysis for Persistent CSMA Systems'," *IEEE Transcations on Communications*, vol. COM-35, no. 2, pp. 243–245, Feb. 1987.

[13] Christian Namislo, "Analysis of Mobile Radio Slotted Aloha Networks," *IEEE Journal on Selected Areas in Communications*, vol. SAC-2, NO. 4, pp. 583–588, Jul. 1984.

[14] Isam M. I. Habbab, Mohsen Kavehard, Carl-Erik W. Sundberg, "Aloha with Capture Over Slow and Fast Fading Radio Channels with Coding and Diversity," *IEEE Journal on Selected Area in Communications*, vol. SAC-7, NO. 1, pp. 79–88, Jan. 1989.

[15] V. C. M. Leung, "Diversity Interconnection of Wireless Terminals to Local Area Networks via Radio Bridges," *IEE Electronic Letters*, vol. 28, pp. 489–490, Feb. 1992.

[16] V. C. M. Leung, "Internetworking Wireless Terminal to Local Area Network via Radio Bridges," in *Proceedings of the IEEE International Conference on Selected Topic in Wireless Communications*, (Vancouver, B.C.), pp. 126–129, IEEE, Jun. 1992.

[17] C. M. Chang, "Multisite Throughput of a Mobile Data Radio Link," *IEEE Transcations on Vehicular Technology*, vol. 39, pp. 190–204, Aug. 1990.

[18] C. M. Chang, "Some Issues on Multisite Throughput of a Mobile Digital Radio Link," *IEEE Transcations on Vehicular Technology*, vol. 41, pp. 526–531, Nov. 1992.

[19] K. Sakakibara, "Performance Approximation of a Multi-Base Station Slotted Aloha for Wireless LAN's," *IEEE Transactions on Vehicular Technology*, vol. 41, pp. 448–454, Nov. 1992.

[20] Mutsumu Serizawa, "A Radio Access Scheme for CSMA/CD," in *IEEE International Conference on Communications*, (Boston, MA), pp. 477–481, Jun. 1989.

[21] J. F. Lemieux, "Experimental Evaluation of Space/Frequency/Polarization Diversity in the Indoor Wireless Channel," *IEEE Transactions on Vehicular Technology*, vol. 40, pp. 569–574, Aug. 1991.

[22] P. Y. Kam, "Optimal Detection of Digitial Data Over Nonselective Rayleigh Fading Channel with Diversity Reception," *IEEE Transactions on Communications*, vol. COM-39, no. 8, pp. 214–219, Aug. 1991.

[23] L. F. Chang, J. C.-I. Chunag, "Diversity Selection using Coding in a Portable Radio Communication Channel with Frequency-Selective Fading," *IEEE Journal on Selected Area in Communications*, vol. 7, pp. 89–98, Jan. 1989.

[24] R. C. Bernhardt, "Macroscopic Diversity in Frequency Reuse Radio System," *IEEE Journal on Selected Area in Communications*, vol. 5, pp. 862–870, Jan. 1987.

[25] Fouad A. Tobagi, "Modelling and Performance Analysis of Multihop Packet Radio Network," *Proceedings of IEEE*, vol. 75, no. 1, pp. 135–155, Jan. 1987.

[26] V. Hayes, "Radio - LAN Standardization Efforts," *IEEE Infocom*, vol. 7, no. 1, pp. 1–4, Sept. 1992.

[27] Fouad A. Tobagi, Leonard Kleinrock, "Packet Switching in Radio Broadcast Channels : Part II - The Hidden Terminal Problem in Carrier Sense Multiple-Access and the Busy Tone Solution," *IEEE Transactions on Communications*, vol. COM-23, no. 12, pp. 1417–1433, Dec. 1975.

[28] Dan Duchamp and Neil Reynolds, "Measured Performance of a Wireless LAN," *Proceedings 17th Conference on Local Computer Networks*, vol. 1, pp. 494–499, May 1992.

[29] K. Bullington, "Radio Propagation for Vehicular Communications," *IEEE Transactions on Vehicular Techology*, vol. VT-26, pp. 295–308, Nov. 1977.

[30] Scott Y. Seidel, Theodore S. Rappaport, "914 MHz Path Loss Prediction Models for Indoor Wireless Channel Communication in Multifloored Buildings," *IEEE Transactions on Antenna and Propagation*, vol. 40, no. 2, pp. 207–217, Feb. 1992.

[31] W. Y. Au, "Multi-Receiver Performance of Slotted Aloha Multiple Access with Direct Sequence Spread-Spectrum Signalling for Wireless In-Building Networks," Master's thesis, University of British Columbia, Nov. 1993.

[32] Dilip V. Sarwate and Michael B. Pursley, "Crosscorrelation Properties of Pseudorandom and Related Sequences," *Proceedings of the IEEE*, vol. 68, no. 5, pp. 593–619, May 1980.

[33] Raphael Rom and Moshe Sidi, *Multiple Access Protocols - Performance and Analysis*. Springer-Verlag, 1990.

[34] Dimitri Bertsekas and Robert Gallager, *Data Network*. Prentice Hall Englewook Cliffs, 2nd ed., 1992.

[35] Randy L. Borchardt and Tri T. Ha, "Analysis of Unslotted Random Access Channel in a Capture Environment," in *IEEE International Conference on Communications*, (Boston), pp. 1263–1267, Jun 1989.

[36] James S. Meditch, Chin-Tau A. Lea, "Stability and Optimization for the CSMA and CSMA/CD channels," *IEEE Transactions on Communications*, vol. COM-31, pp. 763–744, Jun 1983.

[37] James S. Storey, Fouad A. Tobagi, "Throughput Performance of an Unslotted Direct-Sequence SSMA Packet Radio Network," *IEEE Transcations on Communications*, vol. Vol-37, no. 8, pp. 814–823, Aug. 1989.

[38] K.J. Zdunek, D.R. Vcci and J.L. Locicero, "Throughput of non-persistent inhibit sense multiple access with capture," *Electronics Letter*, vol. Vol-25, no. 1, pp. 30–32, Jan. 5 1989.

Appendix A Model Description

The simulation of WLAN involves many parameters or variables. These parameters can be either global, affecting the entire simulation, or local, affecting only a particular routine or process. A complete list of these parameters can be found in each process described below.

A.1 Model Description

The whole WLAN simulation consists of six processes, of which two processes are essential : STATION and RBTR. These two processes have very tight interactions and will be described in details. The other four processes are for calculation purposes : TXRX, RBACKST, STACKRB, STOP.SIM.

Figure 5.6 gives a pictorial model of the WLAN using two types of CSMA as the MAC protocol. The following is a description of the operation of this model. Each procedure labeled in figure is enumerated in the following list.

(1) The system starts with some appropriate initialization of global variables, physical constraints or constants.

a. Global variable :

- arrival rate of packet at each station
- sensing threshold, *THSNR*
- RB threshold, *RBTH*
- maximum propagation delay
- *prno*
- power control method
- packet capture scheme
- processing delay

b. Constraints and constants :

- number of RBs
- processing gain, *PG*

- location of RBs
- network size, N
- room dimension

c. Activation of the two main processes : STATION and RBTR.

d. Activation of the STOP.SIM processes at the end of simulated time. This STOP.SIM process gathers all the statistics of the simulations and writes the results to appropriate files.

e. Simulation starts.

(2) Packet are generated within each station with normalized Poisson arrival rate initialized in (1.a) above. Only idle stations will generate new packets. An idle station is a station that is not in one of these state : tx_packet, tx_ack, recv_packet, recv_ack, waiting_for_ack, backoff.

When there is a new arrival at an idle station (STATION A), the station will sense the state of the channel. For every station, it uses non-persistent CSMA.

a. If the channel is sensed idle, the station transmits the packet using the current power control method.

b. If the channel is sensed busy, the station backoffs according to the equation (3.13) where *prno* is initialized in (1.a) above.

(3) After the packet has been transmitted, two events happen.

a. The transmitting station (STATION A) goes to a waiting_for_ack state and two constraints are applied to this station.

- No new packet is generated at this station.
- This station does not receive any packet except an acknowledgment; therefore, any data packet that is destined to STATION A will not succeed.

b. The transmitted packet and its multipath replica are filed in the channel queue. This queue will be examined by each RB for signal capturing.

(4) Each idle RB will take turn to check the channel queue and capture one of the packets according to the current capture scheme. The packet's BER and PER are

calculated with the received SNR and the maximum ISR according to the equation (3.11), in which P_e is the bit error probability, BER. PER is the packet error probability and is given by equation (3.12). An RB is idle if it is currently not in any one of these states : tx_packet, tx_ack, recv_packet, recv_ack, waiting_for_ack.

a. If this packet is successful, it is stored into the buffer of the appropriate RB (the RB nearest to the destination station). This successful packet is counted as one uplink success.

b. If this packet is unsuccessful, the RB will go back to (4) when the time has reached this end of this packet. Success or failure of reception of a packet is not known until the whole packet is received.

(5) At the end of successful packet reception, an ack packet is generated from the RB and is directed to the previous transmitting station (STATION A) which is now in the waiting_for_ack state. This ack packet and its multipath replica are filed in the channel queue.

(6) Then STATION A will examine the channel queue and see if there is an ack packet.

a. If an ack packet is found, its BER and PER are calculated using the received SNR and maximum ISR according to the equation (3.11) and (3.12) respectively.

b. If no ack packet is found, STATION A will time out and be reactivated by a time out routine. The time out routine is activated at the time

$$pkt.length + ack.pkt.length + 2 * max.propagation.delay \qquad \text{(A.1)}$$

from the start of transmission of STATION A. Then STATION A will backoff according to equation (3.13). The same procedure in (3) above is repeated except the counter will accumulate succeeding transmissions as retransmissions until an ack packet is successfully received.

(7) The ack packet may or may not be successfully received. Determination of the success of downlink ack packet is done by a process called RBACKST.

a. If the ack packet is successful, STATION A will be reactivated and will go to the idle state. A new packet may again be generated from this station. One downlink ack packet success is counted.

b. If the ack packet is unsuccessful, STATION A will be timed out as in (6.b) above.

(8) After a RB has transmitted an ack packet in (5), it will wait until the end of the ack packet. The channel is idle at the end of ack packet. Then, the first packet in the RB's buffer, if any, is retrieved and transmitted over the downlink. If the buffer is empty, the RB becomes idle and (4) will be repeated.

(9) Following the transmission of the packet from its buffer in (8), two events occur.

a. The RB goes to a waiting_for_ack state.

- No further packet transmission from the buffer is possible.
- This RB does not receive any packet from the stations except an ack packet.

b. The transmitted packet and its multipath replica are filed in the channel queue. The queue will be examined by the destination station (STATION B).

(10) This packet from the RB will be captured by the destination station only if STATION B is not in anyone of the tx_packet, tx_ack, recv_packet, recv_ack or waiting_for_ack state, i.e., the station is idle; otherwise, the packet will be discarded and the transmission will be counted as a failure.

If STATION B is idle, it will check the channel queue and will capture the packet directed to it according to the current capture scheme. The packet's BER and PER are calculated with the received SNR and maximum ISR according to equations (3.11) and (3.12) respectively. Calculations are performed in process TXRX.

(11) If this packet transmitted from the RB is successfully received by STATION B, one downlink success is counted. Then STATION B will likewise generate an ack packet back to the RB. Again this ack packet will be filed in the channel queue and examined by a RB that is currently in waiting_for_ack state. The ack packet's BER and PER are calculated using equations (3.11) and (3.12) respectively in a process called STACKRB.

a. If this ack packet is successful, one uplink ack success is counted. This ack packet will reactivate the RB from the waiting_for_ack state to an active state. The first buffer is discarded and the next buffer will become the first buffer in this RB.

b. If this ack packet is unsuccessful, the RB will be time-out with the value of equation (A.1) from the start of transmission of downlink packet in (8).

(12) The reactivated RB performs either one of the following procedures.

a. If the buffer size of this RB is still non-zero, it will again retrieve the first buffer and transmit and (8) will be repeated.

b. If buffer size is zero, it will start to capture any uplink packet in the channel queue and (4) will be repeated.

A.2 Process : STATION

Channel traffic is generated due to the origination of packets from process STATION. Each station generates packet independently and may have a different arrival rate. However the same rate is used in the simulation for simplicity. In each instance of process STATION, the following conditions must be met :

- Single transmission buffer : only one packet is stored in the buffer for uplink transmission. Thus when a packet is not yet successful, the STATION does not generate a new packet.
- Peer-to-peer connection must be done via a RB, even if the two stations are next to each other.

The followings are the global and local variables that may affect the STATION process.

A.2.1 Global

☐ normalized Poisson arrival rate

☐ *THSNR*

☐ *RBTH*

☐ power control method

- ☐ packet capture scheme
- ☐ *prno*
- ☐ non-persistent CSMA

A.2.2 Local

- ☐ x, y location of STATION
- ☐ state of STATION
- ☐ number of transmissions
- ☐ number of ack received

A.3 Process : RBTR

In the WLAN model, the RB itself does not create packet. A transmission from a RB is possible only if it has successfully received an uplink packet or another RB has received a packet and routed the packet to this RB. Therefore, downlink transmissions are highly dependent on the uplink transmissions and the success rate of the RBs. This also gives the reason why the STATION and RBTR processes are tightly related. In each RB, the following conditions must be met :

- Multiple buffers of finite size : each RB has 5 buffers. When the buffers are full, any packet arriving (either from reception or from another RB) will be discarded.
- Upon complete reception of an uplink packet, the RB knows whether to store the packet to its buffers or to forward it to another RB immediately.

The followings are the global and local variables that may affect the RBTR process.

A.3.1 Global

- ☐ *THSNR*
- ☐ *RBTH*
- ☐ power control method
- ☐ packet capture scheme
- ☐ *prno*
- ☐ buffer size

- ☐ 1–persistent CSMA

A.3.2 Local

- ☐ x, y location of RB
- ☐ state of RB
- ☐ number of transmissions
- ☐ number of ack received
- ☐ number of packets remaining in buffer

A.4 Process : TXRX

This is a process used to calculate the success of downlink packets. Calculation of the number of interfering packets is described in [35] but a modified version is applied here. In [35], a tagged packet is interfered by k early interfering packets and j late interfering packets, as illustrated in figure A.1.

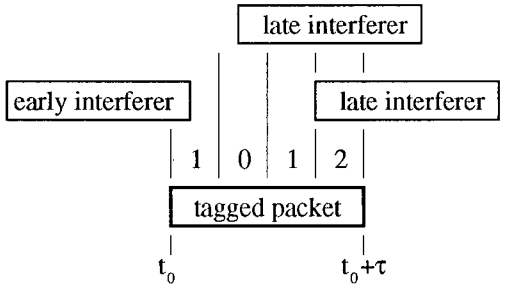

Figure A.1 Tagged packet and interfering packets

As a result of combining the variables k and j, there are $k+j$ independent events that will happen during the time interval $(t_0, t_0+\tau)$, where t_0 is the tagged packet arrival time and τ is the fixed packet length. From there, the probability distribution function of the maximum number of interferers is derived out of the $k+j$ interferers that could be encountered by the tagged packet.

The method above is modified in such a way that a tagged packet may have a maximum of three interfering regions. Region A is defined by the time t_o and the end of early interferer.

Region C is within the beginning of the last late interferer and the end of tagged packet. Region B is the region other than A and C but within the duration of the tagged packet. The three regions are illustrated in figure A.2.

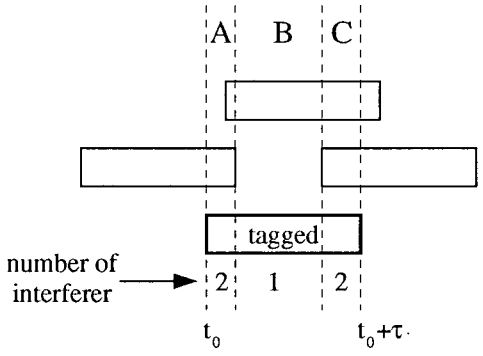

Figure A.2 Calculation of maximum ISR from a tagged packet.

A tagged packet is not yet a successfully received packet. It is merely a packet being locked onto by a receiver using the current capture scheme. The maximum ISR (Interference to Signal Ratio) is calculated in the way that the power of the interfering packets are added columnwise in the three regions shown (A, B, C) producing three different interfering powers. Then among the three ISRs, the maximum is found and substituted in equation (3.11).

A.5 Process : RBACKST

This process is used to calculate the success of downlink ack packets, i.e. the acknowledgments from RBs to stations. In this process, the maximum ISR is calculated by comparing the three possible values of ISR, as illustrated in figure A.3.

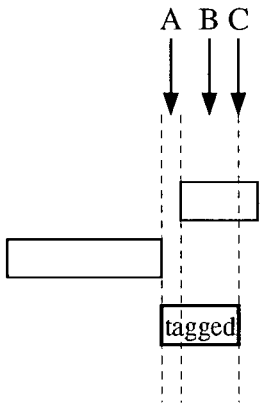

Figure A.3 Calculation of maximum ISR from a tagged ack packet

However, since the length of ack packet is much shorter than the normal packet, most of the interference experienced by the ack packet exist in region B. Note that region B and C are the same region.

A.6 Process : STACKRB

Process STACKRB is similar to RBACKST except that the packet of interest is the uplink ack packet, i.e. acknowledgments from stations to RBs. The method used in this process is identical to the one illustrated in figure A.3 in RBACKST.

A.7 Process : STOP.SIM

This process is activated at the end of the simulation. Its purpose is to gather the statistic during the course of the simulation and produce the results from this simulation. Examples are calculation of the channel offered traffic, the normalized channel offered traffic, the stations' and the RBs' capturing probability, the stations' and the RBs' delay. It also writes the results in proper format for curve plotting. Table A.13 summarizes the functions of the six processes in the protocol.

Table A.13 Functions of the six simulation processes

Process	Function
STATION	to generate packets for transmission
RBTR	to calculate the success of uplink packet and to relay successful uplink packets to the downlink
TXRX	to calcuate the success of downlink packets from RB
RBACKST	to calculate the success of downlink ack packets from RB
STACKRB	to calculate the success of uplink ack packets from STATION
STOP.SIM	to gather statistics for each simulation run